National Institute of BUILDING SCIENCES™

Natural Hazard Mitigation Saves: Case Study

# PORTLAND RESILIENT RUNWAY BENEFIT-COST ANALYSIS

March 2021

# Portland International Airport (PDX) Resilient Runway Benefit-Cost Analysis

## March 2021

**DEVELOPED BY:**

National Institute of Building Sciences
Multi-Hazard Mitigation Council

About NIBS and MMC: National Institute of Building Sciences brings together labor and consumer interests, government representatives, regulatory agencies, and members of the building industry to identify and resolve problems and potential problems around the construction of housing and commercial buildings. NIBS is a nonprofit, non-governmental organization. It was established by Congress in 1974. The Multi-Hazard Mitigation Council (MMC) is one the many councils under NIBS. MMC serves a vital national need by establishing a body of experts in a multitude of related fields of building sciences that can address the challenges associated with the identification and implementation of effective natural hazard mitigation practices. The Council is an independent entity that informs mitigation decisions in ways that lead to effective public policy on many levels. For further information on MMC activities and products, see the Council's website (https://www.nibs.org/mmc) or contact Jiqiu (JQ) Yuan, Executive Director of Multi-Hazard Mitigation Council and Building Seismic Safety Council, at jyuan@nibs.org or 202-289-7800.



SUGGESTED CITATION:
Multi-Hazard Mitigation Council (2021). PDX Resilient Runway Benefit-Cost Analysis. Principal Investigator Porter, K.; Co-Principal Investigators Rose, A., and Santos, J.; Investigator Wei, D.; Yuan, J., Director, MMC. National Institute of Building Sciences. Washington, DC, www.nibs.org.

# Foreword

Every year, natural disasters affect 313 million people in the United States. Disaster losses to events like hurricanes, earthquakes, floods, and wildfire grow about 6% per year — 10 times faster than the population. Future disasters are inevitable, yet their growing frequency and magnitude of destruction substantially are exacerbated by the decisions Americans make in where and how they build.

More than ever, mitigating against natural disasters is of paramount importance.

As cities and communities grow, these events will affect more lives, businesses, and the nation's economy. Fortunately, there are measures that individuals and communities can do to minimize destruction in hazard-prone areas. Pre-disaster mitigation—preparing in advance for future disasters—assures that hazardous events are short-lived and more manageable. Mitigation saves lives and preserves homes, businesses, government facilities, utilities, and transportation infrastructure. It reduces damage to belongings, helps economies spring back faster, and lowers recovery costs.

This report builds on where we started. In 2005, the National Institute of Building Sciences Multi-Hazard Mitigation Council released the initial Natural Hazard Mitigation Saves study, which demonstrated that for every public dollar spent on mitigation, society saves $4. The subsequent studies in 2017, 2018, and 2019 expanded the scope and evaluated broader mitigation measures from adopting up-to-date building codes and exceeding codes to addressing the retrofit of existing buildings and utility and transportation infrastructure. We found that mitigation saves up to $13 per $1 invested (national average) across perils, including riverine flood, hurricane surge, wind, earthquake, and wildland-urban interface fire.

We are happy to support the Portland International Airport to study the long-term benefits of investing in a seismically resilient runway. It is our aim to help decision-makers build a mitigation strategy so they can protect lives, properties, and assets. It is our mission to provide the scientific data that may assist policymakers to develop effective federal programs that support pre-disaster mitigation and encourage more mitigation investments from the public and private sector.

And while we close the chapter on this case study, more work is needed to assess a broad suite of mitigation strategies. We hope you will consider supporting this project moving forward. The National Institute of Building Sciences encourages President Joe Biden, members of Congress and the state legislature, leaders of federal and state agencies, communities, building owners, and officials within the private finance, insurance, and real estate sectors to review our Mitigation Saves report findings and use the results to initiate a greater mitigation dialogue, increasing awareness and encouraging mitigation activities to help develop a more resilient nation.

Sincerely,

Lakisha Ann Woods, CAE
*President & Chief Executive Officer*


F3 B3→
←B3 B B3↗

# Executive Summary

### Background

Oregon has a significant potential in the next 50 years of experiencing an earthquake greater than magnitude-8.7 originating from the Cascadia Subduction Zone (see Figure ES-1). Such an earthquake will cause catastrophic damage and loss of life across Oregon and much of the Pacific Northwest from British Columbia to Northern California. This is a massive risk and a major vulnerability. However, mitigation investments before a disaster can reduce its impacts. With new investments in airfield infrastructure, the Port of Portland (Port) can play a crucial part in the region's earthquake response and recovery.

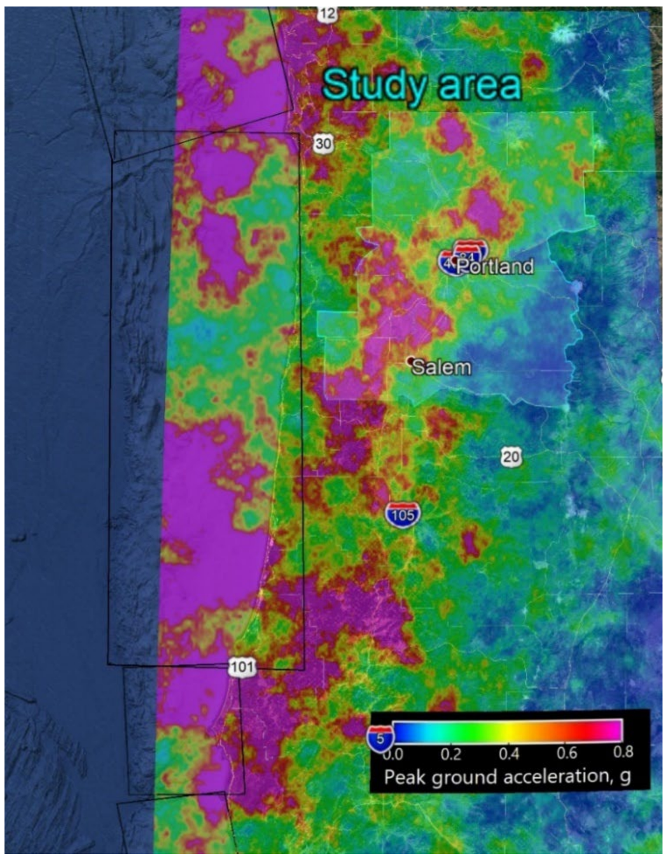


Figure ES-1. Cascadia Subduction Zone (black rectangles), study area (highlight), and one of 100 simulations of peak ground acceleration (color overlay)

When a major Cascadia Subduction Zone earthquake occurs, landslides and bridge damage can isolate the Willamette Valley by road and rail. At Portland International Airport (PDX), which is located on fill in a historic floodplain, such an earthquake will cause the ground beneath the runways to settle and spread, breaking the pavement, and rendering it unusable for aircraft. To repair and rebuild the runway to service large aircraft for air cargo and commercial operations is estimated to take up to approximately one year.

While an earthquake cannot be prevented, it is possible to prepare and build resilience though mitigation. Building resilience lessens the impacts and positions communities to respond, rebuild, and recover quicker and more efficiently. Nationally and locally, mitigation can save billions of dollars in avoided losses.

A seismically resilient runway at PDX that can operate after an earthquake would provide an essential lifeline for the region. Immediately following an earthquake, it would support large-scale medical evacuations that move critically injured people to medical care outside the impact zone. It would make it feasible to bring in aid supplies and workers via large aircraft. It would ensure access to building evaluators within hours or days of an earthquake to evaluate buildings and help people get back in their homes. Returning people to their homes reduces displacement and demand for temporary housing. As commercial passenger and air cargo services resume, it would also reduce business interruption and support economic recovery.

Without a seismically resilient runway at PDX, federal and state response operations for a Cascadia Subduction Zone earthquake will be based in Redmond, Oregon, on the east side of the Cascades. Supplies and aid would need to arrive in the Portland and broader Willamette Valley regions primarily by road. With limited roadway access, air operations would be restricted to small craft, and possibly marine service, significantly constraining recovery operations. Recovery costs are more than financial. Extended recovery times take a physical and emotional toll on people and communities.

The Port began exploring the potential of mitigating one of the runways at PDX in 2017, modeling it on the seismically resilient runway at Sendai Airport in Japan. The Port established a partnership with Oregon State University to develop a site-specific understanding of soil conditions, and then worked with a private consultant, Geotechnical Resources Inc. (GRI) to develop design documents. The Port now has detailed on-site assessments and an initial design and cost estimate for mitigating 6,000 feet of PDX's south runway to be seismically resilient.

### Purpose

This study, prepared under the leadership of the National Institute of Building Sciences (NIBS), presents a benefit-cost analysis of constructing the seismically resilient runway at PDX. It quantifies the financial and life-safety benefits—the present value of avoided future losses—in present-value dollars. The ratio of benefit to cost is referred to as the benefit-cost ratio (BCR). A BCR greater than 1.0 means that the benefits exceed the cost and suggests a desirable investment. The higher the BCR, the more desirable the investment, although other considerations should be considered. The study focuses on avoided losses related to medical evacuations, building-safety evaluations, business interruption while the airport cannot support large aircraft, and runway repairs. This study applies the same principles used in two editions of the landmark nationwide benefit-cost analyses study of natural hazard mitigation entitled *Natural Hazard Mitigation Saves*. Published in 2005 and 2019, both were led by the NIBS project team for the Federal Emergency Management Agency (FEMA) and other public- and private-sector institutions. FEMA, at least partially, credits the 2005 study with inspiring thousands of disaster-mitigation efforts in the last 16 years.

### Process

The project team used a three-step process to determine the losses avoided and to estimate the benefit-cost ratio. The report provides technical details of each step.

1. Probabilistic seismic hazard analysis. The first step described the earthquake hazards to the region. While the Port has an in-depth understanding of risks at PDX, the study focuses on the likely impacts beyond the airport. The benefits of a resilient runway, while significant for PDX, are widely shared. A resilient runway represents a critical asset in the transportation system by facilitating economic and social connections within and outside the region. The project team analyzed ground motion and shaking for 100 earthquake scenarios, using 20 different simulations for each of the five ruptures of the Cascadia Subduction Zone. As shown in Figure ES-1, the project team estimated ground shaking and landslides for only a portion of the geographic area that would be shaken by a Cascadia Subduction Zone earthquake, but one much larger than the study area.

2. Impact assessment. Focusing on the 10-county study area surrounding PDX illustrated in Figure ES-1, the project team used the earthquake scenarios and simulations to estimate how ground motion and shaking would cause:
   - Highway landslides and impaired road access,
   - Bridge closure,
   - Building damage requiring post-earthquake safety assessment, and
   - Traumatic injuries requiring life-saving medical evacuation.

   These impacts will geographically isolate the region, injure people, and cause residential and business displacement. They will also complicate and constrain the delivery of supplies and medical evacuations. The project team assessed conditions during different seasons (to account for ground saturation) and at different times of day (to account for building occupancy).

3. Benefit calculations. Finally, the project team quantified the following impact categories with and without an operational runway at PDX, accounted for occurrence probabilities, and estimated dollar values of each category:
   - Hospital emergency room and intensive care unit capacity to treat traumatic injuries,
   - Ability to perform post-earthquake safety evaluation of buildings and to facilitate the reoccupation of safe buildings,
   - Business interruption at or near PDX and in industries that rely on PDX to operate, and
   - Runway repair costs.

### Findings

The project team found that constructing a resilient runway at PDX will avoid $7.2 billion in future losses, as detailed in Figure ES-2. Considering the estimated cost to improve the runway, the savings represents an overall benefit-cost ratio of 50:1. Details follow.

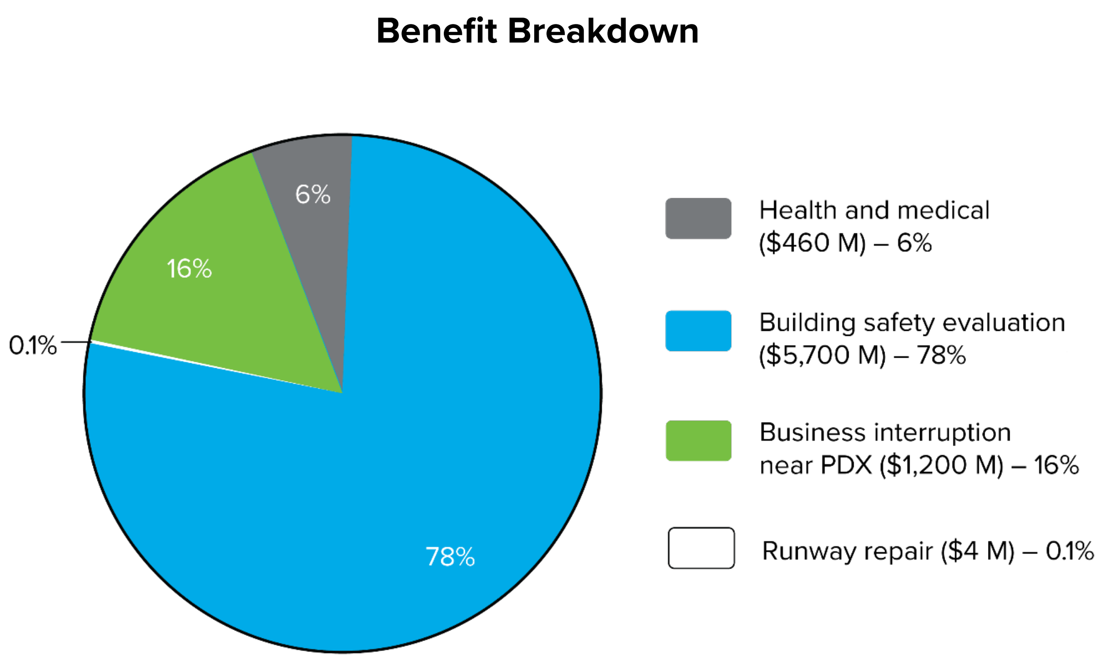


Figure ES-2. Major benefit categories and amounts ($ millions)

1. Medical evacuations ("health and medical" in the figure; $460 million benefit). A major earthquake will damage buildings and injure residents, including up to an estimated 2,400 people who will require medical care in an intensive care unit or emergency department to survive. That number far exceeds local hospital capacity. Under normal conditions, the occupancy rate at local intensive care units (ICUs) and emergency departments is approximately 68%, which existing hospitals in the study area, leaves a bed capacity of 360. The ability to move critically injured patients via large aircraft to hospitals outside of the earthquake zone will save lives and create capacity at hospitals to treat less critical or non-life-threatening injuries.

2. Building safety evaluation ($5.7 billion benefit). The largest scenario earthquakes could damage 600,000 buildings enough that they be rendered unusable until a building safety evaluation is performed on each. Certified building evaluators are needed to inspect buildings to determine under what conditions they are safe to reoccupy. The region will need thousands of inspectors to complete the work in a timely manner. There are fewer than 200 certified inspectors in the northern Willamette Valley. A runway that can serve commercial aircraft will help people get back into their homes and businesses by flying in thousands of certified building safety evaluators to

provide this critical service. Identifying safe structures will help people return to their homes, reduce displacement, and speed recovery.

3. Business interruption ($1.2 billion benefit). This analysis addresses the economic losses that will result from PDX being unable to support large aircraft operations. This includes business at or near PDX, such as hotels and logistics facilities that depend on the airport operating, and off-site businesses that rely on the airport's services. These business interruption losses will result while PDX lacks a functioning runway.

4. Runway repair costs ($4 million benefit). This is the reduction in the cost to repair the runway after an earthquake. Specifically, the remediated part of the runway will not need repair.

**Conclusions**

This study of the benefits and costs of a resilient runway at PDX demonstrates that a proactive investment will help Oregonians and federal and state relief agencies prevent $7.2 billion in foreseeable, avoidable future losses. Without mitigation, PDX's runways are a single point of failure in the transportation chain. Making one runway resilient will provide enormous benefits and make it possible to:

- Save lives by completing more medical evacuations from Oregon's most populous region and bringing in medical staff and supplies to support medical operations.
- Help people return to their homes and businesses by flying in thousands of certified building safety evaluators to determine which of the buildings (up to 600,000) are safe to re-enter and re-occupy.
- Speed the delivery of rebuilding supplies and construction workers.
- Reduce business interruption and make it easier to begin economic recovery.
- Generate immense value for our communities: (a) $460 million in health and medical benefits, (b) $5.7 billion in reduced home and business dislocation, (c) $1.2 billion in business continuity, (d) $4 million in reduced runway repair costs, and (e) allow the Air National Guard to continue operating.

**Limitations**

This study focuses on costs that the project team could confidently estimate. Other costs were omitted because they were too problematic to estimate, such as interrupting the mission of the 142nd Fighter Wing stationed at the Oregon Air National Guard at PDX. Other problematic recovery costs include some public health benefits of a timely recovery and the ability to physically reconnect with family. The project team identifies but does not quantify those costs and benefits. While this study includes an economic impact analysis (mainly focused on business interruption) and quantifies income loss by income level, this study does not estimate racial and social equity impacts. The Port is working with Portland State University (PSU) on an equity-impact analysis that will address racial and social vulnerability and equity and that will complement this study.

# Project Participants

**NATIONAL INSTITUTE OF BUILDING SCIENCES**

Jiqiu (JQ) Yuan, Executive Director of Multi-Hazard Mitigation and Building Seismic Safety Council

**PROJECT TEAM**

Keith Porter, SPA Risk LLC, Denver, CO, Principal Investigator

Adam Rose, University of Southern California, Los Angeles, CA, Co-Principal Investigator

Joost Santos, George Washington University, Washington, DC, Co-Principal Investigator

Dan Wei, University of Southern California, Los Angeles, CA, Investigator

**OVERSIGHT COMMITTEE**

Stephen A. Cauffman, Section Chief, Infrastructure Development and Recovery, Cybersecurity and Infrastructure Security Agency, U.S. Department of Homeland Security

Josh Lehner, Oregon Office of Economic Analysis

Mike K. Harryman, Oregon State Resilience Officer

Shideh Dashti, Associate Professor, University of Colorado Boulder

**PORT OF PORTLAND**

Alexandra Howard, Program Development Manager

Tom Wharton, Project Engineer

Sean Loughran, Planning & Development Director

Ann Gravatt, Federal Affairs & Policy Manager

**About the Oversight Committee**:

NIBS engaged an oversight committee of experts to provide an independent review of the study.

NIBS charged the oversight committee with performing a peer review like that of a technical journal article. Specifically, the committee was asked to review available methods, the project team's choice of methods to apply, and the project's use of data and assumptions. The oversight committee was also tasked with checking that the results were defensible and clear.

The project team presented the work to the oversight committee at three points during the project. At the 20% progress point, the oversight committee reviewed the study's goals, scope, and methods. At the 70% progress point, it reviewed preliminary key findings and a report outline. At the 90% progress point, it reviewed a nearly complete draft report. At each stage, the oversight committee provided verbal or written comments and direction. In total, together with PDX, the oversight committee provided over 170 written and verbal comments on the report. The project team attempted to address all of them.

The project team attempted in each case to respond to every question and recommendation it received from the oversight committee. However, NIBS did not task the oversight committee with checking calculations, approving or rejecting the work, or with ensuring that the project team fully and adequately responded to the oversight committee's questions, comments, and suggestions. The study was greatly improved by the committee's comments, questions, and suggestions. However, because the oversight committee was not tasked with final approval, it is not responsible for any errors the project team made.

# Acronyms and Abbreviations

| | |
|---|---|
| α | Slope angle |
| $a_c$ | Critical acceleration |
| ASCE/SEI | American Society of Civil Engineers Structural Engineering Institute |
| ATC-20-1 | A document used to perform post-earthquake safety evaluation of buildings |
| B | Benefit |
| BCA | Benefit-cost analysis |
| BCR | Benefit-cost ratio |
| BI | Business interruption |
| C | Cost |
| CGE | Computable general equilibrium |
| $D_N$ | Slope displacement |
| EAL | Expected annualized loss |
| EUG | Eugene Airport |
| FEMA | Federal Emergency Management Agency |
| g | Acceleration due to gravity, 9.81 meters per second per second |
| Hazus-MH | Hazards US—Multihazard, catastrophe loss estimation software produced by the Federal Emergency Management Agency |
| HIO | Hillsboro Airport |
| IMPLAN | Economic Impact Analysis for Planning |
| IO | Input-output |
| km | Kilometers |
| MSIDM | Multi-sector income distribution matrix |
| $M_w$ | Moment magnitude, a measure of the energy released by an earthquake |
| NIBS | National Institute of Building Sciences |
| OpenSHA | Open-source seismic hazard analysis software, developed by the United States Geological Survey |
| PDX | Portland International Airport |
| PGA | Peak ground acceleration |
| $P_f$ | Probability of slope failure |
| r | Discount rate |
| $r_{Rup}$ | Distance to fault rupture surface |
| SA10 | 5% damped elastic spectral acceleration response at 1-second period |
| SAP | Safety Assessment Program, a product of the California Governor's Office of Emergency Services that standardizes post-disaster building safety evaluation and trains evaluators |
| SRTM | Shuttle Radar Topography Mission |
| t | Project useful life |
| USGS | United States Geological Survey |

# Table of Contents

## Index of Figures

## Index of Tables

# 1. Introduction

## 1.1 BACKGROUND

The Port of Portland (Port) owns and operates Portland International Airport (PDX). The Port is working to improve seismic resilience at PDX. PDX serves the Portland/Vancouver Metro Area and is the only large hub commercial airport in Oregon. Set within an historic floodplain, the soils at PDX are vulnerable to liquefaction in a major earthquake. Without mitigation, PDX's runways could be inoperable for up to one year, which could significantly impair response and recovery.

The Port worked with Oregon State University (OSU) and Geotechnical Resources, Inc (GRI), to complete a 30-percent design and cost estimate for soil remediation that will make 6,000 feet of PDX's south runway seismically resilient, specifically considering earthquakes originating in the Cascadia Subduction Zone. The Port retained the National Institute of Building Sciences (NIBS) to conduct an independent, peer reviewed, quantitative benefit-cost analysis of the remediation effort. This analysis will help the Port to make an informed investment decision. It will build a foundation of credible science to support proactive investment in seismic resilience more broadly.

The present analysis employs many of the methods and data used in NIBS' groundbreaking study, *Natural Hazard Mitigation Saves: 2019 Report*. The report represents the most exhaustive benefit-cost analysis of natural hazard mitigation, from adopting up-to-date building codes and exceeding codes to addressing the retrofit of existing buildings and utility and transportation infrastructure. It was funded by Federal Emergency Management Agency (FEMA), U.S. Department of Housing and Urban Development (HUD). U.S. Economic Development Administration (EDA), International Code Council (ICC), Insurance Institute for Business and Home Safety (IBHS), American Institute of Architects (AIA), and National Fire Protection Association (NFPA). It was led by a multidisciplinary team of world leaders in structural and earthquake engineering, economics, and disaster social science, including some of the same people who performed the present study.

## 1.2 OBJECTIVES

### 1.2.1 Quantify Benefits in Each of Several Categories

This study seeks to quantify the economic benefits of having a seismically resilient runway at PDX. Specifically, the study estimates how a resilient runway saves lives, helps people to return to safe buildings, restores economic activity associated with air travel, reduces future runway damage, and aids in national defense. It estimates all these benefits in human and monetary terms. It presents the value of benefits in present dollars, accounting for probabilities of future earthquakes and the time value of money. It divides the monetary value of benefits by the estimated cost of the runway remediation, producing a benefit-cost ratio, a number that people often use to decide whether an investment is worthwhile. If the benefits exceed the costs, the benefit-cost ratio is greater than 1.0. The higher the benefit-cost ratio, the greater the implied desirability of the investment. This study does not address design or construction approaches and methods.

The avoided future losses comprise the difference between PDX and regional losses with and without a seismically resilient runway. The difference represents the benefit of mitigation. This study estimates the following benefit categories:

*Medical evacuation.* A resilient runway could conceivably reduce life-safety impacts by allowing for emergency medical care to arrive in Portland from outside the Willamette Valley. Medical personnel could treat some injured victims at or near PDX. Other victims could be evacuated to hospitals in California, eastern Oregon, eastern Washington, Idaho, or elsewhere. Medical evacuation directly benefits people throughout the study area, especially those who live or work in highly seismically vulnerable buildings. This study estimates the number of lives saved and the amount of money that the federal government would deem acceptable to spend to avoid those deaths.

*Building safety evaluation*. The Willamette Valley has a large inventory of buildings that will be heavily damaged in a large earthquake. It is necessary to evaluate damaged buildings for safety prior to reoccupying them. After a disaster, agencies managing response use the Safety Assessment Program (SAP) to evaluate building safety. SAP uses certified professional volunteers and agency staff to complete building safety evaluations. There are approximately 180 certified SAP evaluators in the Willamette Valley. Thousands will be needed for several weeks to respond to the earthquakes examined here. Even when that number increases, it will be far too few to quickly inspect buildings and facilitate the return of people to their homes and workplaces. A resilient runway will facilitate the arrival of SAP evaluators from outside the areas affected by the earthquake. Faster building re-occupancy has health and safety benefits, response and recovery administration benefits, and economic benefits. This study estimates the number of buildings that would require safety evaluation, the delay in performing those evaluations, and the economic benefits that result from being able to use safe buildings sooner.

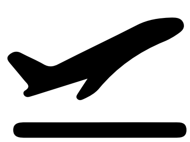

*Reduced business interruption.* Many businesses in the region either directly or indirectly rely on PDX's air operations. A functioning runway will help reduce interruption to businesses throughout the region. A resilient runway would reduce (1) lost revenue to PDX, its tenants, and users; (2) lost revenue to nearby businesses that rely on PDX; and (3) indirect business interruption to businesses that trade with PDX and its nearby businesses. This study estimates the monetary value of increased economic activity from resumption of commercial air travel, as well the monetary benefit to other economic sectors that rely directly or indirectly on PDX.

*Runway repairs.* A resilient runway will suffer less earthquake damage costing less to repair. Other analysts have previously estimated the time required to repair the runway. Their estimates are input into the present analysis of the benefit categories considered here: medical evacuation, building safety evaluation, etc. But lower runway repair costs also represent a benefit not counted in the other categories. Lower runway repair costs primarily benefit PDX. Assuming the earthquake results in a presidential disaster declaration (a likely outcome), the repair costs would eventually be transferred to the federal government through FEMA's Public Assistance program. Thus, reduced runway repair costs benefit all U.S. taxpayers. This study estimates the reduction in runway repair costs.

*National defense.* The Oregon Air National Guard relies on PDX's runway to carry out its mission. Defense benefits are more difficult to quantify rigorously than the foregoing categories. The project team estimates the defense benefit of the resilient runway, but excludes it from the numerator of the benefit-cost ratio calculated here. Defense benefits accrue to the nation.

A resilient runway will provide many other benefits that are not quantified here. See the section 1.3 "Study Limitations" for a discussion of these omitted benefit categories.

### 1.2.2 Study Area

This study estimates the benefits that accrue within a clearly defined geographic boundary called the study area. The study area for this project includes the following ten counties: Clackamas, Columbia, Marion, Multnomah, Polk, Washington, and Yamhill in Oregon, plus Clark, Cowlitz, and Skamania in Washington. See Figure 1-1. Benefits in these counties probably represent most of the benefits that the resilient runway would produce. Benefits could extend geographically much farther, but PDX and the project team selected these study area boundaries to reasonably balance thoroughness with tractability.

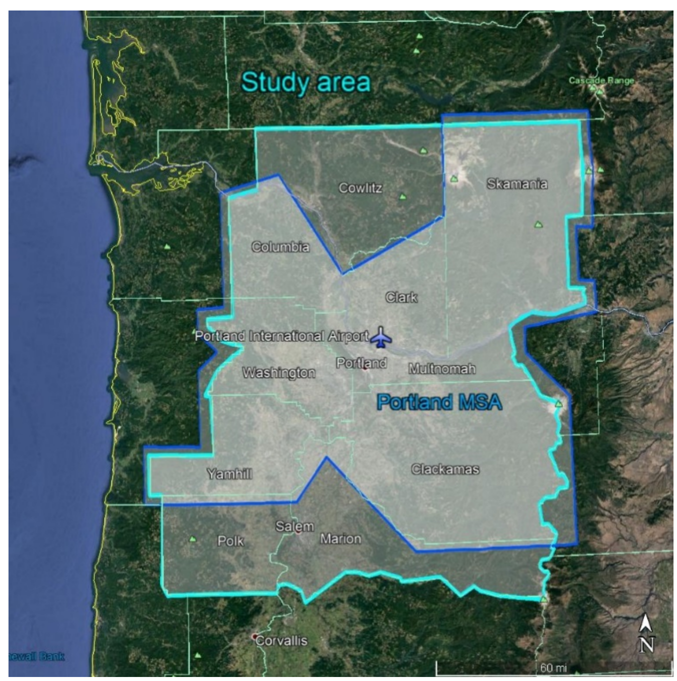


Figure 1-1. Study Area

### 1.2.3 Conform with Natural Hazard Mitigation Saves

The present study aims to conform at least to the state of the practice, not necessarily to advance the field or to equal other similar studies in all respects. It draws, to the extent practical, on methods and data presented in the NIBS study, *Natural Hazard Mitigation Saves*. *Mitigation Saves* represents the most exhaustive, most thoroughly vetted study of the costs and benefits of proactively improving buildings, utilities, and transportation infrastructure to better resist leading natural hazards in the United States, including earthquakes, hurricanes, floods, fires in the wildland-urban interface, and tornadoes. NIBS performed it for three federal agencies and four nonprofit sponsors: FEMA, EDA, HUD, ICC, IBHS, National Fire Protection Association, and AIA.

The present project team also led *Natural Hazard Mitigation Saves*. Like *Natural Hazard Mitigation Saves*, the present study also engaged an independent oversight committee to provide peer review of its assumptions, methods, and findings. Even so, this study expands on *Natural Hazard Mitigation Saves* in several ways. It adds medical evacuation benefits, the benefits of faster building safety evaluation, and defense benefits, and provides new methods to estimate regional access delays associated with landslides and bridge damage. The present study could be used as a template for future similar studies of geographically remote or readily isolated critical infrastructure where these additional benefits apply.

## 1.3 STUDY LIMITATIONS

A resilient runway will produce other benefits that are not quantified here. These likely include some or all the following, and possibly more:

- Provision of trauma care beyond medical evacuation. Earthquakes cause medical needs beyond emergency care for people with life-threatening traumatic injuries. Many people who do not suffer life-threatening injuries will still require hospital care. These people will be triaged yellow—able to wait—and may have to wait days or more for care. A resilient runway will facilitate access by medical professionals and supplies to speed such care.
- Reducing instances of post-traumatic stress disorder and provision of other psychological care. Undoubtedly, the earthquake will frighten many people enough to make them want to leave the Willamette Valley. The earthquake itself will be traumatic and being trapped in the Willamette Valley during what will seem like endless aftershocks will add to the trauma. Likewise, people outside the Willamette Valley will want to come in to support vulnerable or traumatized friends and family. A resilient runway will enable both groups to move quickly and alleviate instances of post-traumatic stress disorder. It will also facilitate access for people providing professional psychological care.
- Reduced environmental impacts. Damaged buildings, utilities, and transportation infrastructure can cause environmental harm. Older buildings contain asbestos and other hazardous materials; earthquakes can damage buildings, thus releasing the hazardous material. Earthquakes damage sewer systems and wastewater treatment plants, potentially releasing untreated wastewater into streets and waterways. Hazardous material spills are

common at industrial facilities strongly shaken by earthquakes. A resilient runway can speed provision of supplies and professionals to address and reduce these harms.

- Reduced cultural impacts. Portland's cultural contribution to the region and the country include music, arts, food, outdoor activities, sports, nightlife, cultural activities among a variety of racial, ethnic, and LGBTQ+ groups, and more. Such activities to some extent involve regional, national, and international exchange: people coming to or visiting away from Portland. A resilient runway will reduce the harm associated with lack of exchange.
- Clearer lessons for the rest of the society. The earthquake will offer reminders and new lessons about society's resilience needs, but only if people can arrive to learn them and people can leave to teach them. Lack of access will cause important lessons to be muted or lost. A resilient runway will reduce that harm.

All these issues have societal value but can only be treated partially or qualitatively. The project will estimate the number of people who need trauma care short of medical evacuation. It will not attempt to quantify the other benefit categories.

The project excludes several other important issues of earthquake damage to PDX. These include:

- Damage and restoration to terminals. Terminal operations rely on safe structures; safety and damage prevention of a variety of architectural elements; the continued operation of mechanical, electrical, and plumbing components; and the provision of resilience measures to allow for continued operation despite damage. The project does not examine these areas.
- Damage and restoration of other pavements. These include taxiways, aircraft and vehicle parking, and hangar paving. The project team assumes that the Port will eventually remediate these to the extent necessary.
- Damage and restoration of utilities and other transportation infrastructure at the airport. These can include potable, cooling, and firefighting water pipelines, reservoirs, and pumping equipment; electrical generation, transmission, and distribution lines, substations, and other equipment; wastewater piping and pumping; fuel storage, pumping, and piping; light rail vehicles, rail, viaduct, stations, and pavements; and probably others. The project team assumes that the port will address the risk to these assets.
- Damage to air traffic control duties. The project does not treat damage and restoration of air traffic control, its structures, architectural elements, mechanical, electrical, and plumbing; radios, radar, towers, and other equipment; or backup equipment and resilience options. Most or all air traffic control can be done temporarily with portable radios and with the assistance of the Seattle Air Route Traffic Control Center.
- Business continuity planning and emergency response, including resilience strategies that can reduce the harm of damage to the runway or other important features of PDX.
- Alternative approaches to runway remediation.

All these issues (and likely many more) matter to the Port of Portland and to the people, culture, and economy of the region, but must remain beyond the practical scope of the present project. The Port is actively working to improve response functions and to build long-term resiliency. It regularly coordinates with local, regional, state, and federal partners and with the private sector to expand resilience.

## 1.4 ORGANIZATION OF THE REPORT

This chapter has introduced the project background, objectives, and listed some important issues that nonetheless must remain outside its scope.

- Chapter 2 summarizes the findings of the study. The chapter summarizes the values exposed to loss, the seismic hazard, the benefits by benefit category, and other considerations such as benefit categories that could not be quantified.
- Chapter 3 reviews the literature that relates to the study. That is, it reviews much of the past pure and applied research on relevant topics: studies that the Port has commissioned on the design of a resilient runway, transit alternatives to PDX, building safety evaluation, hazard, emergency response needs, landslides, hospital capacity, bridge damage, Oregon Air National Guard, future growth, indirect business interruption, equity, aftershocks, and other constraints.
- Chapter 4 presents the methodology employed in the study. Much of the methodology draws on prior applied research, but a few new analytical methods are developed here to account for PDX's unusual features. It presents methods to estimate earthquake shaking, faster building safety evaluation, medical evacuation, defense benefits, aftershock losses, growth, and one or two other topics.
- Chapter 5 presents project data and other analytical details. These include characteristics of the study area, improved commercial air traffic, benefits of faster building safety evaluation, medical evacuation benefits, and defense benefits.
- Chapter 6 lists references cited.

# 2. Findings

This chapter summarizes the study findings. It then quantifies the values exposed to loss, meaning the lives, economic activity, and other functions that a resilient runway affects. It summarizes the seismic hazard that threatens the runway and the region. It describes damage to other Portland infrastructure that matters to the value of resilient runway. It reflects on lessons that the COVID-19 pandemic teaches about community resilience.

## 2.1 BENEFITS AND BENEFIT-COST RATIO

With a resilient runway, the Portland International Airport can help the region respond to and recover from these earthquakes. The airport can return to operation, even if it must rely on temporary structures. Building safety evaluators can fly into the region and begin evaluating buildings within days rather than weeks or more, reducing the time required to get people back into safe buildings. Airport businesses and the nearby businesses that rely on the airport can resume operations faster. Emergency medical resources can be flown in and injured people can be flown out. Fewer runway repairs are required (the parts of the runways that were not remediated). All those savings have value, as summarized in Figure 2-1. The project team estimates the total benefit to be $7.2 billion, excluding national defense. The total estimated cost for a resilient runway is $140 million. The benefit-cost ratio is therefore approximately 50:1.

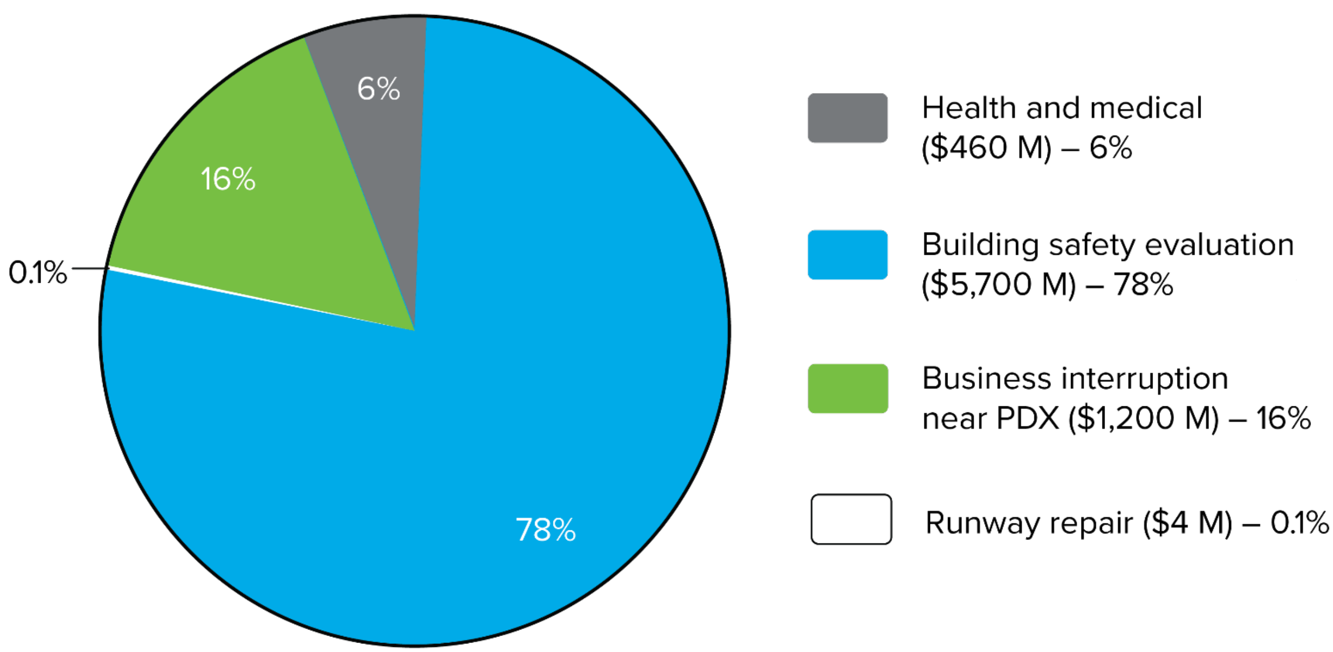


Figure 2-1. Preventing liquefaction under the south runway at PDX would save over $7 billion, counting the four sources shown here (units: $ million)

Figures in the table count benefits over the coming 100 years. A 2.2% real discount rate is applied to the monetary benefits. Business-interruption savings assume that between population growth and increased per-capita productivity, business interruption benefits increase at a rate of 2.9% per year. That is, the business interruption losses increase as the community grows and as people become more productive, so the savings from faster resumption increase at the same rate. Health and medical benefits assume a population growth of 0.9% per year, meaning that in a few years, as the population grows, more people will be injured in a big earthquake, so the benefit of being able to provide medical services increases at the same rate. Runway repair costs are also assumed to remain constant over time, after accounting for inflation.

Table 2-1. Benefits of a resilient runway

| | Benefit ($ millions) | Note |
|---|---|---|
| Health and medical service | $460 | a |
| Faster building safety evaluation | $5,700 | b |
| Reduced business interruption | $1,200 | |
| Reduced runway repair costs | $4 | |
| National defense value | $170 | c |
| Total estimated benefit ($ million) | $7,200 | d |
| Total estimated cost ($ million) | $140 | e |
| Benefit-cost ratio | 50:1 | f |

Some notes on Table 2-1:

(a) Under federal guidelines, it would be acceptable to spend $920 million on a regulation that provides the life savings estimated here. That acceptable cost is used to express a monetary value of safety—the benefit of the safety measure. Here, half of that benefit is attributed to the runway, the other half to the people and systems providing the medical care.

(b) On average, the product of the number of buildings that can be reoccupied, once their safety has been evaluated, and the number of days sooner they can be reoccupied because safety assessment program (SAP) evaluators can arrive sooner via PDX, is 15 million building-days. The number accounts for the number of homes or businesses in each building, the cost for each day the home or business cannot be occupied, the chance that each building will be damaged but re-occupiable once evaluated, and the chance of various size earthquakes.

(c) Defense benefit is provided for information only. It is not included in the total estimated benefit.
(d) Benefits are rounded to two significant figures to reduce the appearance of excessive accuracy, so totals do not match exactly. The total shown here omits national defense value, which is presented for information only.
(e) According to GRI (2020) and the Port.
(f) BCR is rounded to one significant figure to reduce the appearance of excessive accuracy.

*Realism check of the estimated 50:1 benefit-cost ratio*

Several precedents suggest that such a high benefit-cost ratio is unusual but not unique. Multi-Hazard Mitigation Council's (2019) study found that retrofitting weak and flexible ground stories in wood-framed apartment buildings (Figure 3A) exceeds $50 per $1 spent in some locations. It also found that securing residential water heaters to the building frame (Figure 3B) can save over $50 per $1 spent. Multi-Hazard Mitigation Council's (2005) study found that placing an electrical transmission line in Minnesota underground saved $40 per $1 spent (Figure 3C). The later study found that adding a berm to a North Carolina water treatment plant saved $30 per $1 spent (Figure 3D). The last 30 years of building-code development saves up to $32 per $1 added to construction cost, in the highest hazard areas of the United States (Figure 3E). It seems perfectly plausible that improving air access to a region that can be isolated by landslide and bridge damage could produce similarly high benefit-cost ratios. PDX is a key regional asset. Making it resilient produces predictably dramatic benefits. Portland's resilient runway benefits 600,000 homes and businesses with one retrofit. Some of its benefits grow with population and per capita productivity. Its benefits will be experienced for longer than most other mitigation measures. The runway represents a weak, single point of failure in the transportation chain, so fixing it should be enormously beneficial. For all these reasons, the 50:1 figure estimated here seems realistic.

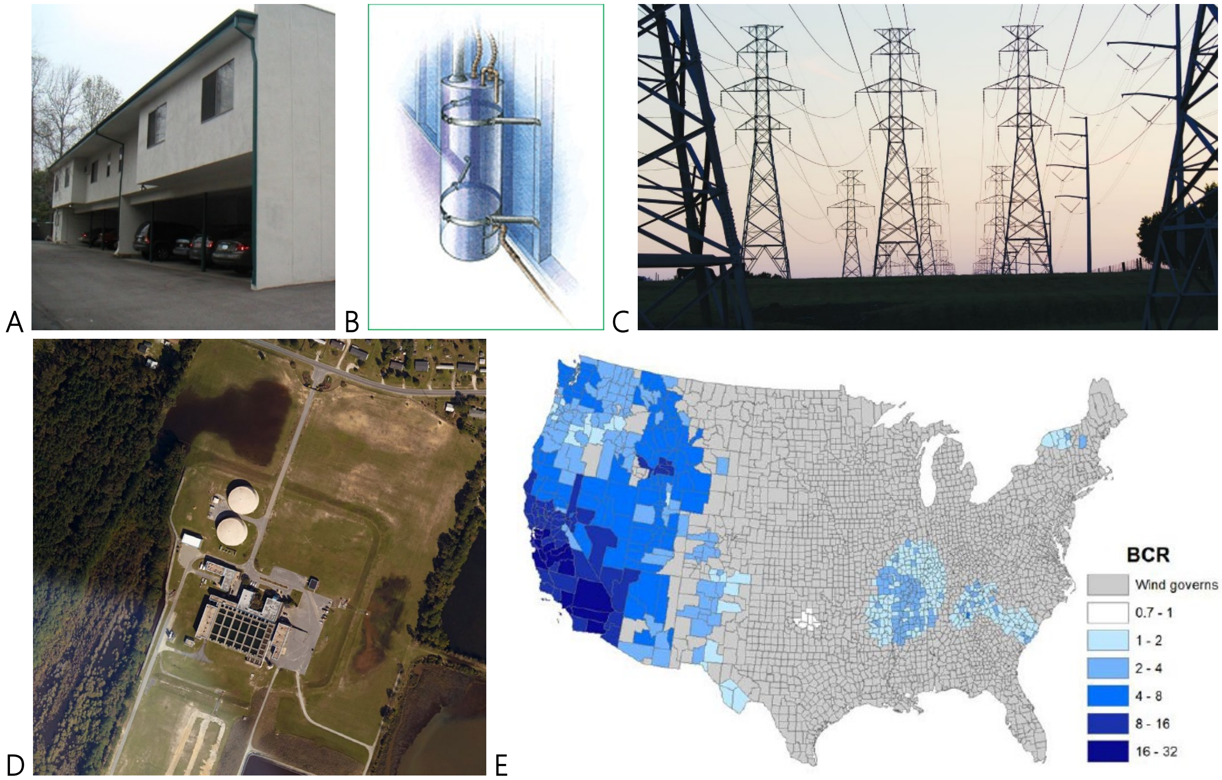


Figure 2-2. Five high-BCR mitigation measures that save at least $30 per $1 spent, some over 50:1: (A) soft-story retrofit, (B) securing residential water heaters to the building frame, (C) undergrounding high-voltage transmission lines, (D) adding a berm to protect a water treatment plant, and (E) building-code development since 1990.

If anything, the estimated benefit-cost ratio is probably low. Throughout this project, when the estimate of benefit-cost ratio relied on uncertain inputs, the project team generally selected best-estimate values of those inputs. However, when the quantities were highly uncertain, the project team attempted to select values that would produce lower estimated benefit-cost ratios rather than higher ones. Notable examples of choices that tended to reduce benefit-cost ratios include:

1. Exclude benefit associated with national defense from the total benefit-cost ratio. The estimated defense benefits are presented separately and are not included in the overall BCR. The reason for omitting defense benefit is that the project team found it too challenging to estimate the chances that aircraft from the 142nd Wing could be transported to other airports and operate out of them. The aircraft need 220 meters of runway to take off, but the project team could not estimate the chance that the damaged runway would have an undamaged stretch 220 meters long.
2. Ignore the possibility of multiple simultaneous disasters, such as an earthquake occurring at the same time as a pandemic that was already taxing hospital resources. Had the project team accounted for this possibility, the estimated benefit-cost ratio would have been somewhat higher.

## 2.2 VALUES EXPOSED TO LOSS

Earthquakes of magnitudes up to 9.3 will inevitably occur on the Cascadia Subduction Zone near Portland, and could occur any day. The Portland International Airport will play several crucial roles in helping the region respond to and recover from those earthquakes. Thousands of volunteer building professionals—engineers, architects, and others—will arrive through the airport to evaluate the safety of the region's building stock of approximately 1.1 million buildings. Industries in the study area generate $200 billion annually. Many of these rely on the airport. The airport acts as a hub for emergency medical resources and medical evacuations for injuries among the region's 2.9 million people. The airport must be functional to provide that value. Runway liquefaction will render the airport nonfunctional for up to 10 months unless the soil beneath the runway is remediated.

Many of the region's 1.1 million buildings will need safety evaluation by volunteer building professionals arriving through PDX from California and elsewhere.

$200 billion in gross domestic product relies to some extent on commercial aviation through Portland International Airport.

2.9 million people live in the study area, which on average has fewer than 400 vacant ICU and emergency department beds. PDX will serve as a hub for emergency medical resources and medical evacuations.

The 142nd Fighter Wing of the Oregon Air National Guard relies on PDX's runway to fulfill its national defense mission.

Figure 2-3. The Portland International Airport will provide crucial value to the region after a great earthquake on the Cascadia Subduction Zone

# 2.3 SEISMIC HAZARD

## 2.3.1 Seismic Sources

*The Ring of Fire.* Portland lies near the so-called Ring of Fire: the boundary of the Pacific Tectonic Plate characterized by volcanoes and large earthquakes (Figure 2-4). Earthquakes larger than magnitude 9 occur on it. The US Geological Survey estimated the March 11, 2011 Tohoku earthquake to have magnitude $M_w$ 9.0 to 9.1. The February 27, 2010 Chile earthquake measured $M_w$ 8.8. The May 22, 1960 Great Chilean earthquake measured $M_w$ 9.4 to 9.6. On January 26, 1700, the Cascadia Subduction Zone, near Oregon and Washington, ruptured to produce an earthquake with an estimated magnitude of $M_W$ 8.7 to 9.2. A repeat of such an earthquake is inevitable, and, as far as is currently known, could happen at any time.

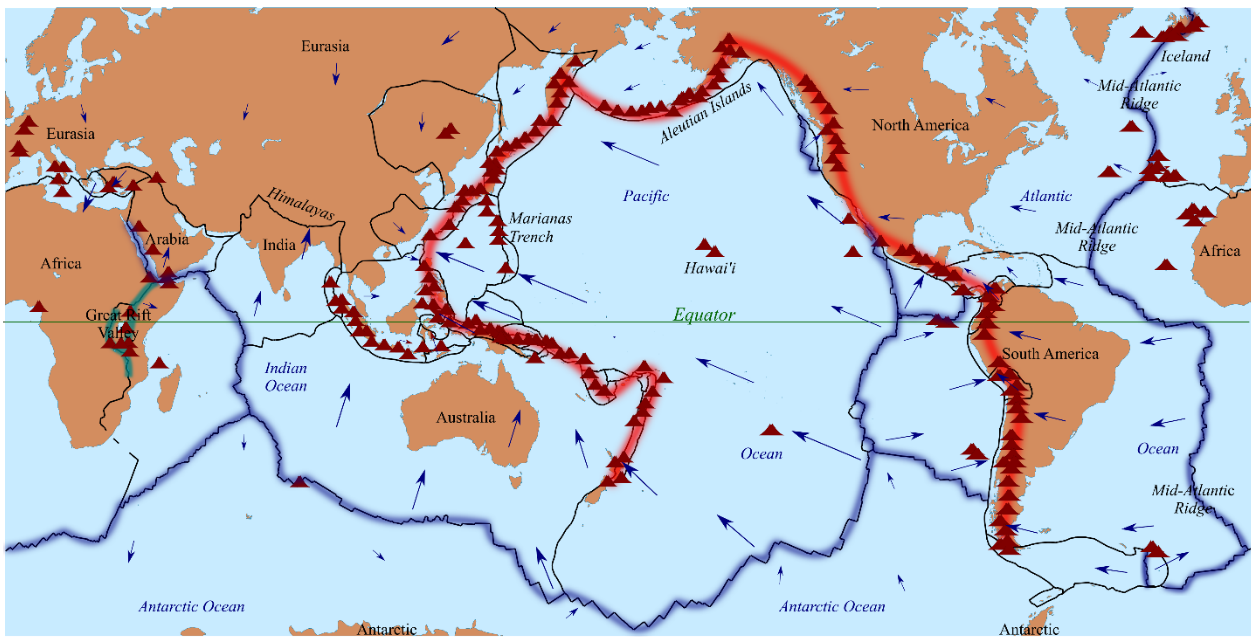


Figure 2-4. The boundary of the Pacific Tectonic Plate is often called the Ring of Fire (CCSA4.0)

*The Cascadia Subduction Zone is a portion of the Ring of Fire.* Figure 2-5 illustrates how the Cascadia Subduction Zone produces earthquakes. It lies off the Oregon coast and dips shallowly beneath North America. The interface between the two plates is locked by friction. Eventually, pressure from the mantle (orange, with black arrows) overcomes friction and the boundary between the two plates suddenly slips, producing an earthquake. Because of the large interface area that can suddenly slip, and because of how far it can slip, Cascadia Subduction Zone earthquakes are larger than any other expected in the Continental United States. It can produce earthquakes as large as $M_W$ 9.34, although smaller earthquakes are also possible. Figure 2-5 shows the Cascadia Subduction Zone's spatial extent. Other, closer earthquake faults (such as the crustal earthquakes illustrated in Figure 2-4) also threaten Portland, but a process called hazard deaggregation indicates that the Cascadia Subduction Zone dominates the region's seismic hazard.

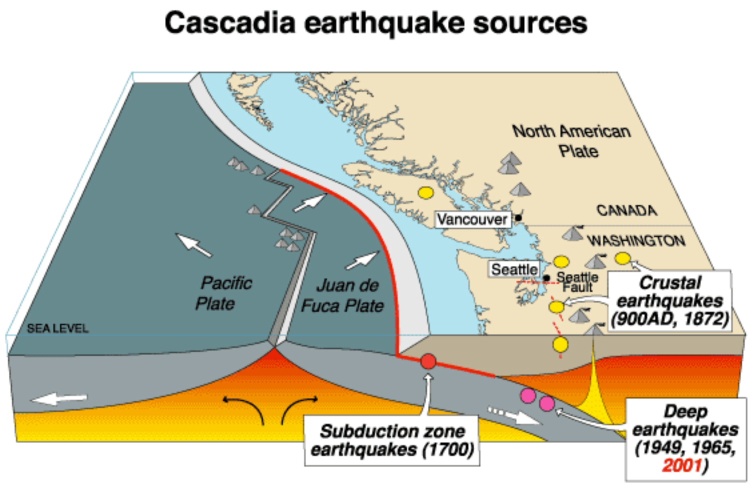


| | Source | Affected area | Max. Size | Recurrence |
|---|---|---|---|---|
| ● (red) | Subduction Zone | W.WA, OR, CA | M 9 | 500-600 yr |
| ● (pink) | Deep Juan de Fuca plate | W.WA, OR, | M 7+ | 30-50 yr |
| ● (yellow) | Crustal faults | WA, OR, CA | M 7+ | Hundreds of yr? |

Figure 2-5. The Cascadia Subduction Zone is a region where the Juan de Fuca Plate dips under North America. (Public domain image)

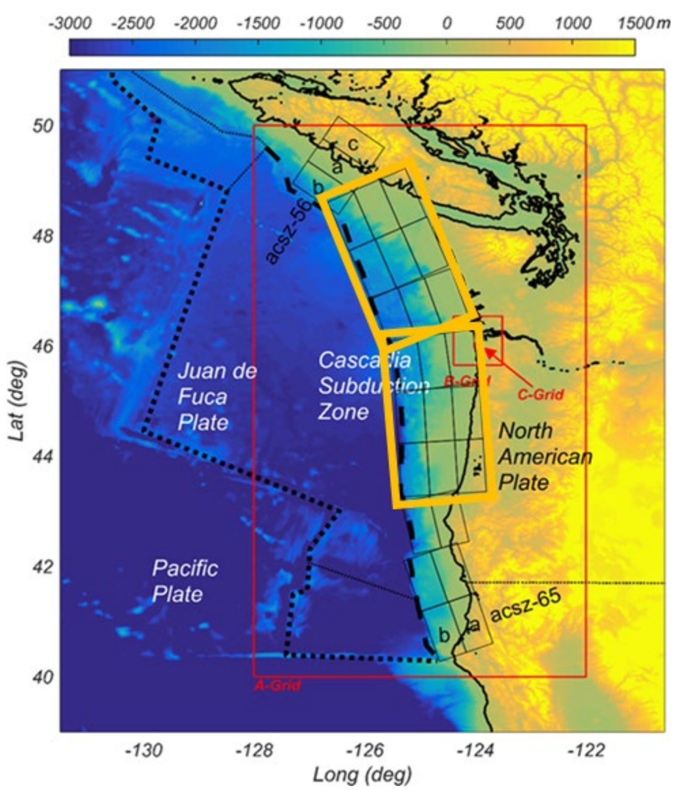


Figure 2-6. Location of the Cascadia Subduction Zone (after Park et al. 2017)

*Only a portion of the Cascadia Subduction Zone is treated here.* For practical purposes having to do with the software used to calculate shaking (OpenSHA, by USGS seismologist Edward Field and colleagues), the present analysis estimates shaking from a rupture of the sections of the fault between about 43 degrees north latitude and about 49 degrees north latitude: the two large central parts highlighted with gold rectangles in Figure 2-6.

Other portions of the fault can (and will) rupture. But the shaking calculated in the study area uses mathematical relationships called attenuation relationships or ground-motion-prediction equations that depend on earthquake magnitude and the closest distance to the fault (among other factors). The rupture of other portions of the fault that are farther away (the parts not highlighted in Figure 2-6), were not addressed by this study. The calculated shaking in the Willamette Valley would not be different if the other portions of the fault were included because they are farther away from the Willamette Valley. See Section 5.3.2 for further detail explaining the choice of rupture area and why the choice made here is conservative, and in the end makes no difference to the estimated results.

### 2.3.2 Seismic Hazard Deaggregation

Table 2-3 summarizes the most likely source of strong shaking at the airport with five commonly considered occurrence probabilities in the coming 50 years according to the US Geological Survey's most recent national seismic hazard maps. The column labeled "probability" indicates the US Geological Survey's estimate of the chance that shaking shown in the column labeled PGA will occur in the next 50 years. That level of shaking will most likely be caused by an earthquake whose magnitude is shown in the column labeled Mw. For example, consider the row labeled earthquake 3. The USGS estimates a 10% probability that an earthquake producing PGA of 0.25g or more will occur in the next 50 years. It will most likely be caused by an earthquake of magnitude Mw 9.12.The scenarios are more subtly defined than that: such an earthquake could produce higher or lower levels of shaking depending on a how quickly the seismic stresses drop during the earthquake, and other features.

The column labeled "percentile" refers to a measure of the shaking probability given the occurrence of that magnitude earthquake. In earthquake 3, the USGS estimates a 66% probability that shaking would be no greater than 0.25g at PDX (the column labeled PGA), given the $M_W$ 9.12 earthquake. The table also measures occurrence probabilities a different way: each earthquake has an associated mean recurrence interval (MRI), meaning the average number of years between earthquakes of the given magnitude and percentile. However, earthquakes are not like clocks; the mean recurrence interval is merely an average. The actual number of years between earthquakes can be much shorter or longer than the average.

The table shows for example that as likely as not (50% probability), an earthquake will occur near Portland causing peak ground acceleration of at least 0.07 g. It will most likely be caused by an Mw 8.7 earthquake on the Cascadia Subduction Zone. Though it is the smallest considered here, an $M_W$ 8.70 earthquake is very large, releasing 16 times the energy of the 1906 San Francisco earthquake. The $11^{th}$ percentile of motion in that earthquake is 0.07 g of peak ground acceleration at PDX. We cannot predict when those earthquakes will occur, but they will inevitably occur, and could happen any day.

Table 2-2. Five scenario earthquakes most likely to cause the peak ground acceleration (PGA) at PDX

| Earthquake | Probability | MRI (years) | PGA (g) | $M_w$ | Percentile |
|---|---|---|---|---|---|
| 1 | 50% | 72 | 0.07 | 8.70 | 11% |
| 2 | 20% | 225 | 0.16 | 9.12 | 39% |
| 3 | 10% | 475 | 0.25 | 9.12 | 66% |
| 4 | 5% | 975 | 0.35 | 9.34 | 39% |
| 5 | 2% | 2,475 | 0.51 | 9.34 | 63% |

### 2.3.3 Estimated Regional Ground Motion

Figure 2-7 shows maps of the ground motion in each of five scenario earthquakes. Each map shows one simulation of peak ground acceleration in a scenario earthquake. "One simulation" refers to the fact that, even knowing the fault rupture location and magnitude, ground motion is uncertain. It is usually higher or lower than the median (the 50th percentile) at any given location. Two nearby locations tend to both have greater or smaller shaking than the expected value; they are said to be spatially correlated. The farther apart, the less correlation. Real earthquake ground-motion maps therefore tend to look blotchy like the ones shown here, rather than smoothly varying with distance from the fault. The present study simulated 20 versions (simulations) of each earthquake, calculated losses in each simulation, and averaged over the simulations. The average loss tends to be greater than what one would calculate from a map of median shaking. The reason for this greater average loss is that a little lower-than-median shaking can produce a little less loss, but a little higher-than-median shaking can produce much higher loss, and the differences do not cancel out. This is important: an entity that manages its earthquake risk based on median shaking will tend to be underprepared for that earthquake.

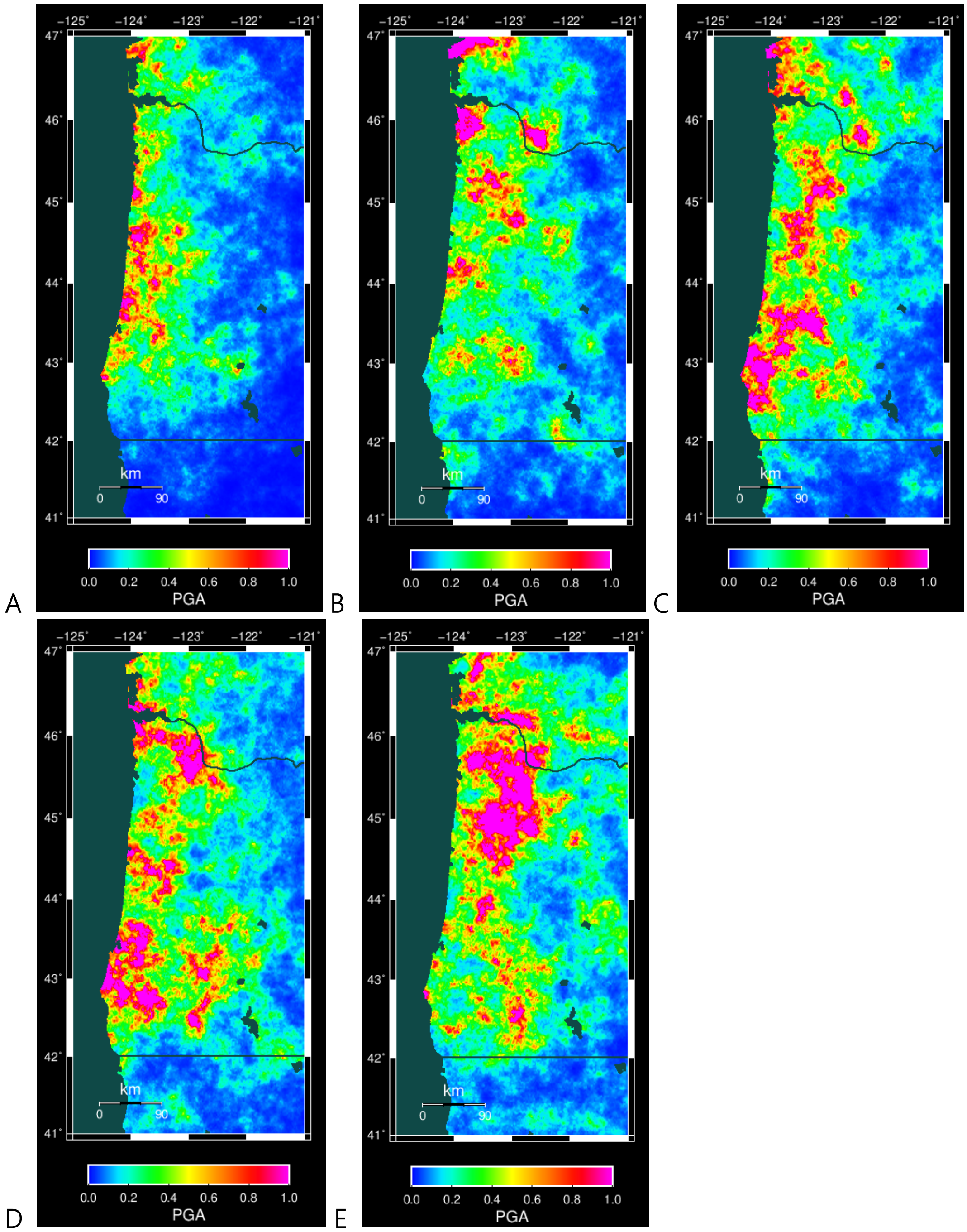


Figure 2-7. One each of 20 simulations of CSZ earthquake A) $M_W$ 8.7, 11th percentile; B) $M_W$ 9.12, 39th percentile, C) $M_W$ 9.12, 66th percentile, D) $M_W$ 9.34, 39th percentile, and 5) $M_W$ 9.34, 63rd percentile

## 2.4 LANDSLIDES AND BRIDGE DAMAGE

The earthquakes and ground shaking illustrated in Figure 2-7 will damage the PDX runway, but they will also damage other infrastructure that affects the value of a resilient runway. First, they damage alternative routes into the Willamette Valley. The more damage to these routes, the more the region needs a functioning runway at PDX.

The earthquakes will damage highway bridges along routes into and through the Willamette Valley. The earthquakes also cause dozens of landslides in dry months, potentially hundreds during the eight months of the year that hills tend to be saturated (Figure 2-8). Table 2-4 shows the average time before the fastest route into the Willamette Valley is fully restored: six days for earthquake 1 in the dry season, up to 81 days for earthquake 5 in the wet season. The fastest route is generally along US-26 from the Redmond Airport. Limited traffic would begin to get through in about half the time shown (three days for earthquake 1 in the dry season to 40 days in earthquake 5 in the wet season).


Figure 2-8. Earthquakes cause landslides and bridge damage, hindering access by road to the Willamette Valley

Table 2-3. Travel delay to clear landslides and repair bridges

| Earthquake | Probability | MRI, years | Delay Jun-Sept (days) | Delay Oct-May (days) |
|---|---|---|---|---|
| 1 | 50% | 72 | 6 | 21 |
| 2 | 20% | 225 | 16 | 66 |
| 3 | 10% | 475 | 20 | 70 |
| 4 | 5% | 975 | 23 | 78 |
| 5 | 2% | 2,475 | 28 | 81 |

## 2.5 BUILDING DAMAGE AND SAFETY EVALUATION DELAYS

The earthquakes would also damage many older, vulnerable buildings. Most can be reoccupied once their safety is evaluated. These re-occupiable buildings have some damage, but remain structurally sound. For example, a building might have stucco cracks at the corners of windows and doors, but remain safe to occupy (Figure 2-9A). Another building might have parapet damage that makes it unsafe to use a door below the parapet, but, if other entrances are safe, the building can still be occupied (Figure 2-9B). In either case, the sooner the building's safety can be evaluated, the sooner the occupants can return. However, volunteer engineers and architects must travel to the Willamette Valley before they can evaluate ("tag") the buildings. Without a resilient runway, the landslides and bridge damage would add to the time required to evaluate the buildings. Table 2-5 shows how long that would take under current conditions (the columns labeled "as-is") and with a resilient runway (the columns labeled "resilient runway"). The column labeled "evaluated buildings" shows an estimate of the number of buildings that would require safety evaluation. The column labeled "re-occupiable buildings" shows an estimate of the number of buildings that could be re-occupied once they are evaluated.

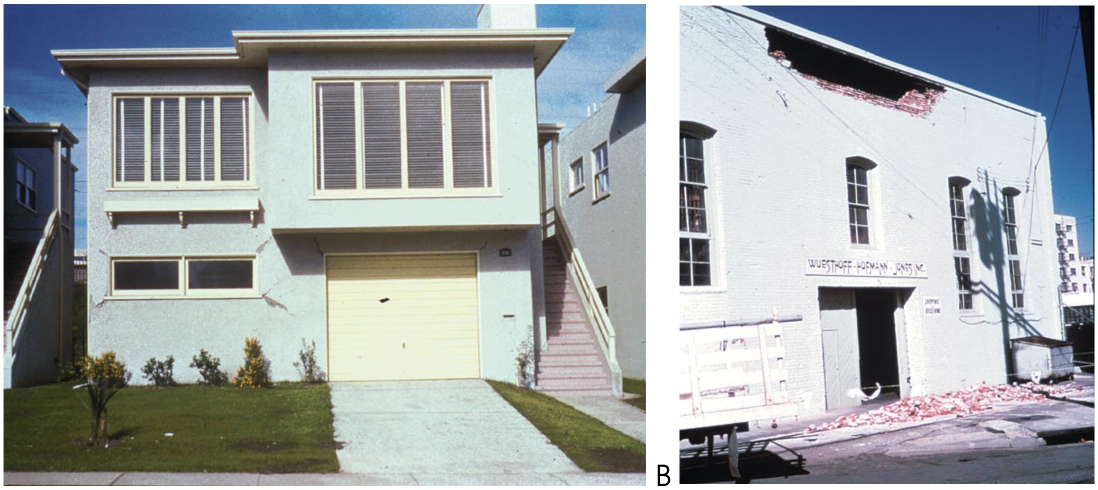


Figure 2-9. Many damaged buildings can be safely occupied. (A) A wood-frame dwelling with cracked stucco at door and window corners would probably be evaluated green, "inspected." (B) An unreinforced masonry warehouse with parapet damage over one of several entrances could nonetheless be used if the entrance beneath the damaged parapet were not used. (Images: public domain)

Table 2-4. Days after the earthquake that safety evaluators finish building safety evaluation, without a resilient runway.

| Earthquake | Evaluated buildings | Re-occupiable buildings | Time to complete evaluations, days | | | |
|---|---|---|---|---|---|---|
| | | | June-Sept | | Oct-May | |
| | | | As-is | Resilient runway | As-is | Resilient runway |
| 1 | 410,000 | 340,000 | 33 | 27 | 48 | 27 |
| 2 | 700,000 | 550,000 | 60 | 44 | 110 | 44 |
| 3 | 750,000 | 580,000 | 67 | 47 | 120 | 47 |
| 4 | 810,000 | 600,000 | 73 | 50 | 120 | 50 |
| 5 | 850,000 | 610,000 | 76 | 52 | 130 | 52 |

## 2.6 MEDICAL IMPACTS

The earthquakes also cause thousands of injuries, some minor, some severe, some fatal. On average, hospital intensive care units and emergency departments have about 30% more capacity than is used at any given time. A large earthquake could cause many injuries that overwhelm the hospitals, greatly exceeding their residual capacity. Daytime earthquakes would cause more injuries than nighttime earthquakes because workplace buildings tend to be more prone to life-threatening damage and collapse than are dwellings. School takes place during the day as well. The number of injuries depends on the earthquake time of day: Table 2-6 summarizes the number of severe injuries over and above hospital capacity. These are the average number of lives saved if they can be treated almost immediately in another hospital.

Table 2-5. Average number of life-threatening injuries over the capacity of regional hospitals

| Earthquake | Probability | MRI, years | Daytime earthquake | Nighttime earthquake | Commute earthquake |
|---|---|---|---|---|---|
| 1 | 50% | 72 | 63 | 0 | 28 |
| 2 | 20% | 225 | 270 | 14 | 160 |
| 3 | 10% | 475 | 320 | 22 | 200 |
| 4 | 5% | 975 | 400 | 35 | 240 |
| 5 | 2% | 2,475 | 470 | 44 | 280 |

## 2.7 THE PANDEMIC AND OTHER CONSIDERATIONS

The 1918 flu took two years to pass, during which time hospitals were overtaxed. COVID-19 shows that the 1918 flu was not unique. It too could absorb hospital resources for two years. If a severe earthquake occurred during a similar pandemic, fewer hospital resources could be available to treat earthquake injuries. The same number of earthquake injuries would occur, which would make a resilient runway more valuable. Conceivably, one could estimate the chance that hospitals were already inundated with pandemic patients, estimate the lower local resources, the greater benefits of a resilient runway, and a weighted average benefit accounting for the chances of an earthquake happening during a pandemic and happening during non-pandemic times. The project team elected not to make such an estimate, which would probably raise the estimated benefits only slightly.

More fundamentally, the pandemic shows that the nation cannot put off solving its natural-hazard problems indefinitely just because they are costly or complicated. Failure to address our problems merely makes them harder to solve. More people needlessly suffer, the economy is more thoroughly impaired, and the divide between the fortunate few and the rest of the people is greater. We will pay for natural disasters one way or another, either by the penny to prevent them when we can most afford it, or the pound to bear them when we can least afford it.

# 3. Literature Review

To the extent practical, the project team draws on the literature reviewed in *Natural Hazard Mitigation Saves* (Multi-Hazard Mitigation Council 2019). This chapter briefly summarizes additional relevant prior works on benefit-cost analysis of airport remediation, scenario loss estimation, and selected relevant topic areas. The literature review shares information on the current state of practice, identifies some knowledge gaps, and provides a basis for the methodology used in this analysis. The literature review sometimes offers competing approaches to estimate benefits and describes their advantages and disadvantages. The choices of which method to use are offered later in chapter 4.

## 3.1 PROBABILISTIC SEISMIC HAZARD ANALYSIS

To estimate the benefits of a resilient runway, the project team will have to estimate landslides that could isolate the Willamette Valley and damage buildings in the metropolitan area. To do so will require characterizing the regional seismic hazard. Methods to characterize probabilistic seismic hazard are discussed in *Natural Hazard Mitigation Saves* (Multi-Hazard Mitigation Council 2019). The present project requires additional hazard calculations, especially disaggregation of seismic hazard at several mean recurrence intervals, calculation of median regional ground motion in each of the same mean recurrence intervals used by HNTB Corporation (2015), and treatment of ground-motion uncertainty, including spatial correlation.

The US Geological Survey provides by far the most authoritative resource for disaggregating seismic hazard, a web page called the Unified Hazard Tool (US Geological Survey ND). With it, one can calculate magnitude and location of ruptures most likely to cause shaking with specified mean exceedance frequencies. It does not create maps of ground motion in those events. Note that as of this writing, the tool reflects hazard as calculated in 2014, before the development of several recent ground-motion-prediction equations for megathrust earthquakes. These ground-motion-prediction equations draw on data from the 2011 Tohoku earthquake. Four such ground-motion-prediction equations are Abrahamson et al. (2018), Zhao et al. (2016), Parker et al. (2020a), and Kuehn et al. (2020).

It seems likely that the Cascadia Subduction Zone will dominate the seismic hazard of interest here. Park et al. (2017) provide a convenient recent recap of some important attributes of the Cascadia Subduction Zone.

Figure 2-6 shows the fault geometry that Park et al. (2017) used. The heavy dashed line along the zone's western edge indicates the fault trace, where the fault intersects the surface of the ocean floor. The subduction zone dips into the earth at about an 11-degree angle.

Four obvious choices present themselves for creation of ground-motion maps.

1. The US Geological Survey and Southern California Earthquake Center provide a state-of-the-art suite of seismic hazard tools called OpenSHA (first introduced by Field et al. 2003), including a

ShakeMap calculator that allows one to specify an earthquake rupture surface, magnitude, ground-motion intensity measure, ground-motion-prediction equation, and other important parameters, as well as calculate ground motion with specified nonexceedance probability. It does not treat spatial variability in ground motion.

2. Hazus-MH represents a second option, but, because of its age, uses outdated ground-motion-prediction equations. It too depicts median motion, which is smaller than average ground motion, and fails to account for spatial variation in ground motion. As a result, using Hazus-MH might significantly underestimate damage.
3. A third option would be to perform hand calculations of ground motion using one of the more recent ground-motion-prediction equations intended for megathrust earthquakes. For example, GRI (2020) calculated weighted average ground motions for PDX by using four such equations: Abrahamson et al. (2018), Zhao et al. (2016), Parker et al. (2020a), and Kuehn et al. (2020). Results are shown in Table 3-1. The table reflects GRI's estimate of ground motion in an $M_W$ 9.0 earthquake on the Cascadia Subduction Zone, assuming soil with 640 m/sec average shearwave velocity in the upper 30 meters of soil, near the boundary of ASCE/SEI (2016) site classes B and C. The estimates also reflect shaking with 84% nonexceedance probability, that is, mean plus one standard deviation motion.
4. Fourth, one could use USGS's scenario ShakeMaps (https://earthquake.usgs.gov/scenarios/), but the USGS does not provide enough of these to characterize hazard at specified exceedance frequencies.

Table 3-1. GRI (2020) weighted average ground motions for an $M_W$ 9.0 earthquake on the Cascadia Subduction Zone (mean plus one standard deviation)

| Ground-motion-prediction equation | Weight |
|---|---|
| BCHydro18 (Abrahamson et al. 2018) | 50% |
| Zhao16 (Zhao et al. 2016) | 20% |
| PSHAB20 (Parker et al. 2020a) | 20% |
| KBCG20 (Kuehn et al. 2020) | 10% |
| GRI (2020) weighted average ground motions assuming soil with 640 m/sec average shearwave velocity in the upper 30 meters of soil, near the boundary of ASCE/SEI (2016) site classes B and C | |
| PGA, g | 0.40 g |
| $S_A$(1.0 sec, 5%), g | 0.33 g |

To treat ground-motion uncertainty, one must start with an attribute of spatial correlation called *range*, which measures the width of the blotches in a ground-motion map. Jayaram and Baker (2009) provide a highly regarded treatment of range. One must then simulate a spatially correlated random field of standard normal distributions (a familiar bell-shaped curve with mean value of zero and standard deviation of 1.0). Many authors have written about how to simulate such a field, e.g., using a

method called kriging, as described by Vanmarcke and Fenton (1991). Porter (2020) section 6.4.3 offers a technique to simulate properly spatially correlated random ground-motion fields from a map of median motion and a suite of maps of properly spatially correlated standard normal random variates.

## 3.2 RESILIENT RUNWAY COST, DOWNTIME, AND REPAIR

HNTB Corporation (2015) estimated the damage, repair cost, and repair duration of the PDX north and south runways, with and without mitigation, under each of five scenario levels of ground motion. The project team can use these values, repeated in Table 3-2. HNTB Corporation (2015, p. ES7) considers remediating the south runway with stone columns at a cost of approximately $67 million, or $137 million for jet grouting (p. 50). The south runway has a lower risk of lateral spreading than the north runway.

In September 2020, PDX and its consultant GRI (2020) neared completion of the 30% design of the runway retrofit. They anticipate moving forward with remediation of 6,000 feet of the south runway (out of about 11,800 ft) to 60-foot depth, based on the outcomes of Oregon State University's blast testing analysis. GRI (2020) estimates that the remediated 6,000-ft portion of the south runway will be operational after an $M_W$ 9.0 earthquake at the median plus one standard deviation level of ground motion. It seems reasonable to interpret the design objective to mean that the remediated portion of the runway will be functional immediately after any of the scenario earthquake considered here. For that reason, half of HNTB's repair costs for the with-mitigation case are shown in Table 3-2 (reflecting the unremediated half of the south runway) and its downtime duration estimates are taken as zero.

The total estimated cost of the preferred option is $140 million. Table 3-3 presents the design estimate. The runway remediation will not prevent damage to the unremediated western portion of the south runway (about 5,800 ft of its 11,800 ft length), so repair costs under the remediated conditions can be taken as half the costs under as-is conditions. Federal Highway Administration's (2013) manual on deep soil mixing makes no mention of maintenance requirements for a foundation that has been subjected to deep soil mixing.

Table 3-2. Post-earthquake runway repair cost and repair duration

| Mean recurrence interval (years) | Repairs (% of runway) | | Repair cost ($ million) | | Downtime (months) | |
|---|---|---|---|---|---|---|
| | Without mitigation | With mitigation | Without mitigation | With mitigation | Without mitigation | With mitigation |
| 72 | <1% | None | $0.3 | $0.15 | 0.75 | 0.001 |
| 225 | 10% | None | $7.7 | $3.85 | 3 | 0.001 |
| 475 | 25% | None | $19 | $9.50 | 7 | 0.001 |
| 975 | 50% | None | $38 | $19 | 10 | 0.001 |
| 2,475 | ≥75% | <1% | $77 | $38 | 10 | 0.001 |

Table 3-3. Runway mitigation 30% design estimate

Runway Seismic Mitigation 30% Design Estimate

**Vertical Mitigation**

| | | | | | | | |
|---|---|---|---|---|---|---|---|
| Mitigation Length | 6000 | ft | Full Depth | 100 | ft | 4,890,000 | $yd^3$ |
| Mitigation Width | 220 | ft | Partial Depth | 60 | ft | 2,930,000 | $yd^3$ |
| Area | 1320000 | $ft^2$ | | | | | |
| Replacement Ratio | 20% | | | | | | |

| Unit Costs: | $/$yd^3$ | Partial Depth | Full Depth |
|---|---|---|---|
| DSM | 120 | $71,000,000 | $118,000,000 |
| Mob/Demob | 6% | $4,000,000 | $4,000,000 |
| Total | | $75,000,000 | $122,000,000 |

**Pavements**

Construction Costs

| | Hard Costs | Contingency | Soft Costs | Contingency |
|---|---|---|---|---|
| PCC Pavement | $36,997,000 | $7,399,000 | $16,057,000 | $4,014,000 |

**TOTAL PROJECT COST**

| PARTIAL DEPTH | Total Project SOUTH Runway |
|---|---|
| PCC Pavement | $140,000,000 |

| FULL DEPTH | Total Project SOUTH Runway |
|---|---|
| PCC Pavement | $187,000,000 |

## 3.3 QUANTIFYING MEDICAL EVACUATION NEEDS

The greater the need for emergency responders to be able to reach the Willamette Valley by air, the greater the benefit of a resilient runway. NIBS and FEMA (2012) offers a model of the deaths and nonfatal injuries resulting from building damage. Porter (2009a, b) shows how one can model deaths and nonfatal injuries in damaged buildings outside of Hazus.

A notable issue with which Hazus does not deal, but the present project must consider: what happens when too many people are injured and need urgent medical care, but local hospitals are overextended? Hazus categorizes injuries in 4 severity levels. Severity-4 injuries are fatal. What about the others? Severity-1 injuries are too severe for self-treatment but can be treated by paraprofessionals outside of a hospital. Severity-2 injuries require "a greater degree of medical care and use of medical technology such as x-rays or surgery, but not expected to progress to a life threatening status." Severity-3 injuries pose an immediate threat to life safety "if not treated adequately and expeditiously," in a hospital.

What does "expeditiously" mean? Can the injured survive long enough to be transported to the airport and thence to a hospital outside the region? NIBS and FEMA (2012) do not say. Paul et al. (2006) report that they interviewed "hospital staff" to establish "survivability times," which they define as "the maximum allowable time before the patient is treated to avoid fatality." They do not offer any detail of the nature of the interviews: what they asked, whom they asked, or how they checked the answers. They report survivability times for severity 1: 390 minutes; severity 2: 270 minutes; severity 3: 80 minutes. Their severity scale seems to mimic that of Hazus—an impression reinforced by their later work (Paul and Hariharan 2012, Paul and MacDonald 2016)—but it is hard to reconcile their figures with Hazus's definitions. Neither severity-1 nor severity-2 injuries are supposed to represent a risk of death, suggesting that either the hospital staff provided poor estimates of survivability time for Hazus injury severities, or the authors' injury severity scale differs substantially from Hazus. In either case, it seems difficult to associate the authors' severity-3 survivability time with the Hazus injury severity 3, especially considering their silence as to interview method, sample size, respondent credentials, or validation.

Later authors reiterate or appear implicitly to adopt Paul et al.'s (2006) survivability times without offering any greater defense or additional study, e.g., Cimellaro et al. (2010), Kaptan (2014), Golshani and Kashani (2018).

Some works in a notable book on human casualties in earthquakes (Spence et al. 2011) deal with morbidity and the urgency of extricating trapped occupants, but do not distinguish the initial injury level of the victims or between initial injuries and deaths associated with delayed treatment, dehydration, or exposure. Within those works, only Ferreira et al. (2011) appear to offer time series about number of fatalities versus the passage of time after an earthquake, but their definitions and methods are too vague to determine whether the time series reflect when people died, when the dead were discovered, or when death certificates were signed.

The project team also sought evidence of mortality resulting from delayed medical care in other contexts: 13% more heart-attack fatalities associated with a 4.4-minute average ambulance delay in communities with a marathon (Jena et al. 2017),

## 3.4 BENEFITS OF FASTER BUILDING SAFETY EVALUATION

A resilient runway can speed access by safety assessment program (SAP) evaluators from outside the Willamette Valley, people whose presence could help to reopen buildings throughout the Willamette Valley (not just PDX) more quickly.

People commonly refer to SAP evaluation as tagging, a reference to the red, yellow, or green placard ("tag") that safety evaluators affix to damaged buildings after earthquakes and other natural disasters to indicate whether the building appears to be safe enough to enter and occupy. The placards are generally affixed under the authority of the local building official and have legal force. A red placard is labeled "unsafe" and legally prohibits entry and occupancy of the building without written authorization by the jurisdiction with authority over the building. A yellow placard is labeled "restricted use," and limits entry and occupancy in any of several ways, usually either restricting entry to portions of the building or restricting use to brief entry for access to contents. A green placard indicates that the building has been inspected and the lawful occupancy is permitted. For details of the SAP evaluation procedures, see a documented usually referred to as ATC-20 (Applied Technology Council 2005). See Figure 3-1 for the ATC-20 placards.

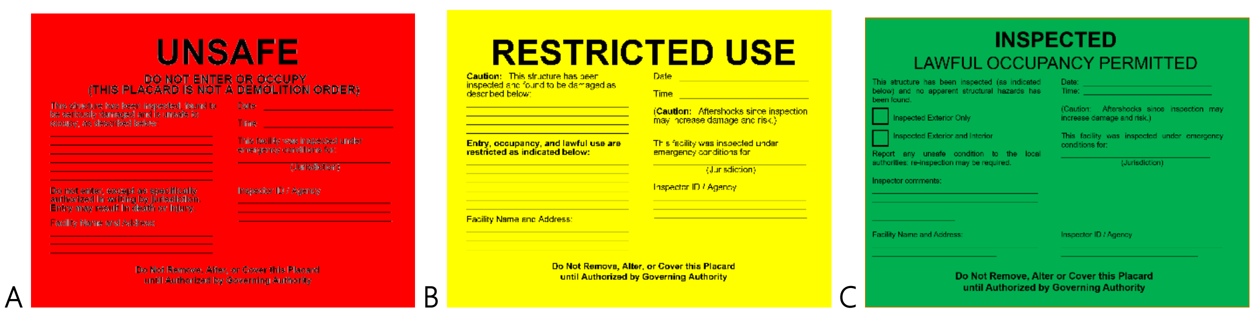


Figure 3-1. ATC-20 placards

The sooner SAP evaluators can determine the safety of damaged buildings, the sooner people can safely reenter their homes, workplaces, schools, and so on, and the less the economic impact of the earthquake. Thus, a resilient runway can facilitate travel of SAP evaluators and reduce those economic impacts. Estimating benefits of faster mutual-aid SAP evaluations requires estimates of:

- The number of buildings that will require safety evaluation.
- The number of evaluators who could mobilize to the Willamette Valley from outside via air or road.
- The rate at which they could evaluate buildings.
- The fraction of the evaluated buildings that are returned to service because of the safety evaluation.

- The daily value of a building returned to service.
- The delay that SAP evaluators would experience mobilizing to the Portland area without and with a resilient runway.

HNTB Corporation (2015) characterized the vulnerability of PDX buildings. "Building seismic vulnerability" refers to the relationship between seismic excitation (ground motion and ground failure) and some measure of loss. The project team relies on that report to estimate the damage and repair needs for PDX buildings in the earthquake scenarios considered here. As for buildings requiring safety evaluation in the greater Portland metro area, researchers involved in the NSF-sponsored M9 Project have estimated building damage in the Pacific Northwest using Hazus-MH. One research product reports an estimate of 44,000 extensively damaged buildings and 9,000 with complete damage, given a magnitude-9 rupture of the Cascadia Subduction Zone (Washington State Department of Natural Resources, 2013).

If the Northridge earthquake is any indicator, 53,000 extensively or completely damaged buildings would represent approximately 12.5% of the total number of buildings damaged enough to require building safety evaluation (EQE International and California Governor's Office of Emergency Services 1995, p. 4-5), meaning perhaps 420,000 buildings might require building safety evaluation.

To supplement the M9 project's estimates of building damage, the project team can use an inventory of buildings in the study area extracted from the Hazus-MH database (NIBS and FEMA 2012), and the vulnerability functions extracted from Hazus-MH as described in Porter (2009a, 2009b, 2010), which relate the fatality risk, repair cost, and loss of function to ground motion, model building type, era of construction, and occupancy class. The vulnerability information in these publications is entirely consistent with Hazus-MH, merely extracted from 15 normalized tables in Hazus-MH relational database and tabulated in a single denormalized lookup table that can be more conveniently used outside of Hazus-MH.

Unpublished, intermediate data in these tables can also be used to estimate the building area that has collapsed and requires urban search and rescue. Porter (2018) provides evidence to relate the area of buildings that have collapsed to the number of buildings that have collapsed, along with the number that are ultimately assigned a red or yellow placard, under the procedures of ATC-20-1 (Applied Technology Council 2005).

Training materials for ATC-20-1 suggest that a 2-person SAP evaluation team can evaluate 13 buildings per day (California Governor's Office of Emergency Services 2020). Would SAP evaluators be as productive in an Oregon earthquake? Probably. SAP training and the evaluation process are standardized. The same process would be used in Portland as elsewhere. Many of the same people who would evaluate the safety of buildings in California would do so in Portland.

EQE International and California Governor's Office of Emergency Services (1995, p. 4-5) report that of 104,000 buildings in Los Angeles and Ventura Counties that required safety evaluation after the 1994 Northridge earthquake, 89% were eventually assigned a green or yellow placard, most of which could be used either fully or with modest restrictions, suggesting that safety evaluation returns 89% or so of buildings to functionality as soon as the safety placard is applied. Would the same fraction return to service in Portland? The total fraction of damaged buildings might be higher, for example because Portland has a higher fraction of fragile buildings. But the fraction of those that could be repaired and returned to service might not be very different, for reasons that are too technical to offer here.

In 2017, the California Governor's Office of Emergency Services (2020) estimated that nationwide, approximately 10,000 building professionals had been trained to perform SAP evaluations. After a major earthquake requiring 500,000 evaluations, perhaps 15% of SAP evaluators would be available until all evaluations were performed (J. Barnes, California Governor's Office of Emergency Services, written commun., June 7, 2017).

## 3.5 QUANTIFYING LANDSLIDES ALONG ACCESS ROUTES

A resilient runway will produce benefits largely in proportion to the degree to which landslides impair access to the Willamette Valley by road, rail, and river. How can one characterize landslides on a regional basis for each of several hypothetical earthquakes?

Hazus-MH (NIBS and FEMA 2012) uses a method proposed by Wilson and Keefer (1985), which offers relationships between so-called critical acceleration ($a_C$, the acceleration necessary to cause a landslide), slope angle, geologic group (generally characterized by chemistry, crystalline structure, degree of compaction), and depth of groundwater. Figure 3-3 shows the relationships in solid lines for dry slope materials and dashed lines for soils that are saturated from the slide plane to the ground surface.

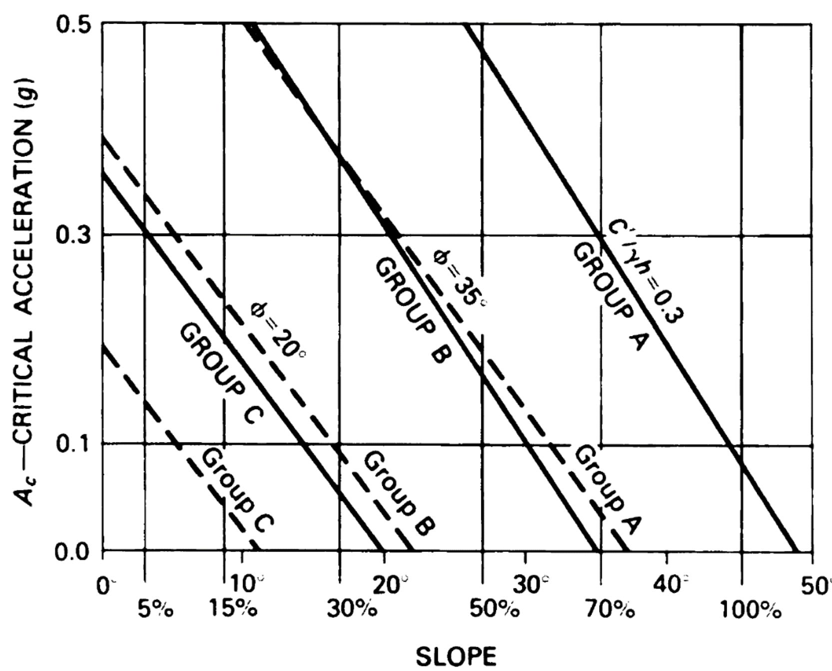


Figure 3-2. Wilson and Keefer (1985) plot of critical acceleration versus slope for three geologic groups

Moisture content varies seasonally in Willamette Valley. Bollman et al. (2013) periodically measured volumetric water content of surface soils (20 cm depth) at 13 locations with various drainage conditions, landforms, and map units in the Willamette Valley in 2010 and 2011, finding high moisture content between November and June, low during the summer and fall.

One can equate Wilson and Keefer's (1985) geologic groups with ASCE/SEI 7-16 site class as defined by (American Society of Civil Engineers 2016), as shown in Table 3-4, using Wells and others (unpublished data, 2017, as reported by Appleby et al. 2019, Tables B-2 and B-10). Equation 3-1 depicts the linear relationships in Wilson and Keefer's (1985) critical-acceleration chart (Figure 3-3), and Table 3-4 provides parameter values for dry soil fit to those lines. (The equation and parameter values were derived in the present work, but presented here, in this literature review chapter, rather than in the methodology or findings sections for convenience.) In the table, $s_1$ has units of gravity (g), $s_2$ has units of gravities per slope angle degree (g/deg), and $\alpha$ has units of degrees (deg). Wilson and Keefer (1985, p. 335) recommend the lower bound of 0.05g considering frequent precipitation loading.

$$\begin{aligned} a_c &= s_1 + s_2\alpha \\ &\geq 0.05g \end{aligned} \quad \text{Equation 3-1}$$

Table 3-4. Mapping ASCE/SEI 7-16 site class to Wilson and Keefer (1985) geologic group, with critical acceleration parameters

| ASCE/SEI 7-16 site class | Geologic group | Examples | Dry | | Saturated | |
|---|---|---|---|---|---|---|
| | | | $s_1$ | $s_2$ | $s_1$ | $s_2$ |
| A | A | | 1.06 | -0.022 | 0.71 | -0.019 |
| B | A | WO17 Volcanic bedrock | 1.06 | -0.022 | 0.71 | -0.019 |
| C | B | WO17 Sedimentary bedrock | 0.70 | -0.020 | 0.40 | -0.018 |
| D | B | WO17 Alluvium | 0.70 | -0.020 | 0.40 | -0.018 |
| E | C | WO17 Alluvial fan deposits | 0.36 | -0.018 | 0.19 | -0.017 |
| F | C | WO17 Colluvium and artificial fill | 0.36 | -0.018 | 0.19 | -0.017 |

For example, a dry hillside with ASCE/SEI 7-16 site class C and a 30-degree slope (common for example along Interstate 5 south of Latham or along US Highway 26 between Portland and Hillsboro) would have a critical acceleration on the order of 0.1g. A saturated hillside with a 20-degree slope would have a critical acceleration of 0.05g.

One can also find geologic information for Oregon in the National Geologic Map Database (NGMDB), developed by 630 agencies, universities, associations, and private companies, and served by the U.S. Geological Survey, e.g., from data.gov (2013). Figure 3-4 shows the geologic map of Oregon (Walker and MacLeod 1991) from the NGMDB, overlain in Google Earth with six mountainous routes to the Willamette Valley from the north, east, and south (red lines).


Figure 3-3. Geologic map of Oregon. Red lines indicate six mountainous routes to the Willamette routes from the north, east, and south

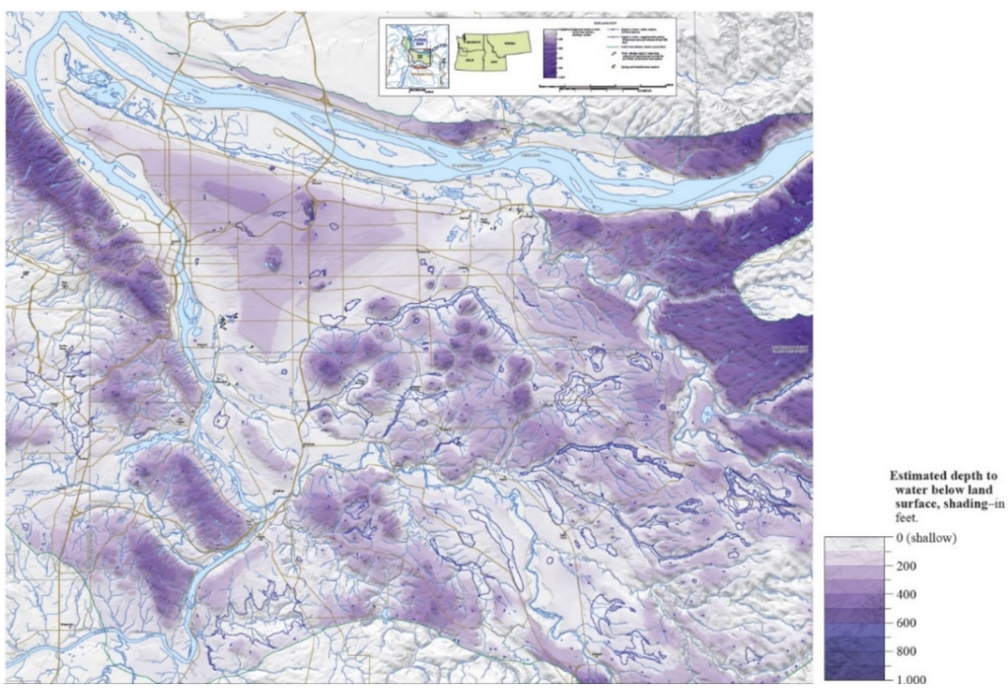


Figure 3-4. Depth to ground water (Snyder 2008)

Snyder (2008) provides a map of estimated depth to ground water in the Portland, Oregon area; it generally exceeds 100 feet on all but the shallowest slopes (any color other than white on Figure 3-5)

Wilson and Keefer's (1985) geologic groups are not mapped in Oregon. However, Appleby et al. (2019) provide useful cross-referencing between geologic unit, Wilson and Keefer (1985) geologic group, and ASCE/SEI 7-16 site class (American Society of Civil Engineers 2016). Particularly useful are assignments that Wells and others (unpublished data, 2017) made of a variety of Oregon geologic units to both Wilson and Keefer and ASCE classifications, as reported by Appleby et al. (2019).

More recently, McCrink and Perez (2017), estimating landsliding for the HayWired Scenario, opted to use the Jibson (2007) Newmark rigid sliding-block displacement analysis regression model, Equation 3-2, which the California Geological Survey Seismic Hazard Mapping Program has adopted. Jibson (2007) recommends it for use in regional, though not site-specific, analysis. In the equation, $D_N$ denotes displacement in centimeters, $a_c$ denotes critical acceleration, meaning the threshold ground acceleration necessary to overcome basal sliding resistance and initiate permanent downslope movement and calculated by Equation 3-3, $a_{max}$ denotes peak ground acceleration, and $M_W$ denotes earthquake magnitude. In Equation 3-3, $c'$ is effective cohesion, $\gamma$ is the unit weight of the slide mass material, $h$ is its thickness (taken as 50 ft), $\alpha$ is the slope gradient of the ground surface, and $\phi'$ denotes the effective friction angle.

$$\log_{10}\left(D_N\right) = -2.710 + \log_{10}\left[\left(1 - \frac{a_c}{a_{\max}}\right)^{2.335} \cdot \left(\frac{a_c}{a_{\max}}\right)^{-1.478}\right] + 0.424 \cdot M_W \pm 0.454 \qquad \textit{Equation 3-2}$$

$$a_c = \left(c'\gamma h \cdot \sin\alpha + \cot\alpha \tan\phi' - 1\right)\sin\alpha \qquad \textit{Equation 3-3}$$

Jibson (2007) limits the applicability of the equation to $5.3 \leq M_W \leq 7.6$, that of his data set. In Portland, larger earthquakes matter, so to use Equation 3-2 will substantially extrapolate from the underlying research. Jibson (2007) also offers a prediction equation that omits $M_W$ but includes Arias intensity, an evolutionary intensity measure that offers an alternative way to account for duration. But the same underlying data set still limits its applicability. Furthermore, it has a substantially larger logarithmic standard deviation: 0.616 rather than 0.454, about 50% more uncertainty.

For example, assuming one is comfortable with such extrapolation, Equation 3-2 implies that a hillside with a critical acceleration of $a_c$ = 0.1g, when subjected to peak ground acceleration on the order of 0.25g, would experience a median displacement of 15 cm, with a factor of 3 error either way.

To estimate the probability of slope failure ($P_f$) in any 10-meter square gridcell, McCrink and Perez (2017) use Jibson et al.'s (2000) relationship derived from 1994 Northridge earthquake data, shown in Equation 3-4; they limited its applicability to cases where $PGV \geq 20$ cm/sec. Note that Equation 3-4 boils down to a 33.5% probability than any particular gridcell will slide if $D_N$ exceeds about 10 cm.

$$P_f = 0.335 \cdot \left[1 - \exp\left(-0.048 \cdot D_N^{1.565}\right)\right] \quad \textit{Equation 3-4}$$

For example, any 10-meter stretch of highway next to a hillside with critical acceleration of 0.1g, shaking with PGA equal to 0.25g, would have a failure probability on the order of 30%. Note that the expected value of $D_N$ in Equation 3-4 must account for the fact that Equation 3-2 shows that Jibson assumed $D_N$ is conditionally lognormally distributed. The expected value of $D_N$ is larger than antilog of $\log_{10}(D_N)$.

Equation 3-3 requires regional geologic data. Burns et al. (2016) offer a statewide map of landslide susceptibility called SLIDO (Statewide Landslide Information Database for Oregon). However, the Burns et al. (2016) landslide susceptibility categories are defined on new grounds, not those of Wilson and Keefer's (1985) categories I-X and not explicitly in terms of critical acceleration ($a_c$) or to any of the underlying cohesion, friction-angle, or slope data.

Where to get topographic slope $\alpha$? Verdin et al. (2007) explain how they derived global topographic slope from shuttle radar topography mission (SRTM) data at 3-arc-second resolution and aggregated them to 30-arc-second resolution with distribution of slopes within each 30-arc-second pixel. SRTM data are now available at 1-arc-second resolution (approximately 30-meter pixels) for most of the world; see Global Multi-resolution Terrain Elevation Data 2010 (GMTED2010) (Danielson and Gesch 2011). Google seems to have acquired those data and implemented them in Google Earth, so one can sample slope $\alpha$ at approximately 30-meter resolution.

Soil moisture can be acquired from various agriculture sources, such as Bollman et al. (2013), who measured soil moisture content in 13 locations of the Willamette Valley in the calendar year 2011, finding soil in all 13 locations to be saturated from about November through June, or 2/3rds of the calendar year.

## 3.6 HIGHWAY DAMAGE AND RESTORATION

A resilient runway will produce greater benefits the longer the Willamette Valley is isolated by landslides and bridge damage along roadways. Wang et al. (2002) offer total landslide repair-cost statistics for Oregon landslides, and include one or two anecdotes in an appendix about the repair duration of slides that caused damage or death.

### 3.6.1 Landslide Damage to Highways

Hopkins et al. (2005) inventory about 1,440 landslides along major highway routes under the jurisdiction of the Kentucky Transportation Cabinet. They describe the severity of the landslides on a scale of A through D, as shown in Table 3-5. In the table, $P[R=r|LS]$ denotes the fraction of landslides with severity $r$. The table shows that about 5% of landslides are serious enough to require closure of the highway or limit access to one lane. One can estimate the probability that a landslide will occur and will have severity $r$ using Equation 3-5. In the equation, $P[R=r]$ denotes the probability that a landslide occurs with severity $r$, $P_f$ denotes the output of Equation 3-4, and $P[R = r|LS]$ is taken from Table 3-5.

$$P\left[R = r\right] = P_f \cdot P\left[R = r \middle| LS\right] \quad \text{Equation 3-5}$$

Thus, in the previously cited example of a highway next to a hillside with critical acceleration of 0.1g, shaken at 0.25g, and thus having a 30% chance of landslide in any 10-meter stretch, would have a 1.5% chance of a very serious slide, or that one could expect a very serious slide approximately every 700 meters (just under ½ mile).

Table 3-5. Relative distribution of highway landslide severity (after Hopkins et al. 2005, as reported by Sun et al. 2005)

| Severity $r$ | Description | $P[R=r/LS]$ |
|---|---|---|
| A | Very serious--failure has occurred or is imminent. Road is closed, one lane condition exists, buildings in danger, or a major safety concern exists. | 4.6% |
| B | Serious--landslide is moving rapidly, requiring constant maintenance (daily, weekly, monthly, etc.). | 24.1% |
| C | Moderate--some movements, breaks in pavement (occurrence over several years). | 57.0% |
| D | Minor--slope failures affecting slope only, slight, or no, movements at the present time. | 14.3% |

Hazus-MH (NIBS and FEMA 2012) offers expert-opinion estimates of repair duration for highway pavements that suffer ground deformation more than a few inches. The authors estimate uncertain repair duration with a mean value of 21 days and a standard deviation of 16 days. This range generally agrees with anecdotal evidence of several landslide repairs discussed in a 2012 highway geology symposium (California Department of Transportation and California Geological Survey 2012).

The project team asked the Oregon Department of Transportation's program lead for unstable slopes whether the range seems realistic. He replied that he tended to think of repair times in terms of cubic yards of soil to be moved: repair crews can generally move 5,000 cubic yards of landslide material per day. But given the size of slides that have closed Oregon roads in the past, Hazus' estimate of three weeks plus or minus 16 days seemed realistic for repairing a slide enough to reopen a road (C. Mohney, Engineering Geology Program Lead, Oregon Department of Transportation, verbal commun., April 22, 2020).

### 3.6.2 Bridge Damage to Highways

Basoz and Mander (1999) offer probably the most-used bridge fragility functions. Hazus-MH adopts them, as does REDARS (Werner et al. 2006). Hazus-MH (NIBS and FEMA 2012) also offer bridge restoration times. Nako et al. (2009) used REDARS, which like Hazus-MH in turn relies on Basoz and Mander (1999), to estimate earthquake damage to Oregon bridges on behalf of the Oregon Department of Transportation. Basoz and Mander's (1999) bridge fragility functions estimate for example that Oregon highway bridges constructed of multi-column bents with simply-supported spans (common near Portland) collapse at a median peak ground acceleration value on the order of 0.65g. Their fragility information includes uncertainty; they recommend a logarithmic standard deviation of 0.6, meaning that one in 10 such bridges would collapse when subjected to about half the median capacity, or 0.3g.

## 3.7 TRANSIT ALTERNATIVES TO PDX

A resilient runway at PDX will produce greater benefits to airport users if other, nearby airports, highway, rail, and river routes cannot be used as an alternative. Figure 3-6A shows alternative commercial airports in and near Oregon. Figure 3-6B shows highway routes into the Willamette Valley.

*Redmond Airport (RDM).* This airport lies within driving distance of Portland while still being far enough away from the Cascadia Subduction Zone that it can be expected to escape serious damage in a large earthquake. To reach Portland from RDM requires a drive over the highlighted route on US 26 through the Cascade Mountain Range, a driving distance of 150 miles, about a three-hour drive under normal conditions. The red highlighted portion of the route passes steep terrain, with the potential for earthquake-induced landslides.

*Hillsboro Airport (HIO).* Much closer to Portland than RDM, HIO is the closest of many general aviation airports in the Willamette Valley, shown in Figure 3-7. HNTB Corporation (2015) estimated that the runway at HIO could be used for emergency response purposes after a major regional earthquake. It seems reasonable to assume that firefighters and emergency medical service personnel could use HIO, but because HIO does not support commercial aviation, engineers and building professionals needed for post-earthquake safety evaluation would be effectively prevented from arriving by air while PDX is impaired.

*Eugene Airport (EUG).* This is a small hub for regional commercial aviation: Alaska, Allegiant, American, Delta, and United all fly through EUG. Travel from EUG to Portland is about 130 miles and takes about two hours via Interstate 5. The route crosses the McKenzie, Willamette, and Tualatin Rivers. The National Bridge Inventory (Federal Highway Administration 2020) indicates that the route includes at least 148 bridges with an average age of 46 years. Most bridges appear to be nonductile concrete multi-span, multi-column bents, hinting at the possibility of such extensive damage that a large regional earthquake could render Portland inaccessible via Eugene and I-5.

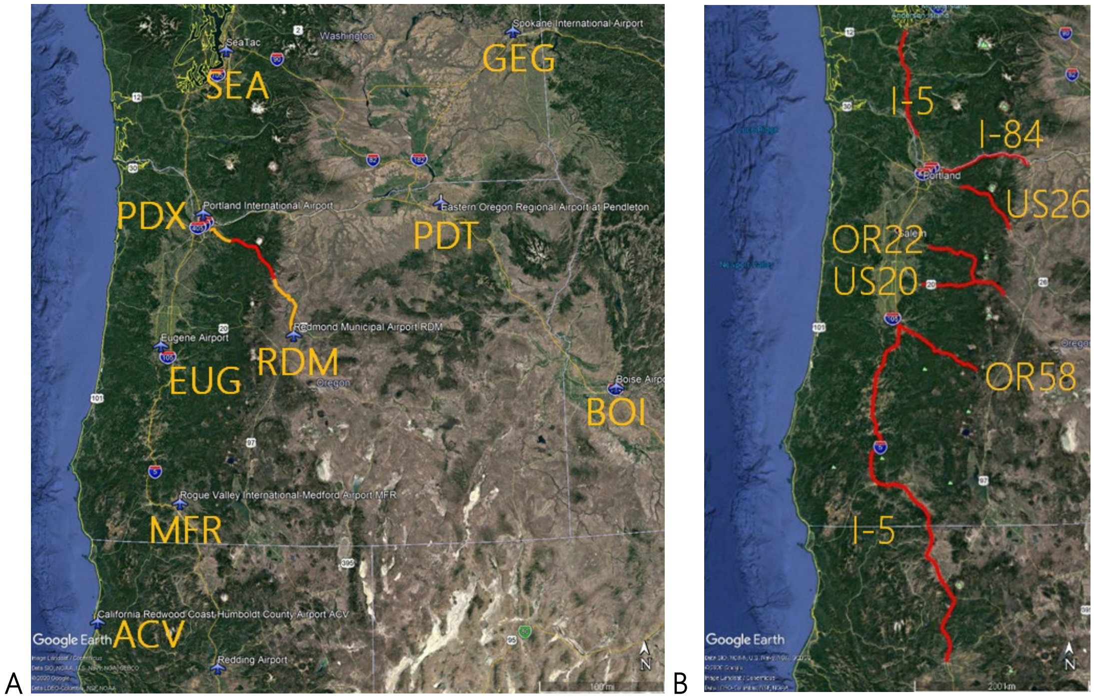


Figure 3-5. (A) Commercial airports in and near Oregon, and (B) highway routes into the Willamette Valley

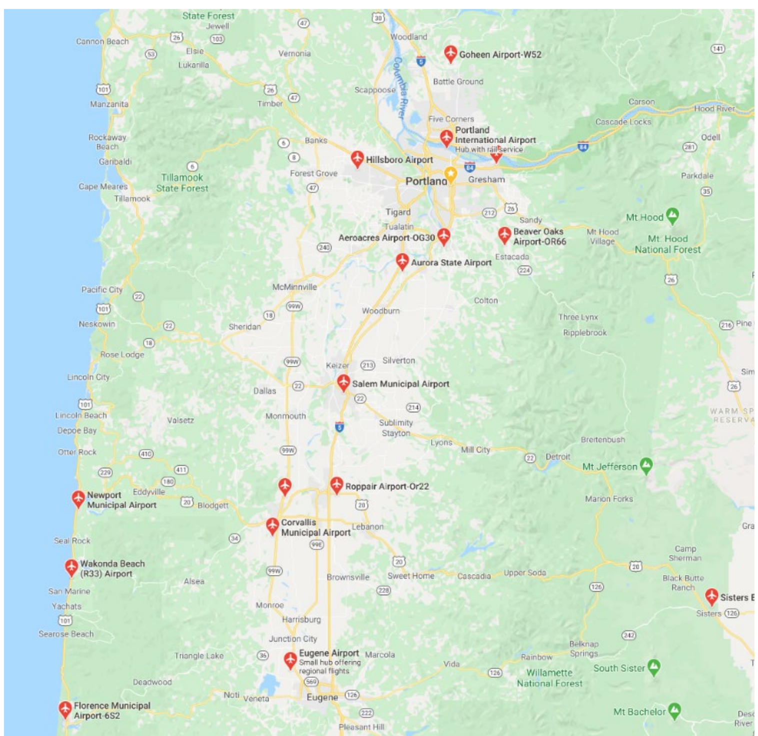


Figure 3-6. Airports in the Willamette Valley

## 3.8 HOSPITAL CAPACITY

Table 3-6 summarizes hospital capacity in the study area: an estimated 5,200 beds, including approximately 600 ICU beds and 550 emergency department beds. See also Figure 3-8. Data come from Portland International Airport (2019, App II-9-1), with additions by Oregon Health Authority and Google Maps. For some records, breakout of beds was unknown and estimated based on ratios for which beds were known. Halpern et al. (2016) found that in 2010, hospital and ICU occupancy rates were 64.6% and 68%, respectively, and that occupancy rates vary by hospital size, with higher occupancy rates associated with larger hospitals.

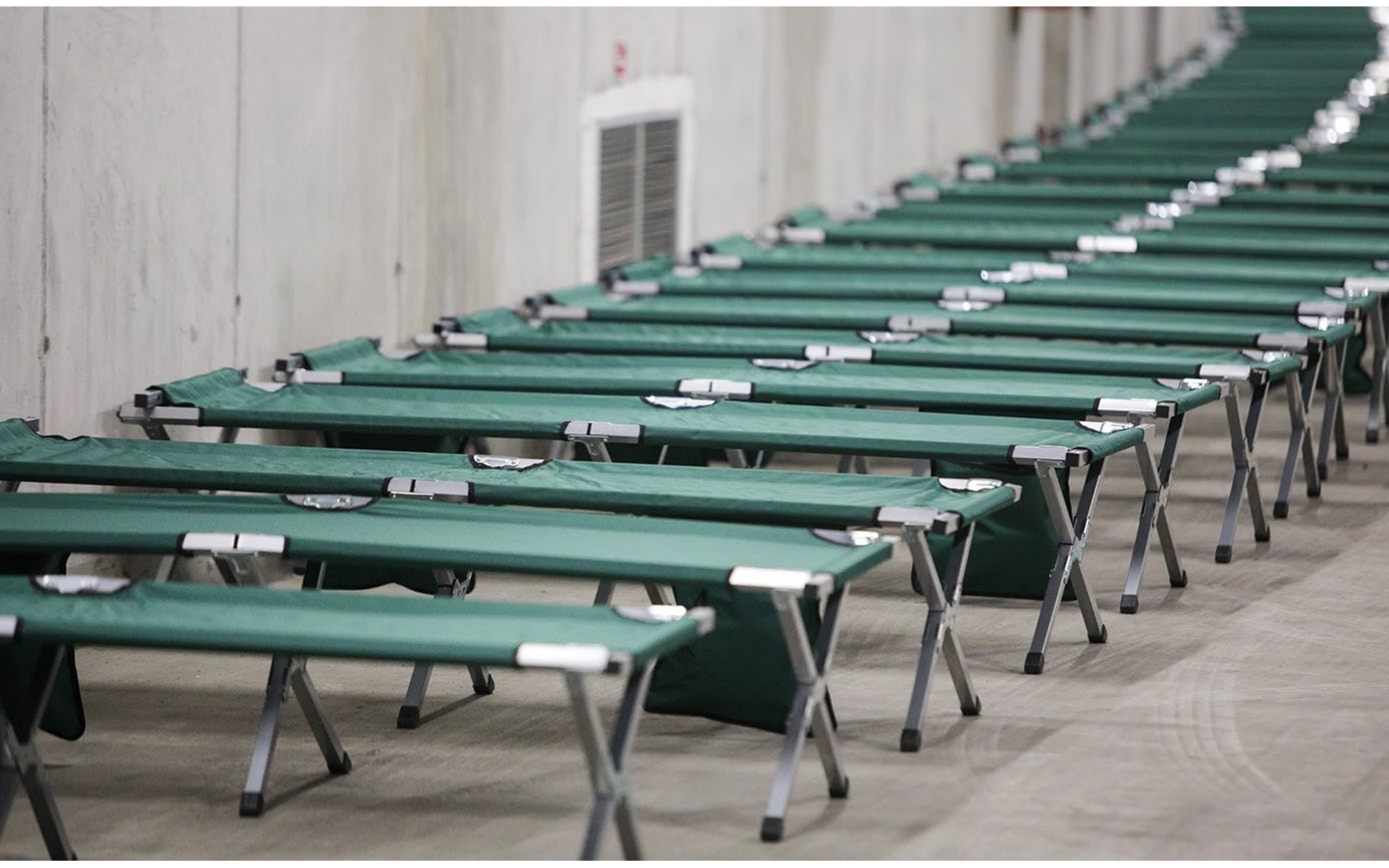

Table 3-6. Regional hospitals

| Name | Latitude deg N | Longitude deg E | Beds | | | |
|---|---|---|---|---|---|---|
| | | | Total | Regular | ICU | ED |
| Kaiser Sunnyside Medical Center | 45.4321 | -122.5629 | 337 | 267 | 39 | 31 |
| Legacy Meridian Park | 45.3784 | -122.7431 | 150 | 117 | 16 | 17 |
| Providence Milwaukie Hospital | 45.4492 | -122.6305 | 97 | 71 | 6 | 20 |
| Providence Willamette Falls Med Ctr | 45.3563 | -122.5893 | 155 | 128 | 8 | 19 |
| Adventist Health Portland | 45.5133 | -122.5605 | 255 | 211 | 12 | 32 |
| Randall Children's Hospital at Legacy Emanuel | 45.5446 | -122.6723 | 554 | 441 | 55 | 58 |
| Legacy Good Samaritan Medical Ctr | 45.5310 | -122.6988 | 299 | 246 | 28 | 25 |
| Legacy Mt. Hood Medical Center | 45.5166 | -122.4098 | 98 | 71 | 10 | 17 |
| OHSU Hospital | 45.4993 | -122.6871 | 563 | 382 | 139 | 42 |
| Providence Portland Medical Center | 45.5277 | -122.6148 | 565 | 483 | 36 | 46 |
| Portland VA Medical Center | 45.4963 | -122.6851 | 174 | 131 | 24 | 19 |
| Adventist Health Tillamook | 45.4566 | -123.8567 | 35 | 21 | 4 | 10 |
| Kaiser Westside Medical Center | 45.5415 | -122.8752 | 148 | 100 | 20 | 28 |
| Providence St. Vincent Medical Ctr | 45.5105 | -122.7738 | 721 | 536 | 135 | 50 |
| Tuality Community Hospital | 45.5196 | -122.9804 | 167 | 137 | 9 | 20 |
| Tuality Forest Grove Medical Plaza | 45.5189 | -123.0927 | 48 | 42 | 2 | 4 |
| Legacy Salmon Creek Medical Ctr | 45.7208 | -122.6500 | 203 | 155 | 16 | 32 |
| PeaceHealth Southwest Medical Ctr | 45.6250 | -122.5833 | 354 | 272 | 24 | 58 |
| Legacy Silverton Medical Center | 45.0046 | -122.7925 | 50 | 39 | 6 | 5 |
| Santiam Hospital | 44.8052 | -122.7873 | 50 | 39 | 6 | 5 |
| Salem Health West Valley Hospital | 44.9186 | -123.3126 | 50 | 39 | 6 | 5 |
| Unity Center for Behavioral Health | 45.5320 | -122.6660 | 107 | 87 | 10 | 10 |
| | | **Total** | **5,180** | **4,015** | **611** | **553** |

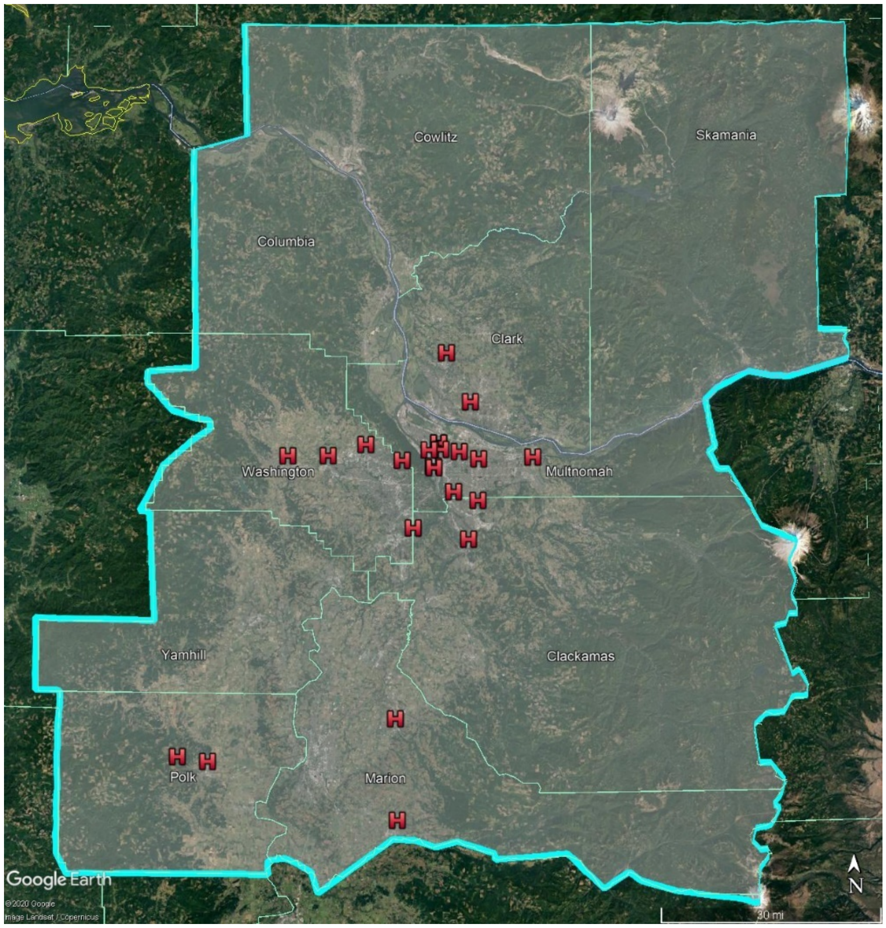


Figure 3-7. Hospitals in the study area

## 3.9 QUANTIFYING HIGHWAY BRIDGE REPAIRS

Basoz and Mander (1999) provide perhaps the most often-used set of U.S. highway bridge fragility functions. They group highway bridges in six categories: simply supported spans on multi-column bents; discontinuous box girders on single-column bents; continuous concrete spans; continuous steel spans; single spans, and major bridges. They subdivide the six categories in into three subcategories each: conventionally designed bridges outside of California; conventionally designed California bridges; and seismically designed bridges. They offer fragility functions for four damage states: slight, moderate, extensive, and complete, numbered 2 through 5, respectively. (They denoted the undamaged state by damage state 1). They derived fragility functions analytically, that is, considering structural limit states that a structural model would realistically enter conditioned either on member forces or deformations. The authors supplemented their analysis with empirical observations of damage to California highway bridges in the 1989 Loma Prieta and 1994 Northridge earthquakes. Table 3-7 presents the authors' estimated median PGA capacity values for conventionally designed non-California bridges. They recommend a uniform logarithmic standard deviation of $\beta$ = 0.6. Table 3-8 presents the repair durations assumed by Hazus-MH, which its authors took directly from expert opinion elicited by the authors of ATC-13 (Applied Technology Council 1985).

Table 3-7. Basoz and Mander (1999) bridge fragility median capacities for non-California conventional bridge design

| Classification | NBI class | Damage state | Conventional design, non-CA, median PGA (g) |
|---|---|---|---|
| 1. Multi-column bents, simply-supported | 101-106<br>301-306<br>501-506 | 2 slight | 0.26 |
| | | 3 moderate | 0.35 |
| | | 4 extensive | 0.44 |
| | | 5 complete | 0.65 |
| 2. Single column bents, box girders, discontinuous | 205-206<br>605-606 | 2 | Not applicable |
| | | 3 | |
| | | 4 | |
| | | 5 | |
| 3. Continuous concrete | 201-206<br>601-607 | 2 | 0.60 |
| | | 3 | 0.79 |
| | | 4 | 1.05 |
| | | 5 | 1.38 |
| 4. Continuous steel | 402-410 | 2 | 0.76 |
| | | 3 | 0.76 |
| | | 4 | 0.76 |
| | | 5 | 1.04 |
| 5. Single span | All | 2 | 0.8 |
| | | 3 | 0.9 |
| | | 4 | 1.1 |
| | | 5 | 1.6 |
| 6. Major bridge | | 2 | 0.4 |
| | | 3 | 0.5 |
| | | 4 | 0.6 |
| | | 5 | 0.8 |

Table 3-8. Hazus-MH highway bridge repair durations

| Damage state | Mean repair time (days) | Standard deviation (days) |
|---|---|---|
| 2 Slight | 0.6 | 0.6 |
| 3 Moderate | 2.5 | 2.7 |
| 4 Extensive | 75 | 42 |
| 5 Complete | 230 | 110 |

## 3.10 VALUE OF AIR NATIONAL GUARD OPERATIONS

PDX hosts the U.S. Air Force 142nd Wing Oregon Air National Guard, which supports the North American Aerospace Defense Command (NORAD) and Air Combat Command. The mission of the 142nd Wing is to "maintain 24-hour Aerospace Control Alert in the Pacific Northwest and provides Air Superiority mission capabilities as well." (United States Air Force, ND.)

One might think of the continued performance of that mission as the product or value to be preserved by a resilient runway. The runway appears to be necessary to delivering that product. The air wing primarily operates McDonnell Douglas/Boeing F-15A/C Eagle fighter aircraft, which require 275 meters of runway for takeoff and 1,100 meters of runway to land (Skybrary 2014). With 275 meters of runway, the 142nd Wing can effectively relocate to another, undamaged facility. With 1,100 meters of runway to land, the 142nd Wing can continue to perform its mission (or in a sense deliver its product) without disruption.

Portland Air National Guard Base Finance Office (2019) reports that the annual economic impacts of operating the 142nd Wing totals $130 million: $80 million in payroll, $17 million operation and maintenance expense, $2 million in training, uniforms, meals, and other expenses, and $31 million in other jobs.

Various authors have estimated the benefit of military expenditures in several contexts. The United States Air Force (2018, 2019) estimated benefit-cost ratios for its requested appropriation for working capital funds that "provide warfighters the key services needed to meet global mission capability requirements." It estimated various elements of the appropriation provide benefits of 3.5 and 5.22, (U.S. Air Force 2017 pp. 99 and 103 respectively), and 2.97 (U.S. Air Force 2019 p. 110) times the expenditure. For later purposes of finding a weighted average, the expenditures that produced these BCRs were, respectively, $239 million (2012 USD), $562 million (2017 USD), and $33.6 million (2019 USD). Hill et al. (2009, p. 22) examined the total fiscal impact on Kansas from $104 million (2006 USD), spent for military employment, retirees, and contracts in Kansas and found a benefit-cost ratio of 2.59.

## 3.11 ACCOUNTING FOR FUTURE GROWTH

A resilient runway will produce greater benefits the more the airport is used, and use will likely increase as population grows. Metro Research Center (2016) provides growth estimates of the Portland-Vancouver-Hillsboro, OR-WA, Metropolitan Statistical Area through the year 2060. To the extent necessary, the project team can extrapolate future growth beyond 2060 from that study. It is unclear how long-lasting the economic and demographic effects of the COVID-19 pandemic will be. Parker et al. (2020b) suggest that recovery may take three years or. In the meantime, it seems reasonable to continue to use those of Metro Research Center (2016), which suggests annual population growth in the MSA of 0.85%.

Real per capita gross domestic product in Oregon has also generally increased at a rate of 1.5% per year since 2000 or 2.0% per year since 2010. The project team takes the former for present purposes since it is both more conservative and longer term.

## 3.12 INDIRECT BUSINESS INTERRUPTION

Business interruptions (BI) that are caused by disasters and other disruptive events can lead to costly economic losses. The inherent interdependencies across various sectors of the economy further exacerbate the direct effects of disruptive events, often resulting in significant indirect and induced effects. A survey by Webb et al. (2000) indicates that the direct and indirect business interruption losses triggered by disasters are as significant as the magnitude of the resulting physical infrastructure and property damages. Business interruption losses have been identified as a key contributor to disaster risks. Notably, the Allianz Global Corporate & Specialty (2020) has concluded business interruption to be a leading risk concern among businesses. In estimating business interruption losses, it is essential to understand the magnitude and extent of linkages that exist across interdependent sectors of the affected regional economy.

Wassily Leontief was awarded a Nobel Prize in Economics in 1973 for what became known as the input-output (IO) model for the economy (Leontief 1936). Miller and Blair (2009) provide a comprehensive introduction of the model and its applications. The input-output model is a useful tool in economic decision-making processes used in many countries. It presents a framework that can describe the interactive nature of transactions among economic systems. The input-output model and an extension known as computable general equilibrium (CGE) analysis are two of the most popular methods typically used in evaluating the efficacy of resilience management to reduce BI and other economic losses in interdependent sectors. Rose (2009) provides detailed reviews of economic resilience definitions, categories, and enhancement strategies. Computable general equilibrium shares the capabilities of input-output models in itemizing the effects of a disruptive event across interdependent sectors. In this project, the estimation of indirect business interruption losses will be assessed using input-output modeling and data analysis. The U.S. Bureau of Economic Analysis and IMPLAN are the agencies primarily responsible for releasing input-output accounts for the United States at both national and regional levels.

## 3.13 BENEFITS BY INCOME LEVEL AND RACIAL OR ETHNIC GROUP

One can use a multi-sector income distribution matrix (MSIDM) to estimate the social economic impacts of an earthquake. This tool has been developed and utilized in several studies over the past 30 years, most recently to analyze the income distribution impacts of a major Southern California earthquake scenario and its effect on the regional transportation system of major ports and highway networks (see, e.g., Rose et al. 1988; Li et al. 1999; Rose et al. 2012; and Wei et al. 2020). The MSIDM can be used formally to describe impacts across income brackets and informally to describe impacts across racial and ethnic groups. This type of analysis can help to analyze the social equity of mitigation measures, environmental justice concerns, and potential public support of major policies, the latter by more precisely determining who gains and who loses.

## 3.14 AFTERSHOCK LOSSES

Large earthquakes always produce aftershocks. In general, the larger the mainshock, the larger and more numerous the aftershocks, and the longer they will continue. A magnitude-9 mainshock can be followed by one or more magnitude-8 aftershocks, several magnitude-7 or larger aftershocks, and several dozen magnitude-6 and larger aftershocks, all occurring years or decades after the mainshock. The magnitude-9.1 2011 Tohoku earthquake has so far produced 60 aftershocks over magnitude 6.0. (About 5% of earthquakes are preceded by smaller events called foreshocks, but whether the present project treats associated smaller events in the earthquake sequence as occurring before or after the mainshock seems immaterial.)

For aftershock magnitudes and dates after the mainshock, one could use the statistical model of aftershock rate developed by Reasenberg and Jones (1989, 1994). For aftershock distances, one could use Felzer and Brodsky's (2006) power-law distribution of distance, as in HayWired (Wein et al. 2017).

Alternatively, one can estimate the losses due to all aftershocks as an approximate factor of mainshock losses, drawing for example from the HayWired scenario, which modeled losses from an earthquake sequence beginning with a magnitude-7.0 mainshock on the Hayward Fault in the San Francisco Bay area. The authors of that study estimate the aftershocks add about 25% to the economic losses resulting from the mainshock (Detweiler and Wein 2018, p. 41).

## 3.15 OTHER CONSTRAINTS ON RESTORING PDX OPERATIONS

Even if a resilient runway sustains little damage, would other damage at PDX hinder restoration of service? Experience at other airports in past disasters provides some guidance.

The $M_w$ 8.8, February 27, 2010 Chile earthquake shook Santiago International Airport with peak ground acceleration of approximately 0.25g and modified Mercalli intensity MMI 7 (U.S. Geological Survey National Earthquake Information Center, NDa). The earthquake caused the collapse of suspended ceilings and above-ceiling systems (Earthquake Engineering Research Institute 2010, p. 12) and "shook glass out of doors and windows" (Saavedra 2010). By Sunday, February 28, commercial airline services had been partially re-established, and aircraft were being allowed to land in Santiago (Franklin and Gabbatt 2010). Service returned to about 50% of normal activity by March 4, 2010, five days after the earthquake (MercoPress 2010).

The $M_w$ 6.2 Christchurch earthquake of Tuesday, February 21, 2011, (U.S. Geological Survey National Earthquake Information Center, NDb) caused peak horizontal ground acceleration about 0.25g, and modified Mercalli intensity 7 shaking at the Christchurch International Airport. The earthquake caused nonstructural damage in the terminal: Taylor et al (2011) report fallen plaster and ceiling tiles. The airport reopened to emergency flights on February 22 (RNZ News 2011), one day after the earthquake and to commercial flights on February 23 (Forgione, 2011), two days after the earthquake.

The 1994 Northridge earthquake caused minor flooding at Los Angeles International Airport after a sprinkler system was activated, but the airport reopened after approximately two hours. Hollywood Burbank Airport reopened following inspections the day after the earthquake, according to EQE International (1994). Shaking was estimated at about 0.3g of peak ground acceleration and MMI 7.5 at Hollywood Burbank Airport and approximately 0.2g of peak ground acceleration and MMI 6.5 at Los Angeles International Airport (U.S. Geological Survey National Earthquake Information Center, NDc).

# 4. Methodology Employed in this Study

## 4.1 MOST METHODS FROM NATURAL HAZARD MITIGATION SAVES

The project team employs the methods from *Natural Hazard Mitigation Saves* (Multi-Hazard Mitigation Council 2019). Its general procedures are summarized in section 4.2. Many of the decisions required to apply these general methods are also summarized in this chapter. Where the present analysis requires new methodological details, this chapter also explains them and notes why they are required.

## 4.2 ENGINEERING APPROACH TO BENEFIT-COST ANALYSIS

Much of the methodology employed to assess the benefit of a resilient runway can be taken from other parts of *Natural Hazard Mitigation Saves* (Multi-Hazard Mitigation Council 2019). This section briefly explains how an engineering approach to benefit-cost analysis works. Subsequent sections explain any problem-specific aspects of the analysis that cannot be borrowed from *Natural Hazard Mitigation Saves*.

As done in the *Natural Hazard Mitigation Saves 2019 Report*, the project team used an engineering approach to estimate the benefit-cost ratio (BCR). Figure 4-1 and the process below qualitatively summarize the steps of an engineering approach. The quantitative details follow.

1. *Exposure data.* Acquire available data about the assets exposed to loss. Often these data come in formats intended for uses other than those to which the analyst intends to put them.
2. *Asset analysis.* Interpret the exposure data to estimate the engineering attributes of the assets exposed to loss. These attributes (denoted by $A$) may include quantity (e.g., square footage), value (e.g., replacement cost), and other engineering characteristics (e.g., model building type) exposed to loss in one or more small geographic areas. Occasionally assets are described probabilistically (e.g., the probability $P$ that each asset has some set of attributes $A$, given the exposure data $D$, denoted by $P[A|D]$). Combine the data $D$ and the asset model $P[A|D]$ to estimate the probability that the assets have attributes $A$, denoted by $P[A]$.
3. *Hazard analysis.* Select one or more measures of environmental excitation $H$ to which the assets are assumed sensitive (e.g., peak ground velocity), and estimate the relationship between the severity of those measures and the frequency (events per unit time) with which each of many levels of excitation is exceeded. The relationship is denoted as $P[H|A]$, (e.g., the probability that the environmental excitation will take on value $H$, given attributes $A$). Combine $P[A]$ and $P[H|A]$ to estimate the probability of various levels of excitation, denoted by $P[H]$.
4. *Loss analysis.* Select loss measures to quantify, for example, property repair costs, casualties, duration of loss of function, etc. For each taxonomic group in the asset analysis, estimate the relationship between the measure of environmental excitation $H$ and each loss measure $L$. This relationship is called the vulnerability model, denoted by $P[L|H]$. Loss measures are usually expressed at least in

terms of expected value, and often in terms of the probability distribution of loss conditioned on (e.g., given a level of) environmental excitation. Use the theorem of total probability to estimate either the expected value of loss or the probability of exceeding one or more levels of loss, for each loss measure. Sometimes one estimates and separately reports various contributors to loss by asset class, by geographic area, by loss category, etc. One combines $P[H]$ and $P[L|H]$ to estimate the probability of various level of loss, denoted by $P[L]$.

5. *Decision-making.* The results of the loss analysis are almost always used to inform some risk-management decision. Such decisions always involve choosing between two or more alternative actions, and often require the analyst to repeat the analysis under the different conditions of each alternative, such as as-is and assuming some strengthening occurs.

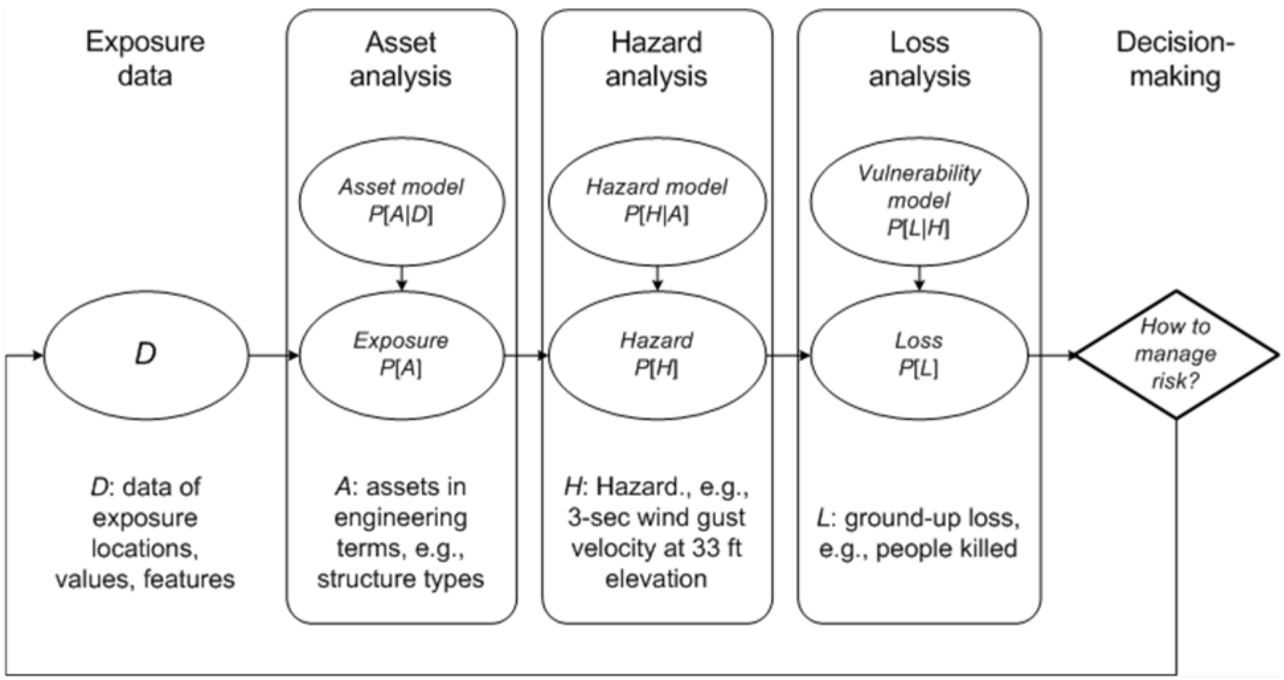


Figure 4-1. An engineering approach to risk analysis (image credit: Porter 2017, used with permission)

This project quantifies the desirability of mitigating the PDX runway using a benefit-cost ratio, meaning the ratio of the present value of reduced future losses (the benefit) to the retrofit cost of the mitigation effort (the cost). The benefit expresses a long-term average over time, considering large and small disasters that may occur at any point in time during the economic life of the mitigation measure, and considering the likelihood that these events will happen at all. The more likely a disaster is to occur, or the more severe its outcomes, the greater the expected value of the benefit that mitigation will produce.

As a consequence of this averaging process, benefit-cost analysis (BCA) has an important limitation when applied to natural hazard mitigation: a benefit-cost ratio by itself tells the decision-maker nothing about the chance that the mitigation measure will actually be needed during the economic life of the project. The rarer the disaster, the less likely that a mitigation measure will produce value by reducing loss. While the benefit-cost ratio accounts for that likelihood through the averaging process, some decision-makers may object to the fact that money is being spent up front to reduce a loss that may never occur during the life of the asset (i.e., the runway), that the benefit of mitigation may only be enjoyed by somebody else, or by nobody at all, and that the money spent on mitigation might have been diverted from another, better, investment with surer, greater, or more near-term benefits.

The foregoing outlines qualitatively how a benefit-cost analysis is performed. Quantitatively, it works as show in Equation 4-1 through Equation 4-3. The equations can be explained as a three-step process:

Step 1. Calculate the project's expected (e.g., average) annualized loss (*EAL*) due to earthquakes in the absence of mitigation, as shown in Equation 4-1. In the equation, $G(x)$ denotes the mean exceedance rate of environmental excitation $x$ (for example, peak ground velocity) to a sample facility; $y(x)$ denotes the mean loss to the facility (as a fraction of value exposed to loss, e.g., replacement value) when subjected to excitation $x$ absent mitigation; and $V$ denotes the value exposed to loss, absent the mitigation. Note that the vulnerability function $y(x)$ represents more than property loss. It also comprises time-element losses, losses associated with deaths and nonfatal injuries, loss of employment, and may include a variety of financial, social, and cultural losses. Then repeat this calculation under remediated conditions, that is, with a mitigation strategy applied. That is, calculate *EAL'* (what-if-mitigated *EAL*) using a what-if-mitigated vulnerability function $y'(x)$, using the same Equation 4-1. In the present case, where the project team uses a few scenario events, each scenario is associated with a mean exceedance frequency $G(x)$ where $x$ is ground motion at PDX, its scenario loss is represented as $V \times y(x)$, and Equation 4-1 is evaluated numerically, assuming $\ln(G(x))$ decreases linearly with $x$ and $V \times y(x)$ increases linearly with $x$.

In some situations, Equation 4-1 involves integration over time. That is, $V$, $G$, and perhaps $y$ may also be functions of time, so the equation more properly has a second integral over time. The second integral is omitted from the equation for clarity. Nonstationary value and hazard are serious concerns for a long-lived asset like a runway. Nonstationary vulnerability is more dubious than time-varying value and hazard. The temporal changes of material strength and stiffness observed in the laboratory, such as with concrete cylinder strength, are small compared with uncertainty in vulnerability. The analysis generally assumes therefore that engineering vulnerability $y$ remains constant over time.

Step 2. Calculate the benefits for the mitigation (denoted by $B$) over time $t$, as shown in Equation 4-2. The term $r$ denotes the after-inflation annual discount rate (which measures the time value of money), and $t$ denotes the number of years that mitigation strategy $i$ is effective. Note that Equation 4-2 accounts for the possibility that the mitigation measure is never actually used—that the earthquake does not occur during the effective life of the mitigation measure. It also says that benefits do not accrue after time $t$.

In the present case, the project team analyzes benefits using both a 3% discount rate, approximately consistent with the government's after-inflation cost of borrowing, and 7%, consistent with OMB Circular A-94's base case. No discount rate is applied to the acceptable cost to avoid future statistical deaths and injuries, because OMB's logic to justify a discount rate speaks solely to people's preference for money now versus money later, not to their view of the value of human life.

What about the project life *t*? While the useful lifespan of a runway typically is 15 to 20 years, its foundation soils have an effectively infinite life; any repaving of the runway would be done over the remediated foundation soils, so the remediation has an effective useful life if the airport will continue to serve the Portland metropolitan area, conceivably for centuries. A useful project life of *t* = 100 to 150 years seems defensible, but the difference in the present value of a constant annuity of 100 years versus 150 years is very small, even at a 3% annual discount rate. The project team therefore uses a useful project life of *t* = 100 years, consistent with the assumptions in Natural Hazard Mitigation Saves for utilities and transportation infrastructure.

Step 3. Calculate the benefit-cost ratio (BCR), as in Equation 4-3. In the equation, *C* denotes the cost of the mitigation measure.

$$EAL = V \int_0^\infty -\frac{dG(x)}{dx} y(x) dx \qquad \text{Equation 4-1}$$

$$B = \frac{EAL - EAL'}{r}\left(1 - exp(-rt)\right) \qquad \text{Equation 4-2}$$

$$BCR = \frac{B}{C} \qquad \text{Equation 4-3}$$

Alternatively, loss may be expressed as a function of mean exceedance frequency, e.g., the loss given the shaking with mean recurrence intervals of 72 yr, 225 yr, 475 yr, 975 yr, and 2475-yr exceedance frequencies. EAL can be exactly numerically integrated by assuming that loss is linearly proportional to the natural logarithm of exceedance frequency. In such a case, let:

$g$ = excitation exceedance frequency in $yr^{-1}$

$V$ = value exposed to loss

$y(g)$ = loss per unit value conditioned on excitation with exceedance frequency $g$
$\approx m \cdot \ln(g) + b$, perhaps piecewise linear over $n+1$ points (or $n$ increments) $\{g_0, g_1, g_2, \ldots g_n\}$

Integrating over the $n$-1 increments,

$$
\begin{aligned}
EAL &= \sum_{i=0}^{n-1} \int_{g_i}^{g_{i+1}} V \cdot y(g) \cdot dg \\
&= \sum_{i=0}^{n-1} V \cdot \int_{g_i}^{g_{i+1}} \left(m_i \cdot \ln(g) + b_i\right) dg \\
&= \sum_{i=0}^{n-1} V\left(m_i \cdot \left(g \cdot \ln(g) - g + c_i\right) + b_i g + d_i\right)\Big|_{g_i}^{g_{i+1}} \\
&= \sum_{i=0}^{n-1} V \cdot m_i \cdot \left(g_{i+1} \ln(g_{i+1}) - g_i \ln(g_i) - g_{i+1} + g_i\right) + V \cdot b_i \cdot \left(g_{i+1} - g_i\right)
\end{aligned}
$$

*Equation 4-4*

Where

$$
m_i = \frac{y_{i+1} - y_i}{\ln(g_{i+1}) - \ln(g_i)}
$$

*Equation 4-5*

$$
b_i = y_i - m_i \ln(g_i)
$$

*Equation 4-6*

It is necessary to estimate the value of *g* associated with the initiation of loss. In cases where we do not already know that value, we extrapolate from the relationship between peak ground acceleration and mean recurrence interval.

## 4.3 BENEFIT CATEGORIES CONSIDERED HERE

Most of the benefit categories considered here were also considered in *Natural Hazard Mitigation Saves*. Relevant benefit categories considered here include:

- Medical evacuation, which helps to avoid deaths among severely injured people who would overwhelm local hospital resources. The estimated number of injuries relies largely on methods previously described in *Natural Hazard Mitigation Saves*, with some novelties described later in this chapter.
- Reduced business interruption and additional living expenses associated with faster safety evaluation of buildings damaged throughout the study area. The benefit category appears to be new. That is, the project team is unaware of any prior study estimating these benefits. The analysis relies partly on methods used in *Natural Hazard Mitigation Saves*. Novel aspects are described later in the chapter.
- Business interruption at PDX and in nearby businesses that rely on PDX, such as nearby hotels. Methods are largely identical to those used in *Natural Hazard Mitigation Saves*, albeit with some enhancements (described later in the chapter) made possible by the local nature of the study, that is, because the study addresses one particular metropolitan area rather than the whole nation.

- Runway repair costs. These are taken from HNTB Corporation's (2015) estimates, shown in Table 5-2, except that downtime is taken to be zero thanks to GRI's (2020) remediation design.
- Defense benefits. This benefit category was not addressed in *Natural Hazard Mitigation Saves*, and a new approach was required. It is detailed later.

## 4.4 SEISMIC HAZARD ANALYSIS

*Natural Hazard Mitigation Saves* used a different hazard method than the one described here because it mostly dealt with individual assets rather than geographically dispersed systems. For the latter, seismic hazard must be characterized via a handful of earthquake scenarios rather than with a hazard curve that depicts ground motion versus exceedance frequency. First, because liquefaction depends on ground-motion duration, in addition to ground-motion intensity. Second, because simultaneous landsliding on access routes reflects a regional problem, not hazard at a point; only with a suite of ground-motion fields can we realistically reflect that regional problem. To design the scenarios requires several steps:

1. Select a geographic point at which to calculate hazard.
2. Select exceedance frequencies on the hazard curve at which to calculate scenarios.
3. Deaggregate hazard at that location and at each exceedance frequency to identify scenarios, each characterized by rupture source, magnitude, location, and epsilon (a measure of the degree to which ground motion in the event exceeds or falls below the median).
4. Calculate maps of median shaking in each scenario.
5. Overlay one or more spatially correlated random fields to represent between-event and within-event uncertainty. Here, "uncertainty" refers to the fact that real ground-motion maps tend to be blotchy and differ from the median value one would calculate for a given earthquake magnitude and distance. "Between-event uncertainty" refers to the fact that earthquakes tend to produce overall motion that is somewhat higher or lower than one would expect over the whole shaken area. "Within-event uncertainty" refers to the blotchiness of real ground-motion maps, with some spots experiencing above-median motion, others experiencing below-median motion, and still others experiencing motion around the median. "Spatially correlated" refers to the fact that the closer two addresses are together, the more likely they are to experience similar motion—similarly higher or lower than the median—which gives blotches a characteristic width.

The project team selected the geographic location of the Port of Portland, 7200 NE Airport Way, Portland OR, for want of a demonstrably better choice. Its geographic coordinates are 45.5871N, 122.5911W.

The project team used the same mean recurrence intervals as HNTB Corporation (2015) did: 72 years (50% exceedance probability in 50 years), 225 years (20% exceedance probability in 50 years), 475 years (10% exceedance probability in 50 years), 975 years (5% exceedance probability in 50 years), and 2,475 years (2% exceedance probability in 50 years).

The project team used the U.S. Geological Survey's (ND) Unified Hazard Tool to disaggregate hazard and select scenarios. The tool provides a 3-dimensional bar chart of the earthquake magnitude-distance pairs most likely to cause ground motion with a given exceedance frequency. Each bar corresponds to one magnitude-distance pair. Its height reflects the degree to which that magnitude-distance pair contributes to the likelihood of shaking with the specified mean exceedance frequency. The tallest bar is the one most likely to cause the specified ground motion, and therefore represents the leading choice for a scenario. Figure 4-2 shows an example: the disaggregation at PDX of the ($M_w$, $r_{Rup}$) pairs that are most likely to cause 5%-damped, elastic spectral acceleration response at 1-second period (SA10) with 20% exceedance probability in 50 years.

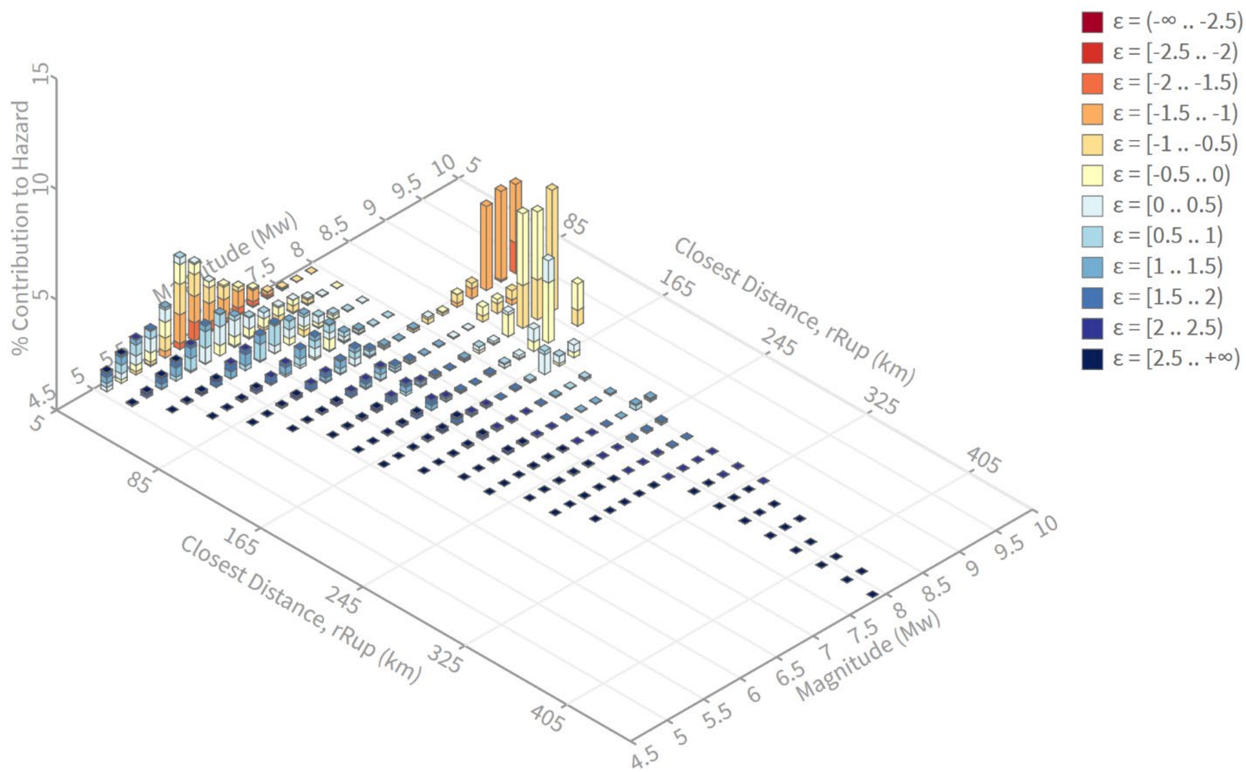


Figure 4-2. Hazard deaggregation for 5%-damped, 1-second elastic spectral acceleration response with 20% exceedance probability in 50 years

The unified hazard tool disaggregates hazard in combinations of moment magnitude ($M_w$), rupture distance ($r_{Rup}$) and the number of standard deviations of a single predicted value of the natural logarithm of the ground motion measure above or below the mean of the natural logarithm of ground motion. The number is denoted by $\varepsilon$. For example, $\varepsilon$ = -0.62 indicates that in a combination of $M_w$ and $r_{Rup}$, the natural logarithm of ground motion is 0.62 standard deviations smaller than the mean of the natural logarithm of ground motion. Part of the standard deviation is attributable to between-event uncertainty (variability of the whole ground-motion field from earthquake to earthquake), part to within-event uncertainty (variability of ground motion in each earthquake from location to location).

To calculate maps of shaking in each scenario, the project team used a product of the U.S. Geological Survey and the Southern California Earthquake Center. These organizations provide by far the most powerful, authoritative resource to create such maps: a suite of Java applications collectively called OpenSHA (Field et al. 2003).

Key input parameters for the OpenSHA tool are as follows. One can take the rupture surface from any of a variety of sources. For example, for the Cascadia Subduction Zone, Park et al. (2017) provide the fault location. Between-event probability level is taken as equal to ε from the hazard disaggregation. Within-event variability is discussed later. For the Cascadia Subduction event, one can estimate the hypocenter (the place where the rupture initiates) at the midpoint between the north and south ends of the fault trace. For a large subduction earthquake, one can use Zhao et al.'s (2006) ground-motion-prediction equation (which estimates ground motion such as peak ground acceleration as a function of earthquake magnitude, earthquake location, and site characteristics). Site characteristics are taken from Wald and Allen (2007).

As of this writing, OpenSHA lacks the newer ground-motion-prediction equations discussed earlier, on which GRI (2020) and therefore the Port of Portland rely. The project team therefore calibrated ground motions estimated using OpenSHA by factoring PGA estimates by a single factor selected so that when one calculates PGA with OpenSHA and multiplies by this factor, it matches GRI's (2020) weighted-average estimate shown in Table 3-1. The project team similarly scaled all SA10 motions. Note that the project team performs the calibration on an apples-to-apples basis:

- Same geographic location: midpoint of the 6,000-ft remediated segment of the south runway, near GRI's boring B-3, at approximately 45.5846N, -122.5945E.
- Same site conditions as GRI's calculations: a hypothetical rock outcrop with average. shearwave velocity in the upper 30 meters of soil (*Vs30*) of *Vs30* = 2,100 ft/sec (approximately 640 m/sec) as defined in ASCE/SEI 7-16 (2016).
- Same earthquake fault rupture: a megathrust interface earthquake on the Cascadia Seismic Zone.
- Same magnitude: $M_W$ 9.0.
- Same nonexceedance probability: 84%, to which GRI refers as the mean plus one standard deviation of ground motion.
- Where spatial interpolation is required, it is performed assuming that within a rectangular grid of four nearby points, ground motion at some midpoint takes on the value $z(x,y)$ as shown in Equation 4-7. In the equation, $x$ and $y$ are the longitude and latitude of a point on the earth's surface, and the four nearest gridpoints are located at $(x_0,y_0)$, $(x_1,y_0)$, $(x_0,y_1)$, and $(x_1,y_1)$. The coefficients $a_0$ through $a_3$ are calculated so that $z(x,y)$ matches the estimated motions at the four nearby gridpoints.

$$z(x,y) = a_0 + a_1\frac{(x-x_0)}{(x_1-x_0)} + a_2\frac{(y-y_0)}{(y_1-y_0)} + a_3\frac{(x-x_0)}{(x_1-x_0)}\frac{(y-y_0)}{(y_1-y_0)} \quad \text{Equation 4-7}$$

See Porter (2020) section 6.3.4 for details of the approach used here to simulate properly spatially correlated random fields of ground motion. The project team randomly selected among a number of previously-generated maps of properly spatially correlated random fields of a standard normal distribution. Figure 4-3 presents an example. In the figure, the horizontal and vertical axes measure distance in kilometers east and north, respectively, from an arbitrary geographic location, and the map color (denoted by ePGA in the legend) measures the value of the standard normal variate at that location. Then the ground motion at any given location in a scenario is estimated as

$$y_o^{(i)} = \hat{y}_o e^{\left(\varepsilon_0 \cdot \tau + \varepsilon_1^{(i)} \phi\right)}$$ *Equation 4-8*

where:

$o$ = an index to a geographic location

$i$ = an index to a realization of $M$ spatially correlated random ground-motion fields, $i \in \{0, 1, \ldots M\text{-}1\}$

$y_o^{(i)}$ = realization $i$ of ground motion at $o$, with inter- and intra-event uncertainty and spatial correlation

$\hat{y}_o$ = median ground motion at location $o$

$\tau$ = between-event uncertainty term in ground-motion prediction equation

$\phi$ = within-event uncertainty term in ground-motion prediction equation

$\varepsilon_0$ = the number of standard deviations of the predicted value of the natural logarithm of the ground motion measure above or below the mean of the natural logarithm of ground motion

$\varepsilon_1^{(i)}$ = realization $i$ of spatially correlated zero-mean, unit-standard-deviation normal variate at location $o$ for within-event uncertainty

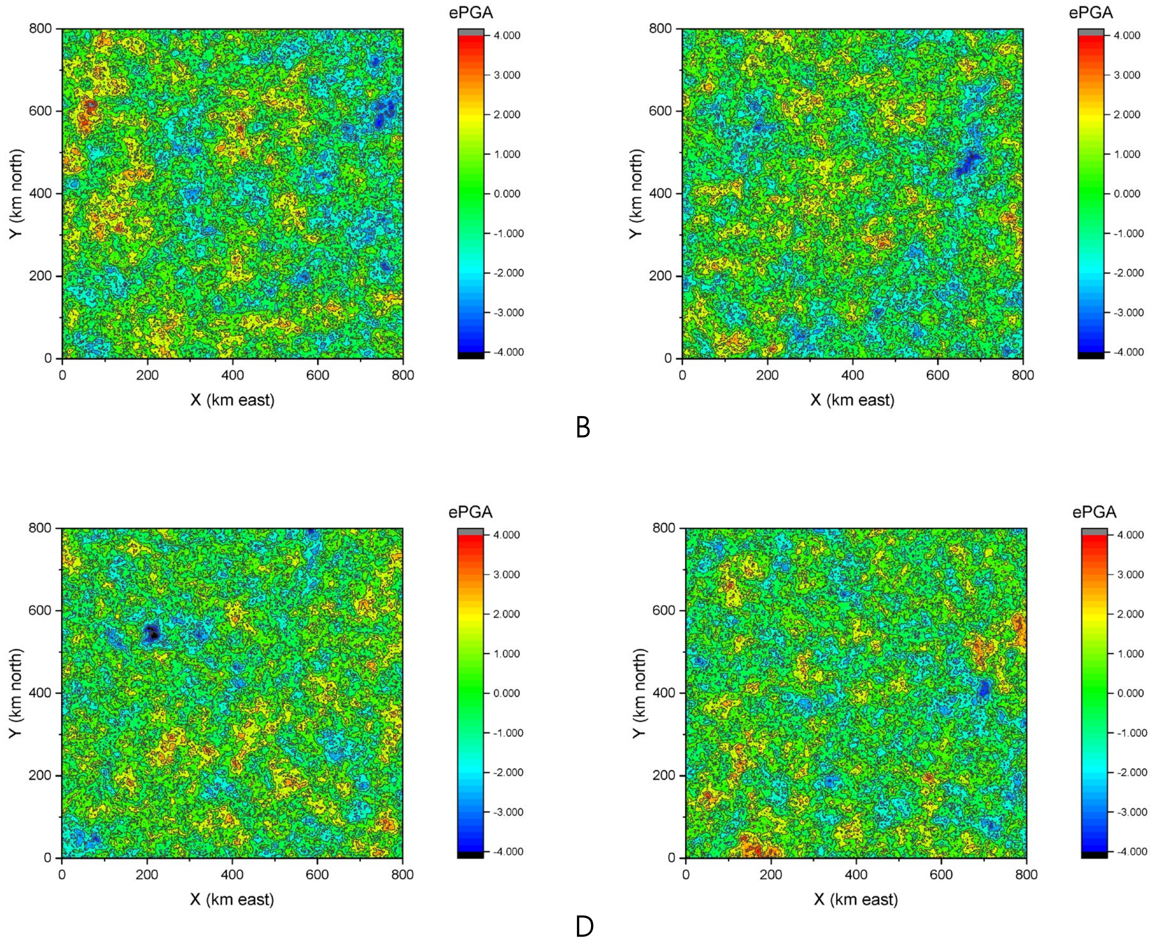


Figure 4-3. Four realizations of a spatially correlated random field of Gaussian variates (Porter 2020)

Note that equation 4-7 applies $\varepsilon_0$ to between-event ground motion uncertainty, but not to within-event ground-motion uncertainty. The project team considered at least three choices: (1) adjust median ground motion by a factor exp($\varepsilon_0 \cdot \tau + (\varepsilon_0 + \varepsilon_1^{(i)}) \cdot \phi$), (2) adjust median ground motion as shown in equation 4-7, or (3) something in between. Option 1 tends to overestimate uncertainty in ground motion because it would treat the within- and between-event variability as perfectly correlated, that is, treating total uncertainty as the simple sum of $\tau$ and $\phi$, whereas seismologists sum their squares. Because of nonlinearity in vulnerability, greater ground-motion uncertainty tends to increase the expected value of loss and therefore the expected value of the benefit of retrofit. Option 2 tends to underestimate uncertainty, because $\varepsilon_1$ is a zero-mean variable. It would therefore tend to underestimate benefit. One can imagine a middle-ground approach (3) with a factor exp($\varepsilon_0 \cdot \tau + (\alpha \cdot \varepsilon_0 + \varepsilon_1^{(i)}) \cdot \phi$), with the parameter $\alpha$ chosen within $0 < \alpha < 1$ so that total uncertainty comes out somewhere near $(\tau^2 + \phi^2)^{1/2}$. The project team is unaware of any precedent for such an approach and opts not to introduce one. Given a choice between over- and under-estimating benefit—options 1 and 2—the project team opts for the latter, more conservative approach.

To estimate ground motion requires a modeling element called a ground-motion-prediction equation, which is a mathematical relationship that estimates ground motion as a function of earthquake magnitude, distance, site conditions, and other parameters. OpenSHA offers many options for ground-motion-prediction equation to use. However, only one applies to megathrust earthquakes like the Cascadia Subduction Zone events considered here. That one ground-motion-prediction equation is documented in Zhao et al. (2006).

The seismological community has learned much since 2006. The 2011 Tohoku earthquake occurred after Zhao et al. developed their ground-motion-prediction equation for megathrust earthquakes. It produced a large quantity of new earthquake observations that informed several new ground-motion-prediction equations. Among these are ground-motion-prediction equations by Zhao et al. (2016), Abrahamson et al. (2018), Parker et al. (2020a), and Kuehn et al. (2020). A map of ground motion derived using these models differs somewhat from maps created using Zhao et al. (2006).

It was impractical either to add these newer ground-motion-prediction equations to OpenSHA or to use alternative software to create the maps of ground motion, so the project team addressed the problem as follows.

1. Estimate ground-motion maps in OpenSHA using the Zhao et al. (2006) ground-motion-prediction equation.
2. Estimate the $84^{th}$ percentile ground motion in terms of peak ground acceleration (PGA) and 1-second 5% damped elastic spectral acceleration response (denoted SA10) at PDX with OpenSHA using the Zhao et al. (2006) ground-motion-prediction equation.
3. Compare the results of step 2 with estimates offered by GRI (2020, Table 1C).
4. Calibrate maps from OpenSHA from step 1 by the ratio of GRI's ground-motion estimate to that of step 2. Factor maps of PGA by the ratio of GRI's PGA to that of OpenSHA. Factor maps of SA10 by the ratio of GRI's SA10 to that of OpenSHA.
5. The project team did *not* attempt to calibrate motions so that they also match the PGA values estimated by USGS in the hazard deaggregation. The USGS's ground-motion estimates date to 2014, so they predate the newer ground-motion-prediction equations. The USGS hazard deaggregation is used solely to identify the best proxy earthquake (with magnitude, location, and nonexceedance probability) for a 72-year mean recurrence interval, 225 years, etc.

## 4.5 ESTIMATING MEDICAL EVACUATION BENEFITS

PDX expects that a resilient runway will enable it to provide for transport of health and medical resources after the first 24 to 72 hours (Portland International Airport 2019 p. II-9). The project team estimated the benefits of enhanced life safety from having a resilient runway based on these assumptions:

- The demand for medical care could exceed local resources
- Additional care and mutual aid will be transported through PDX if the runway is operational
- One can partly attribute the provision of care above local capacity to the resilient runway

- Care transported through PDX can prevent severe nonfatal injuries from becoming fatal
- Care transported through PDX can alleviate the distress of less severely injured people who nonetheless require hospital treatment
- Care will be transported through PDX for the portion of the study area that is closer to PDX than to Hillsboro, taken here as Multnomah, Columbia, Cowlitz, Clark, Skamania, and Clackamas counties.

The project team therefore quantified benefits associated with transporting health and medical resources through PDX as follows.

1. Use building-stock information discussed previously to estimate the number of people in each of many building types by census tract and time of day (day, night, commute)
2. Estimate ground motion by earthquake scenario (72-year, 225-year, etc.) and census tract with Equation 4-7.
3. Use the life-safety vulnerability functions by Porter (2009b) to estimate deaths and nonfatal injuries by census tract in each combination of scenario and time of day. Note that *Natural Hazard Mitigation Saves* also used these functions.
4. Assume that area hospitals are functional and can receive patients to the extent of their capacity, and that at the time of the earthquake they are already at 68% capacity (Halpern et al. 2016).
5. All severity-2 injuries (those that are not life-threatening but require medical technology) will be treated at a hospital emergency room, but will be triaged for treatment after severity-3 injuries.
6. All severity-3 (life-threatening) injuries are also treated at a hospital emergency room and require an ICU or ED bed. Assume all severity-3 injuries that cannot be treated at a hospital result in fatalities. Thus, one can estimate avoided fatalities by PDX having an operating runway as:

$$\Delta F = \left( I_3 - 0.32 \cdot H \right) \cdot O \qquad \textit{Equation 4-9}$$

   Where $\Delta F$ denotes fatalities avoided conditioned on an earthquake, $I_3$ denotes the expected value of the number of severity-3 injuries in the subset of counties near PDX, given the earthquake, $H$ denotes the number of ICU and ED beds in hospitals in those counties, and $O$ is variable to indicate the fraction of the first 72 hours that PDX can provide life-saving resources, e.g., $O$ = 2/3 if victims can be transported to emergency medical care within 24 hours, 1/3 if it will be 48 hours before victims can receive care, 0 if 72 hours or more. The equation assumes that hospital staffing and resources approximately match the availability of beds.
7. The acceptable cost to avoid the resulting fatalities is taken as

$$B = \Delta F \cdot \left( V_4 - V_3 \right) \qquad \textit{Equation 4-10}$$

   Where $V_3$ denotes the acceptable cost to avoid a severity-3 injury and $V_4$ denotes the acceptable cost to avoid a statistical death, taken here as $4.0 million and $10.2 million, respectively, from US Department of Transportation (2015), increased for inflation using the Consumer Price Index.

8. The value of Δ*F* varies by time of day. It is calculated at 2 PM, 2 AM, and 5 PM. The three values can be weighted according to the average number of hours people occupy workplaces, are at home, and in transit, taken here as 25%, 67%, and 8%, respectively.
9. Only a fraction of the benefit *B* is attributable to having a resilient runway; emergency medical personnel and their logistical support also contribute to the benefit. For simplicity, the project team split the benefit evenly between PDX and the other necessary resources.

# 4.6 ESTIMATING BENEFITS OF FASTER SAFETY EVALUATION

## 4.6.1 Motivation and Approach to Estimating Access Delays

A large regional earthquake will cause heavy damage to the building stock. Many buildings will experience alarming visual damage that will cause users to vacate buildings until the buildings are either repaired or determined to be safe to enter and occupy. Judging by past earthquake experience, such as in the 1994 Northridge earthquake, most buildings with visually alarming damage will probably be safe to enter and occupy. The California Governor's Office of Emergency Services has designed the de facto standard process for evaluating post-earthquake building safety, a process called Safety Assessment Program (SAP). The process requires brief (15-30 minute) in-person inspection by teams of trained building professionals (structural engineers, architects, building inspectors, and a few others) called SAP evaluators.

SAP evaluation cannot take place remotely. SAP evaluators must be able to travel to the building. SAP evaluators must receive advanced training and certification. Potentially hundreds of thousands of buildings in the Pacific Northwest will require SAP evaluations after a large Cascadia earthquake, requiring thousands of SAP evaluators, far more than are available within the Willamette Valley. Almost all the evaluators will have to travel from outside the Willamette Valley to perform the evaluations. The longer it takes the evaluators to arrive, the longer it takes before possibly tens of thousands of buildings can be reoccupied, at the cost of potentially millions of dollars or more in lost business per day.

SAP evaluators can arrive by air through PDX or by road, through a few routes. The roads are subject to damage by landslides and bridge damage. A resilient runway can make the difference between a few days' travel delay and several weeks. To assess the value of a resilient runway in speeding SAP evaluations, the project team calculated the travel delays without and with a resilient runway and the resulting benefit of faster re-occupancy of buildings. The decreased future losses contribute to the estimated benefits of a resilient runway.

## 4.6.2 Steps to Calculate Safety Evaluation Delays

The following sections explain the project team's methodology to estimating that benefit, in the following steps. The next five sections detail the project team's methodology for each of these steps.

1. Identify access routes: SAP evaluators can arrive in the Portland area by air or by a finite number of highway routes. Identify them.
2. Calculate access delays from landslide damage to roads: how long will it take to reopen mountainous highway routes into the study area?
3. Calculate access delays from bridge damage within the study area: how long will it take to reopen roads within the Willamette Valley so that SAP evaluators can reach the study area?
4. Synthesize access delays: for each route in step 1, find the time required to clear landslides (step 2) and repair bridges (step 3). SAP evaluators can be assumed to arrive shortly after the first route opens, perhaps 2-3 days.
5. Building stock: estimate the quantity, location, and engineering attributes of buildings exposed to damage in the study area.
6. Quantity with delayed re-occupancy: how many buildings evaluated using the ATC-20 methodology (Applied Technology Council 2006) will be deemed safe to reenter and occupy (assigned a green placard under ATC-20)?

### 4.6.3 Identify Access Routes

The roadway network is quite complex. One could perform a full analysis of the entire roadway network to enumerate probably tens or hundreds of thousands of routes. The project team simplified the available routes to approximately 10, reasoning that after a major earthquake, drivers will only try to arrive using a route over interstate freeways, U.S. highways, and Oregon state highways. This network is much simpler.

### 4.6.4 Estimate Access Delays from Landslides

The landslide analysis aims to estimate the potential for earthquake-induced landslides to block roadway access to the study area. Earthquake-induced landslides tend to occur in steep terrain, so the analysis focuses on roads that follow mountainous routes to the study area from just outside regions of steep terrain. The first step in the analysis is to identify such routes.

For each such route, one selects a starting point on a highway into the study area just outside the mountainous parts. Additional points are selected based solely on distance along the road from the previous point. The project team used Google Earth to sample highway slopes at points spaced approximately 5,000 meters apart along the routes into the study area. That distance seems to provide enough resolution of the distribution of slopes that closer spacing would not substantially increase the accuracy of the distribution, while remaining practical to carry out manually.

One estimates the hillside slopes adjacent to both edges of pavement by measuring out a 30-meter horizontal distance perpendicular to the roadway alignment and observing and recording the elevation change from the edge of the pavement to the point 30 meters away. The vertical angle from the edge of the pavement to the point 30 meters away in plan is calculated using trigonometry. One records the larger of the two angles, since that side is more likely to experience a landslide.

At each sample location, one estimates geologic unit of soil using an authoritative map of geological units. The project team used Walker and MacLeod's (1991) geologic map of Oregon. From the description of the geologic unit, one identifies Wilson and Keefer's (1985) geologic group.

Using the geologic group and slope, one calculates critical acceleration $a_c$ with Equation 3-1. Peak ground acceleration ($a_{max}$ of Equation 3-2) at each site is calculated for each scenario earthquake and each of many realizations of within-event ground-motion variability. With $a_c$, $a_{max}$, and $M_w$, one calculates slope displacement $D_N$ using Equation 3-2, slope failure probability $P_f$ using Equation 3-4, and probability that the landslide will have severity $A$ using Equation 3-5. Since the equations provide probability that a landslide will occur in any 10-meter gridcell, one estimates the number of severity-$A$ landslides by multiplying the output of Equation 3-5 by the distance between sample locations divided by 10 meters.

Such a calculation is slightly conservative (underestimating number of landslides), because it assumes that only landslides in the gridcell immediately adjacent to the roadway will affect the road. That is, landslides that occur farther than 10 meters from the edge of the road but not immediately adjacent to the edge of the road are ignored. The calculation also assumes that only one side of the road will experience a landslide, ignoring the possibility that both sides experience a landslide.

Why make *any* conservative assumptions about landslides? The more landslides one estimates, the greater will be the estimated benefit of mitigating the PDX runway. Erring on the side of lower estimated landslides reduces the chance that the benefit-cost analysis will overestimate benefit, which makes the benefit-cost analysis more defensible.

The landslide repair duration is calculated by multiplying the number of estimated landslides by the estimated repair duration divided by the number of available repair crews, as in Equation 4-4:

$$\tau_L = \frac{L \cdot D}{F}$$

*Equation 4-11*

In the equation, $\tau_L$ is the number of days required to restore access to the study area, $L$ is the estimated number of very severe landslides along highway access routes, $D$ is the number of days to clear one landslide (3 weeks plus or minus 16 days), and $F$ is a factor to account for the number of landslides that can be accessed from either end of the route and from side roads that intersect it. Note that to open one lane takes about half as long as the time required to complete repairs, aside from guardrails, signs, and other accoutrements (C. Mohney, Oregon Department of Transportation, Engineering Geology Program Lead, verbal commun., July 22, 2020).

How to estimate $F$? The following analytical procedure was developed in conversation with the Oregon Department of Transportation to estimate restoration time (C. Mohney, Oregon Department of Transportation, Engineering Geology Program Lead, verbal commun., July 22, 2020). Consider three possible situations illustrated in Figure 4-4, Figure 4-5, and Figure 4-6 involving a hypothetical highway (double line), landslides (ovals), junctions with other roads that provide alternate access to the highway (single lines that meet the highway) and repair crews (bulldozers). Let *L* denote the number of landslides, *J* denote the number of junctions, and *C* denote the number of repair crews.

First, see Figure 4-4. In this situation, there are many more landslides than junctions ($L >> J$), so repairs are limited by access. Each junction provides access to two nearby landslides (green ovals), and the ends each provide access to one landslide. One must at least partially clear one landslide to access the next (red ovals). Thus, $F = 2J + 2$, because each junction provides access to two landslides.

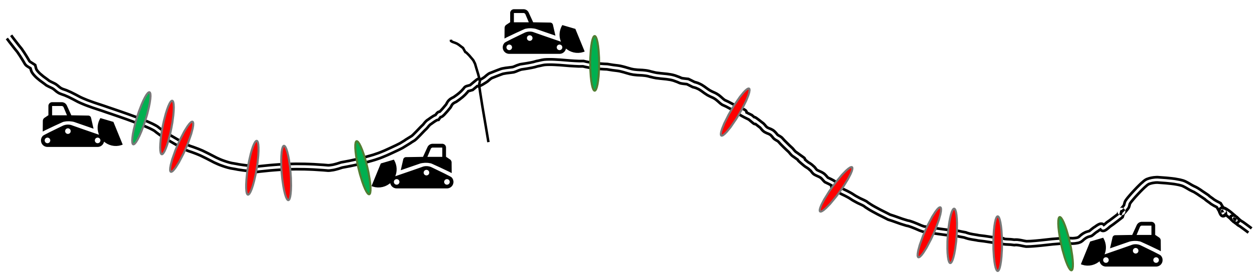

Figure 4-4. Accessing landslides in situations of limited access

In the second situation, junctions provide plenty of access ($J >> L$), so one can access all, or almost all, landslides simultaneously, and $F = L$.

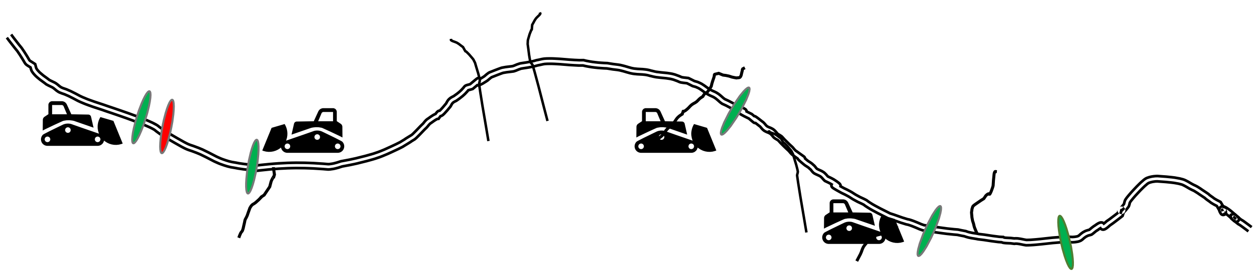

Figure 4-5. Accessing landslides in situations of plentiful access

In the third situation, repairs are limited by the number of available crews ($L >> C$), so $F = C$. More precisely, one assumes that each very severe landslide requires 3 crews to repair, so $F = C/3$.

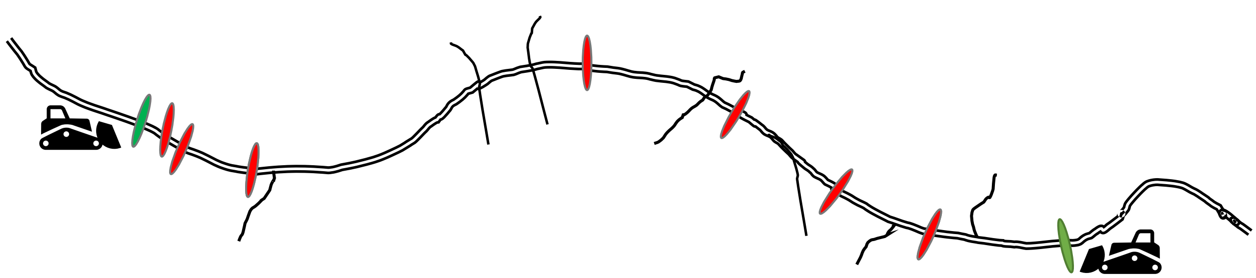

Figure 4-6. Repairing landslides in situations of limited repair resources

Then one can estimate $F$ as:

$$F = \min\left(2J + 2, L, \frac{C}{3}\right)$$ Equation 4-12

where $J$ denotes the number of junctions between the end points along the route, $L$ denotes the number of landslides, and $C$ denotes the number of available repair crews. The number of available repair crews is taken as 2 to 3 times the number of grading contractors available to ODOT, based on the assumption that some contractors can field multiple crews, some can only field one, and some will be available from outside of Oregon (C. Mohney, Oregon Department of Transportation, Engineering Geology Program Lead, verbal commun., July 25, 2020).

The time required to clear landslides along a given route, denoted by $\tau_{L,r}$, will depend on how crews are allocated. Oregon Department of Transportation will probably prioritize certain routes over others, rather than try to allocate crews so that every route opens at the exact same time. As calculated above, $\tau_L$ is the time when the last landslide is cleared, but some routes will have their landslides cleared before the others. The project team approximates landslide repair time along each route as proportional to the number of landslides on that route.

$$\tau_{L,r} = \tau_L \cdot \frac{L_r}{Max_r\{L_r\}}$$ Equation 4-13

### 4.6.5 Estimate Access Delays from Bridge Damage

It may not be only the landslides that isolate the Portland area from outside aid, but damage to highway bridges within the Willamette Valley. The project team estimated damage to highway bridges using Basoz and Mander's (1999) bridge fragility functions, which are also adopted by Hazus-MH, and the restoration times used by Hazus-MH (NIBS and FEMA 2012). The project team only considers Basoz and Mander damage states 4 and 5 as likely to close a bridge. Mean bridge repair time for a given bridge $i$ can then be estimated using the theorem of total probability as follows:

$$E\left[\tau_{B,i} \middle| X = x, C = c\right] = \sum_{d=4}^{5} P\left[D = d \middle| X = x, C = c\right] \cdot E\left[\tau_{B,i} \middle| D = d\right]$$ Equation 4-14

$$\begin{aligned} P\left[D = d \middle| X = x, C = c\right] &= \Phi\left(\frac{\ln\left(x/\theta_{c,d}\right)}{\beta_{c,d}}\right) - \Phi\left(\frac{\ln\left(x/\theta_{c,d+1}\right)}{\beta_{c,d+1}}\right) \qquad 1 < d < 5 \\ &= \Phi\left(\frac{\ln\left(x/\theta_{c,d}\right)}{\beta_{c,d}}\right) \qquad d = 5 \end{aligned}$$ Equation 4-15

Where

$E[Q|B]$ = expected value of quantity $Q$ given that $B$ is true

$P[A|B]$ = probability that $A$ is true given that $B$ is true

$\Phi(z)$ = Gaussian cumulative distribution function evaluated at $z$

$\tau_{B,i}$ = bridge re-opening time for bridge $i$; expected values taken from Table 3-8.

$X$ = uncertain level of shaking (PGA)

$x$ = a value of $X$

$D$ = uncertain bridge damage state

$d$ = a value of $D$

$C$ = Basoz-Mander bridge class

$c$ = a value of $C$

$\theta_{c,d}$ = median capacity of bridge class c and damage state $d$, from Table 3-7.

$\beta_{c,d}$ = standard deviation of the natural logarithm of capacity of bridge class $c$ and damage state $d$, which as noted in chapter 3 can be taken as 0.6 regardless of $c$ and $d$.

Figure 4-7 presents the results of the foregoing calculations using the selected parameter values.

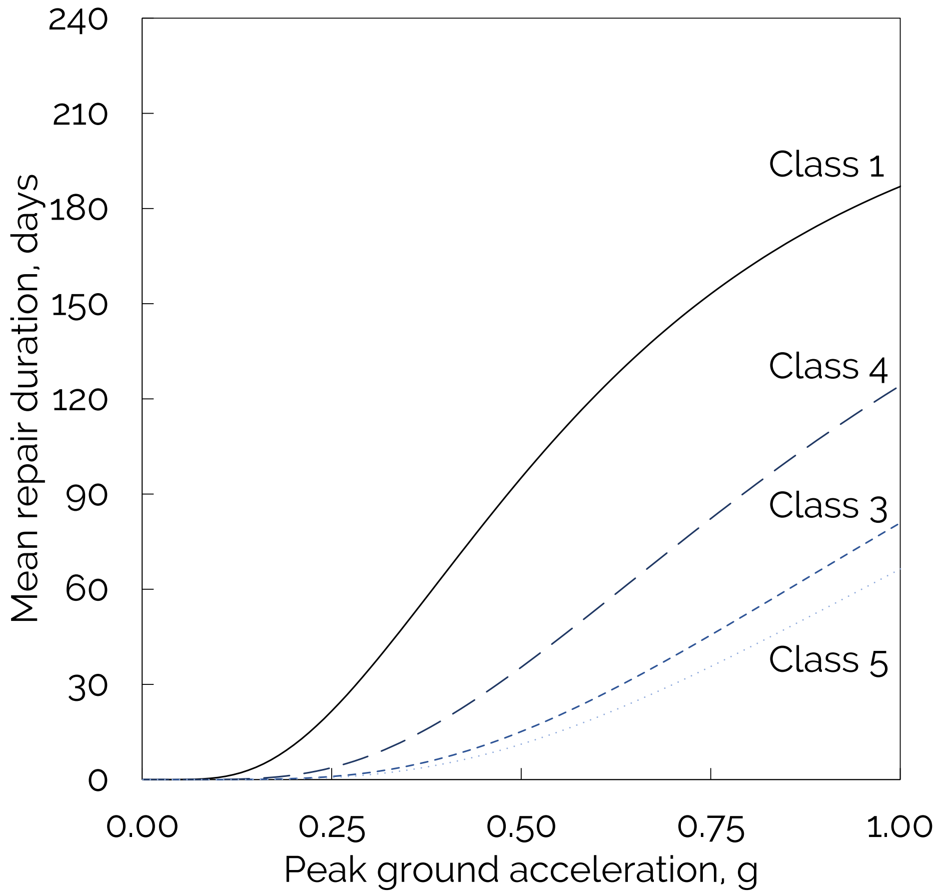


Figure 4-7. Mean bridge repair duration as a function of peak ground acceleration

One could in principle use sophisticated highway network analysis tools, especially Reference Engineering Data Automated Retrieval System (REDARS, Werner et al. 2006), which was used in *Natural Hazard Mitigation Saves*. Doing so would be excessively burdensome, so the project team used a more-approximate approach, as follows. Highway bridge damage only prevents SAP volunteers from mobilizing to the Willamette Valley if each of the key highway routes has at least one bridge that cannot be safely used (technically, in the extensive or complete damage state), ignoring damage to bridges with modest (no more than 10 km) detours. Highway bridge locations, routes, classification under Basoz and Mander's grouping, and detour distance are taken from the National Bridge Inventory (Federal Highway Administration 2020).

Conceivably, limited quantities of bridge designers and repair crews could cause additional delays beyond those modeled by Hazus-MH, but it seems both more practical and more conservative (in the sense of estimated lower losses and therefore smaller mitigation benefits) to ignore this possibility.

## 4.6.6 Aggregate SAP Mobilization Time

The repair duration for roadway route *r*, denoted here by $\tau_r$, can be taken as the larger of the landslide and bridge repair durations for that route, $\tau_{L,r}$ and $\tau_{B,r}$. The equation includes appropriate mobilization times $\tau_{LMob}$, and $\tau_{BMob}$, meaning mobilization time to perform landslide and bridge damage reconnaissance, contract with repair crews, and time for repair crews to arrive and begin work.

$$\tau_r = Max\left\{\tau_{L,r} + \tau_{LMob}, \tau_{B,r} + \tau_{BMob}\right\}$$ Equation 4-16

The time between the mainshock and when SAP evaluators arrive by road, denoted here by $\tau_{Road}$, can be taken as the smallest of the access delays for all routes, plus two added delays: $\tau_{SAP}$, the delay associated with activating the SAP volunteers, and an added travel time $\tau_{Drive}$ that accounts for the added drive time associated with flying to an airport outside the Willamette Valley and driving into the study area.

$$\tau_{Road} = \tau_{SAP} + Min_r\left\{\tau_r\right\} + \tau_{Drive}$$ Equation 4-17

The time between the mainshock and when SAP evaluators arrive through PDX, denoted here by $\tau_{Fly}$, can be taken as $\tau_{SAP}$, the delay associated with activating the SAP volunteers, and the time required to repair the runway, $\tau_{PDX}$, from Table 3-2.

$$\tau_{Fly} = \tau_{SAP} + \tau_{PDX}$$ Equation 4-18

The aggregate SAP mobilization time, denoted here by $\tau$, is taken as the smaller of the time between the mainshock occurrence and when SAP evaluators can arrive in study area by road, $\tau_{Road}$, or via PDX, denoted by $\tau_{Fly}$:

$$\tau = Min\left\{\tau_{Road}, \tau_{Fly}\right\}$$ Equation 4-19

### 4.6.7 Building Stock

Hazus-MH provides a database containing an estimate of the building stock based on measured proxies such as number of housing units and employment statistics, factored by estimates of square footage per housing unit and per employee. The Hazus-MH software automatically integrates these, and related quantities coded into its databases to estimate, among other things, the quantity of buildings (square footage, building count, replacement cost, and occupancy loads) by census area (including tracts) and engineering features, especially the lateral force resisting system, height, and era of construction. The project team carried out the calculations specified in FEMA (2012) Chapter 3 to estimate the inventory. To update the underlying Hazus-MH database from 2002, the project team increased building quantities in proportion to the study area's population growth. The new buildings are assumed to comply with post-2002 model codes of the International Code Council.

Let $N_{tract,type}$ denote the estimated number of buildings in a given census tract and belong to a particular combination of Hazus-MH model building type, height category, and code era (that is, a qualitative description of the seismic design provisions to which the building was designed and constructed). Let $N_{buildings}$ denote the total number of buildings in the study area:

$$N_{buildings} = \sum_{tract} \sum_{type} N_{tract,type}$$ Equation 4-20

### 4.6.8 Improved Resilience from Faster Building Safety Evaluation

Hazus-MH provides fragility functions that relate the probability that a building experiences structural damage in each of one of four overall states—slight, moderate, extensive, and complete—to peak ground acceleration. Hazus's structural fragility functions take the following form:

$$P\left[D \geq d \middle| X = x\right] = \Phi\left(\frac{\ln\left(x/\theta_d\right)}{\beta_d}\right)$$ Equation 4-21

Where *D* refers to uncertain structural damage state, *d* to a particular value of *D* (slight, moderate, extensive, and complete in that order), *X* to ground motion (here, uncertain peak ground acceleration), *x* to a particular value of *X*, and $\theta_d$ and $\beta_d$ to parameters of the fragility function for damage state *d*. They vary by Hazus-MH model building type, height category, and code era. Following common practice, the project team equated extensive structural damage with ATC-20's restricted use (yellow) placard, and equated complete structural damage with ATC-20's unsafe (red) placard. Applying the equation to red and yellow placards, one can estimate the probability that a building will be evaluated red ($P_{red}$), yellow ($P_{yellow}$), or green ($P_{green}$) as follows:

$$P_{red} = \Phi\left(\frac{\ln\left(x/\theta_{red}\right)}{\beta_{red}}\right)$$ Equation 4-22

$$P_{yellow} = \Phi\left(\frac{\ln\left(x/\theta_{yellow}\right)}{\beta_{yellow}}\right) - \Phi\left(\frac{\ln\left(x/\theta_{red}\right)}{\beta_{red}}\right)$$ Equation 4-23

$$\begin{aligned} P_{green} &= 6.3 \cdot \left(P_{yellow} + P_{red}\right) \\ &\leq 1 - \left(P_{yellow} + P_{red}\right) \end{aligned}$$ Equation 4-24

The first line of the last equation acknowledges that many buildings have frightening-looking damage that does not actually impair their safety. In the 1994 Northridge earthquake, 6.3 buildings were placarded green for every building with a red or yellow placard (EQE International and California Governor's Office of Emergency Services, 1995, Table 4-1). The second part of the equation also acknowledges that in some places, shaking may be so high that virtually every building will be evaluated.

One can estimate the total number of buildings in the study area evaluated red, yellow, and green (denoted $N_{red}$, $N_{yellow}$, and $N_{green}$, respectively), and the total number of placards (denoted by *N*) as follows:

$$N_{red} = \frac{1}{n_{sims}} \cdot \sum_{sim} \sum_{tract} \sum_{type} N_{tract,type} \cdot P_{red,sim,tract,type}$$ *Equation 4-25*

$$N_{yellow} = \frac{1}{n_{sims}} \cdot \sum_{sim} \sum_{tract} \sum_{type} N_{tract,type} \cdot P_{yellow,sim,tract,type}$$ *Equation 4-26*

$$N_{green} = \frac{1}{n_{sims}} \sum_{sim} \sum_{tract} \sum_{type} N_{tract,type} P_{green,sim,tract,type}$$ *Equation 4-27*

$$N = N_{green} + N_{yellow} + N_{red}$$ *Equation 4-28*

In the equations, $n_{sims}$ denotes the number of simulations of within- and between-event ground motion for each scenario earthquake, sim denotes an index to simulations, tract denotes an index to census tracts in the study area, type denotes an index to the combination of Hazus-MH model building type, height category, and code era, and $N_{tract,type}$ is as defined in the previous subsection. The terms $P_{red,sim,tract,type}$, $P_{yellow,sim,tract,type}$, and $P_{green,sim,tract,type}$ refer to the red, yellow, and green placard probabilities defined above, acknowledging that peak ground acceleration *x* varies by simulation (sim) and census tract and that $\theta$ and $\beta$ parameters vary by Hazus-MH model building type, height category, and code era (type).

The fraction of all buildings in the study area whose safe re-occupancy is delayed because SAP evaluators cannot reach the Willamette Valley, is estimated as follows:

$$Q = \frac{N_{green} + 0.75 \cdot N_{yellow}}{N_{buildings}}$$ *Equation 4-29*

The equation uses the simplifying assumptions that (1) people immediately re-occupy buildings that do not show symptoms of damage sufficient to call for safety evaluation; (2) people will not re-occupy a building that is ultimately assigned a green placard until the building's safety is evaluated, because of symptoms of damage that seem to require a safety evaluation; (3) 75% of buildings that are assigned a yellow placard can be safely re-occupied except for limited areas with falling hazards; and (4) most of the delay re-occupying buildings with a red placard and the remaining yellow-placard ones results from the time required to repair damage.

Some of the *N* placards will be assigned by SAP evaluators who live inside the Willamette Valley, others by volunteers mobilized from outside the Willamette Valley. Let *L* denote the number of local evaluators (those who live within the study area) and let *M* denote the number of remote volunteers, that is, SAP evaluators who live outside the study area and who could be allocated to the Portland metropolitan area (as opposed to the Seattle-Tacoma area, which would also require volunteer SAP evaluators).

Let *F* denote the fraction of all evaluators who will be able to perform safety evaluation on any given day—for large numbers of required evaluations, SAP evaluators may rotate in and out of volunteer duty. Let *R* denote the number of evaluations that each SAP evaluator team can perform in a day. The project team assumed that in a large earthquake, each certified SAP evaluator will be teamed with one non-certified or newly trained SAP evaluator, so each SAP evaluation team will contain one certified SAP evaluator and one non-certified or newly trained evaluator.

Let *T* denote the time required to perform all *N* evaluations. Let $\tau$ denote the time required to mobilize SAP evaluators from outside the study area and have them arrive in the study area, whether by road from outside the Willamette Valley, or through PDX. Then the time required to evaluate all the buildings can be estimated as follows:

$$N = T \cdot R \cdot F \cdot L + (T - \tau) \cdot R \cdot F \cdot M \qquad \text{Equation 4-30}$$

Reorganizing to express the total evaluation time *T* as a function of SAP evaluator mobilization time $\tau$,

$$T(\tau) = \frac{N + \tau \cdot R \cdot F \cdot M}{R \cdot F \cdot (L + M)} \qquad \text{Equation 4-31}$$

One can calculate the number of placards completed by day *t*, denoted here by *n*(*t*) as follows.

$$\begin{aligned} n(t) &= t \cdot R \cdot F \cdot L && t < \tau \\ &= t \cdot R \cdot F \cdot L + (t - \tau) \cdot R \cdot F \cdot M && \tau < t < T \\ &= N && t > T \end{aligned} \qquad \text{Equation 4-32}$$

The average time between the earthquake mainshock and the time when an arbitrary building is evaluated is then given as the area above the curve *n*(*t*)/*N*, which one might call the safety-evaluation progress curve, as shown in Figure 4-8. The figure shows two curves: the blue one illustrates the progress of safety evaluation with a resilient runway, the red, without. The shallow sloping part of the safety-evaluation progress curve indicates evaluation by local SAP evaluators only; the steep part after remote evaluators arrive.

The difference in area between the red and blue curves is a measure of the improvement in the regional resilience associated with faster safety evaluation. The area is measured in days, and represents the reduction in the average number of days it takes between the earthquake mainshock and the day when a placard is assigned to a building. Let us denote the improved resilience associated with faster building safety evaluation (the difference in area) as $\Delta T_{tag}$. The Greek capital letter delta (Δ) denotes the improvement caused by some resilience measure, such as remediating the PDX runway.

Denoting the safety-evaluation progress curve without a resilient runway by $n_0(t)$ and the safety-evaluation progress curve with a resilient runway by $n_1(t)$, and the time required to complete evaluation under the two conditions by $T_0$ and $T_1$, respectively, one can calculate the improved safety-evaluation resilience $\Delta T_{tag}$ as follows. Note that it is not simply the difference between $T_0$ and $T_1$, because of the complexity of the two curves.

$$\Delta T_{tag} = \int_0^{T_0} \left(1 - \frac{n_0(t)}{N}\right) dt - \int_0^{T_1} \left(1 - \frac{n_1(t)}{N}\right) dt \qquad \text{Equation 4-33}$$

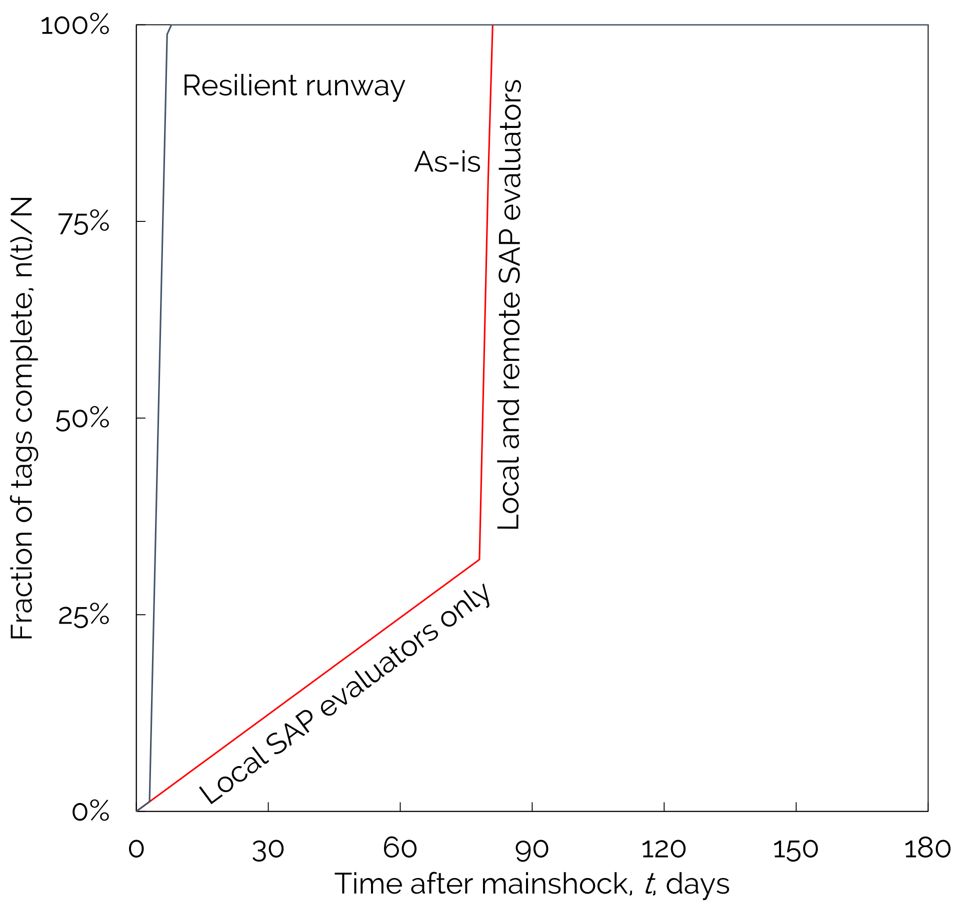


Figure 4-8. Illustration of the effect of a resilient runway on delays in building safety evaluation

## 4.7 ESTIMATING BENEFIT FOR AIR NATIONAL GUARD

The project team is unaware of any prior study that estimated the defense benefit of a resilient runway. The mission of the 142nd Wing of the Oregon Air National Guard relies on flying F-15 A/Cs. Its product, in an economic sense, is the performance of that mission. Its aircraft cannot fly (and therefore cannot add to the production of national defense) while the PDX runway is inoperative. Because it is problematic to estimate the benefit of these expenditures, the project team relied on the concept of benefit transfer, with which one estimates nonmarket economic values based on their similarity to something known from prior study. It seems reasonable therefore to estimate the national-defense benefit of having the 142nd Wing to be the expense times a weighted average of the benefit-cost ratios estimated by US Air Force (2017, 2019) and Hill et al. (2009).

One can estimate the 2020-equivalent value of the expenditures those authors drew from as a weighting factor. Present values are calculated using the U.S. Bureau of Labor Statistics (ND) CPI Inflation Calculator, taking June values of the consumer price index for purposes of calculating buying power. Using benefit-transfer, the daily national defense value of the PDX runway is therefore taken as the daily expenditure times the weighted average benefit-cost ratio of military expenditures.

The defense benefit of faster restoration of the runway is taken as the daily defense value of the 142nd Wing times the number of days sooner a resilient runway is restored.

## 4.8 AFTERSHOCK LOSSES

Rather than attempt to simulate a full aftershock sequence, the project team used the expedient of increasing benefits by 25% to approximate the losses avoided in aftershocks, consistent with the findings of the US Geological Survey's HayWired scenario (Detweiler and Wein 2018, p. 41).

## 4.9 POPULATION AND GDP GROWTH

Some benefits will remain constant whether an earthquake happens next year or 20 years hence, such as reduced cost of runway repairs. Some benefits increase as population increases, such as number of excess fatalities avoided. And some increase with both population growth and growth in per-capita gross domestic product, such as reduction in business interruption losses.

Consider a benefit that increases with population and real per-capita gross domestic product. If population grows at a rate $x_1$ per year, and real per capita gross domestic product at a rate of $x_2$ per year, expected annualized benefits can be estimated to grow at a similar rate, $g = (1+x_1)\cdot(1+x_2) - 1$. The present value of an annuity that grows at a rate of $g$ per year, with discount rate $r$ over $n$ periods is given by

$$P = A_1\left(\frac{1-(1+g)^n(1+r)^{-n}}{r-g}\right) \qquad \text{Equation 4-34}$$

As noted in Chapter 3, the Portland Metropolitan Statistical Area is growing in population at a rate of $x_1$ = 0.85% per year and its real GDP per capita is growing at a rate of $x_2$ = 2.0% per year, implying a GDP growth rate of $g$ = 2.87%. To which benefits would which growth factors apply?

- Emergency medical care: As PDX provides emergency medical transport, its value certainly increases with population. The value of a statistical fatality avoided probably increases with per-capita GDP. But future, safer buildings will slowly replace existing, more-dangerous ones, reducing life-safety benefits in the future as people occupy safer, newer buildings. Newer buildings grow stronger at a rate of about 1% per year, which seems to roughly offset the increase in GDP. The project team therefore counts only population growth for life-safety benefits, i.e., $g$ = 0.85%.

- Building safety evaluation: As PDX provides transit for SAP evaluators, its value will grow with population, but that growth will be offset by the growth in the number of evaluators. As people become more productive, the avoided business interruption from faster safety evaluation will grow with real per-capita GDP, but newer buildings will also need fewer evaluations than older ones, offsetting the growth in per-capita GDP. The project team therefore neglects both population growth and growth in per-capita GDP to evaluate benefits of building safety evaluation, i.e., $g$ = 0%.
- Business interruption: PDX business activity will grow with population and real per-capita GDP growth. Both factors are considered for business interruption, i.e., $g$ = 2.87%.
- Defense: The size of the military would seem to grow with population. Military compensation between 2010 and 2020 has increased with inflation (1.82% per year; U.S. Department of Defense 2020), suggesting that the budget for the Oregon Air National Guard will scale approximately with population but not real per capita GDP. The project team estimated the defense benefit from the 142$^{nd}$ Wing using its budget and benefit transfer, suggesting the use of $g$ = 0.85%.
- Runway repair: Construction costs since 2010 have increased approximately with inflation. Runway repair costs will not grow with population. The project team used $g$ = 0% for runway repairs.

## 4.10 SPECIAL METHODS FOR INDIRECT BUSINESS INTERRUPTION

Recent studies on disaster risk analysis have underscored the significance of business interruption (BI) losses in the aftermath of disasters. There have been a significant number of scenarios where the indirect business interruption losses from disasters have been assessed to be economically costlier than the direct losses (Webb et al. 2000). In this study, the project team estimated the indirect BI losses by using the input-output (IO) model, particularly using the IMPLAN model. For a given runway disruption scenario to the PDX airport, the approach is to estimate the following model inputs: (i) regional scope, (ii) percentage of direct loss to the airport operations, and (iii) duration of restoration. Once the scenario parameters are identified, the next step is to determine the primary sectors that are affected by the scenario. IMPLAN data were acquired for all the counties of Oregon and three counties in the state of Washington that are proximate to the PDX airport (Clark, Cowlitz, and Skamania). Furthermore, the IMPLAN model currently maintains a database comprising of 546 sectors, of which the sector code "414" is assigned for air transportation (IMPLAN 2020). For this project, the team considered the direct business losses to sectors that operate within the airport including stores, restaurants, and couriers, among others. The direct business interruption disruptions to such sectors along with air transportation were then modeled in IMPLAN, which led to estimates of indirect and induced losses. IMPLAN results are presented in annual values; hence the estimated losses are scaled accordingly to the assumed duration of the scenario.

# 4.11 SPECIAL METHODS TO ESTIMATE BENEFIT BY INCOME LEVEL, RACIAL, AND ETHNIC GROUP

To estimate the social economic impacts of the major Portland earthquake and mitigation measures, the project team constructed a multi-sector income distribution matrix (MSIDM). Figure 4-9 presents a schematic depiction of a MSIDM. The matrix provides the earnings profile according to nine income brackets for each producing sector in the economy, i.e., what proportion of the personal income (including both labor income and capital income) paid out by each sector accrues to each income bracket.

| Industry \ Income Bracket | <5k | 5-12.5k | 12.5-17.5k | 17.5-25k | 25-32.5k | 32.5-42.5k | 42.5-55k | 55-77.5k | 77.5-130k | >130k |
|---|---|---|---|---|---|---|---|---|---|---|
| Agriculture | x | x | x | x | x | x | x | x | x | x |
| Construction | x | x | x | x | x | x | x | x | x | x |
| Manufacturing | x | x | x | x | x | x | x | x | x | x |
| Transportation | x | x | x | x | x | x | x | x | x | x |
| Service | x | x | x | x | x | x | x | x | x | x |
| . | | | | | | | | | | |
| . | | | | | | | | | | |
| . | | | | | | | | | | |

Figure 4-9. Schematic depiction of a multi-sector income distribution matrix

In 2018, the total personal income in the Portland metropolitan area was $893 million (U.S. Bureau of Economic Analysis 2020). Table 4-1 presents the major components of the personal income accounts for the metropolitan statistical area. The data in this table represent a key input into the development of the Portland MSIDM. It served as a major set of control totals for adapting an analogous matrix from California to the region of interest. Construction of the matrix proceeds as follows:

1. Begin with the California matrix and adjust for the Portland metropolitan area economy.
2. Adjust for sectoral composition differences.
3. Adjust for total income payment differences by sector.
4. Adjust for relative differences in income components.

The MSIDM was applied here to total sectoral personal income impacts using an input-output methodology, with which the MSIDM is most compatible.

Table 4-1. Personal income by major components for Portland OR-WA MSA, 2018

| | |
|---|---|
| Earnings by place of work | 103,525 |
| Wages and salaries | 75,782 |
| Supplements to wages and salaries | 16,821 |
| Employer contributions for employee pension and insurance funds | 10,626 |
| Employer contributions for government social insurance | 6,195 |
| Proprietors' income | 10,922 |
| Farm proprietors' income | 148 |
| Nonfarm proprietors' income | 10,774 |
| Less: Contributions for government social insurance | 12,521 |
| Plus: Adjustment for residence | 79 |
| Plus: Dividends, interest, and rent | 30,359 |
| Plus: Personal current transfer receipts | 19,826 |
| Personal income | 141,270 |

Source: U.S. Bureau of Economic Analysis (2020).

# 5. Project Data and Other Analytical Details

## 5.1 STUDY AREA

The project team estimated economic impacts of a resilient runway that accrue to communities within a study area that comprises the seven counties of the Portland Metropolitan Statistical Area plus Polk and Marion Counties, Oregon, and Cowlitz County, Washington, as illustrated in Figure 5-1, and whose population is shown in Table 5-1.

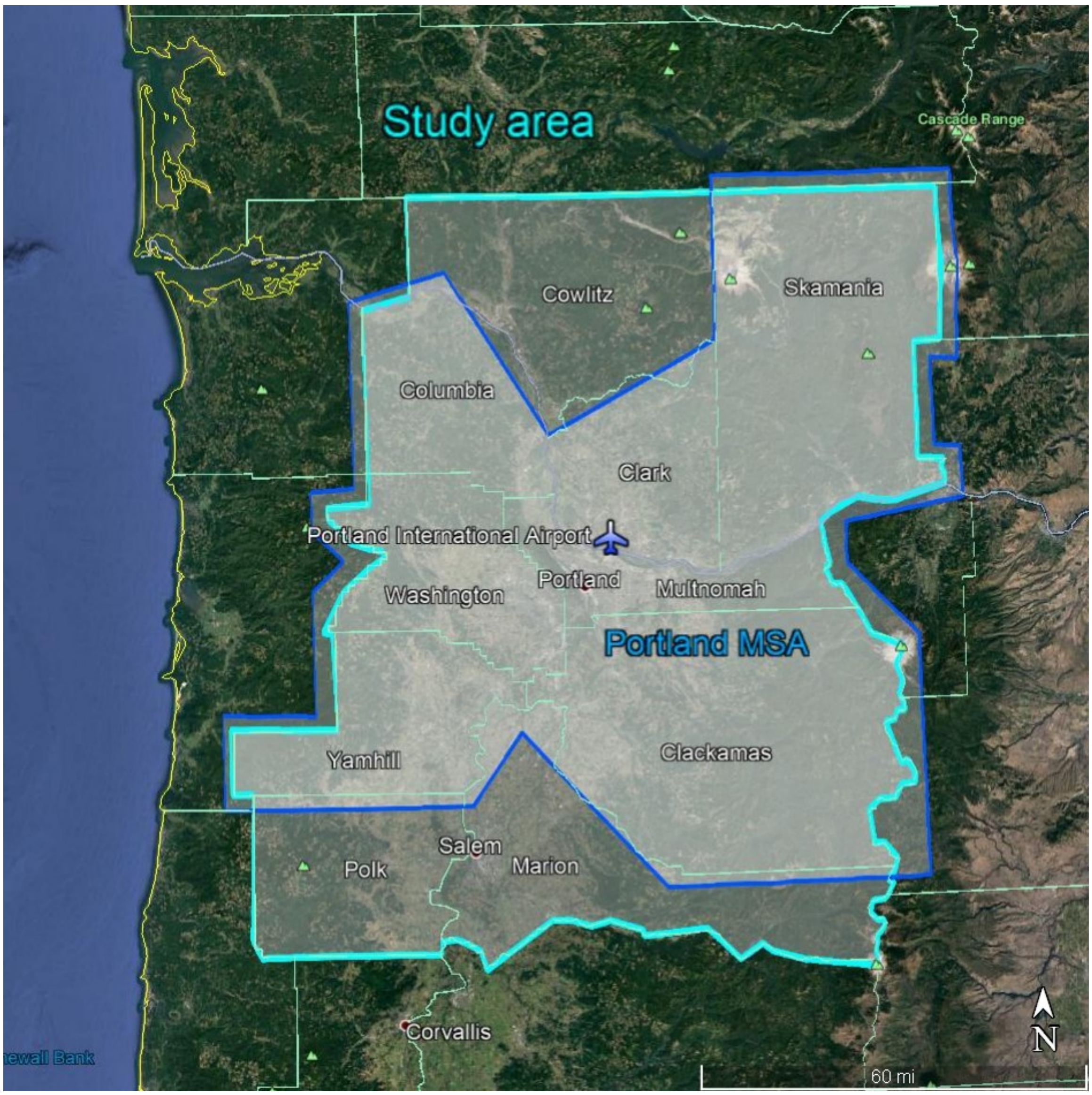


Figure 5-1. Study area boundaries: the Portland MSA plus three nearby counties

Table 5-1. Study area population

| County | State | FIPS | 2019 population |
|---|---|---|---|
| Clackamas | OR | 41005 | 404,980 |
| Columbia | OR | 41009 | 52,354 |
| Marion | OR | 41047 | 333,950 |
| Multnomah | OR | 41051 | 790,670 |
| Polk | OR | 41053 | 79,730 |
| Washington | OR | 41067 | 583,595 |
| Yamhill | OR | 41071 | 104,990 |
| Clark | WA | 53011 | 488,241 |
| Cowlitz | WA | 53015 | 110,593 |
| Skamania | WA | 53059 | 12,083 |
| **Total** | | | **2,961,186** |

## 5.2 IMPROVEMENT IN COMMERCIAL AIR TRANSPORTATION

HNTB Corporation (2015) estimated the damage, repair cost, and repair duration of the PDX north and south runways, with and without mitigation, under each of five scenario levels of ground motion. These levels are characterized both in terms of peak ground acceleration and mean recurrence interval. Mean recurrence intervals are 72 years, 225 years, 475 years, 975 years, and 2,475 years. If these recurrence intervals seem strange, understand that they correspond to 50% probability of being exceeded in 50 years (the assumed but probably underestimated economic life of an ordinary building), 20% probability in 50 years, 10% in 50 years, 5% in 50 years, and 2% in 50 years.

At these mean recurrence intervals, peak horizontal ground accelerations at the runways are estimated to be approximately 9%, 18%, 25%, 30%, and 39% of the acceleration due to gravity, respectively. Figure 5-2 presents HNTB Corporation's (2015) estimates of downtime. Repair costs without mitigation vary from $250,000 in the 72-year ground motion to $77 million in the 2,475-year

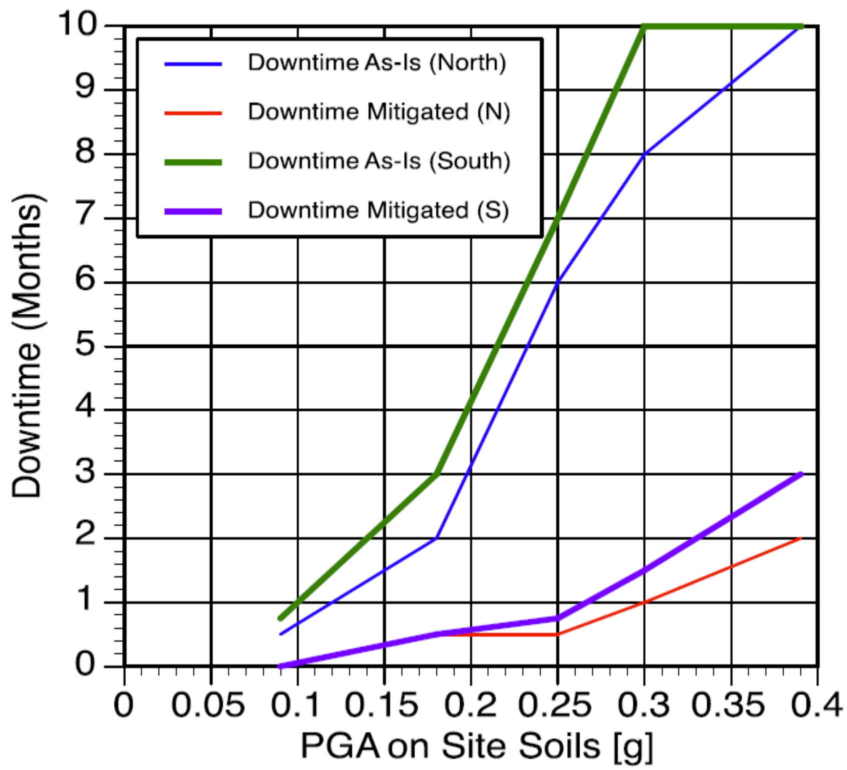


Figure 5-2. Estimated runway repair duration as a function of ground motion, as-is and mitigated (HNTB Corporation 2015, p. 49). Only the as-is curves are used.

ground motion. With mitigation, repair costs range from zero to $7.7 million depending on the severity of ground motion.

Table 5-2 summarizes repair costs and downtime for the south runway before and after mitigation according to HNTB Corporation, except that mitigating half the south runway (6,000 ft out of 11,800 ft) is expected to approximately halve repair costs. The retrofit also eliminates downtime. The table reflects these revisions.

The project team interprets these data to mean 100% reduction in commercial air transportation through PDX for the duration of repairs to the runway that has been mitigated (shown as downtime in the right-hand table column), and something between 0% and 50% reduction in air transportation until the second runway (the one without mitigation) is repaired, that is, for the remainder of the downtime shown in the fourth column.

The Federal Aviation Administration reports 200,000 commercial flight operations occurred at PDX in 2017 (Port of Portland, 2019). With PDX commercial air traffic operating between 6:00 AM and 11:00 PM, it seems practical to carry out an upper bound of 186,150 operations per year on a single runway (93% of the 2017 total), with one operation occurring every two minutes, a reduction of 7% overall, a modest reduction that seems reasonable to take as essentially zero.

Table 5-2. Runway performance summary

| Mean recurrence interval (years) | PGA (g) | Without mitigation | | | With mitigation | | |
|---|---|---|---|---|---|---|---|
| | | Repairs | Cost | Downtime (months) | Repairs | Cost | Downtime (months) |
| 72 | 0.09 | <1% of runway | $300,000 | 0.75 | None | $150,000 | 0 |
| 225 | 0.18 | 10% of runway | $7,700,000 | 3 | 5% of runway | $3,850,000 | 0 |
| 475 | 0.25 | 25% of runway | $19,300,000 | 7 | 12% of runway | $9,650,000 | 0 |
| 975 | 0.30 | 50% of runway | $38,500,000 | 10 | 25% of runway | $19,250,000 | 0 |
| 2,475 | 0.39 | ≥70% of runway | $77,000,000 | 10 | 35-50% of runway | $38,500,000 | 0 |

Table 5-2 does not provide the threshold level of shaking required to damage the runway, or the mean recurrence interval associated with that level of shaking. However, linear extrapolation of downtime versus PGA suggests a 0.06-g threshold, associated with approximately 49-year mean recurrence interval (from linear extrapolation of the natural logarithm of exceedance frequency versus PGA).

# 5.3 SEISMIC HAZARD

## 5.3.1 Hazard Deaggregation

The project team performed seismic hazard disaggregation at the geographic location of the Port of Portland, 7200 NE Airport Way, Portland OR, 45.5879N, -122.5915E, using Vs30 = 180 m/sec (DE boundary, as suggested by HNTB Corporation 2015 Appendix 2, PDF p. 133), the Conterminous U.S. 2014 (update) (v4.2.0), and peak ground acceleration (PGA), for comparison with HNTB Corporation (2015). PGA values at these return periods are not the same as HNTB Corporation calculated, possibly because they used a weighted average of results for D and E soils, rather than soils at the DE boundary. Or it could be that they used a slightly older hazard model. In any case, it seems reasonable to use HNTB's estimates of as-is runway damage, repair time, and recovery cost at the specified mean recurrence intervals. It also seems reasonable to use the rupture magnitudes and locations de-aggregated at these mean recurrence intervals for estimating regional landsliding and other regional effects.

Table 5-3 shows the earthquakes most likely to cause shaking with several commonly used mean recurrence intervals. In the table, "EQ" denotes an index to five earthquakes. "Mean recurrence interval" refers to the expected value of the time between earthquakes producing shaking that exceeds the intensity of ground motion shown in the column labeled "*PGA*," which denotes peak ground acceleration in units of gravities. $M_w$ refers to moment magnitude of the earthquake most likely to cause that ground motion. Columns labeled $r_{Rup}$, $\varepsilon_0$, and percentile, respectively denote distance from the site (here, PDX) to the earthquake fault, a measure of how high or low the ground motion is relative to the median that one would expect from such a magnitude and distance, and the non-exceedance probability associated with that difference from the median. Source denotes the earthquake fault that ruptures. Lon and Lat denote the epicenter location in decimal degrees east longitude and north latitude.

The table shows that a whole-fault rupture of the Cascadia Subduction Zone is the largest contributor to seismic hazard at PDX at these mean recurrence intervals. The ruptures can produce shaking as low as 0.07g and as high as 0.51g in terms of peak ground acceleration at PDX. These levels of shaking reflect the hazard as estimated by the 2014 National Seismic Hazard Mapping Program, which predate the ground-motion-prediction equations on which GRI (2020) rely, and therefore on which PDX relies.

Note that, to perform the benefit calculations, it will be necessary to estimate the level of shaking at which damage just initiates, along with its mean exceedance frequency. Using the USGS Unified Hazard Tool, and, assuming damage begins when strong shaking occurs (commonly taken as peak ground acceleration exceeding 5% of gravity), the project team estimates that damaging shaking currently has a mean exceedance frequency of 0.0241 times per year, or on average every 42 years.

It was also necessary to estimate the level of shaking and mean exceedance frequency at which the mitigation provides no further benefit, that is, where damage is just as bad with the mitigation as without, or an upper bound of the benefit integral above which to stop counting benefits. The project team assumed that losses at shaking with 1% exceedance probability in 100 years (10,000-year mean recurrence interval) are approximately the same as those in the 2% in 50 year shaking level (2,475-year mean recurrence interval), and that therefore the losses are the same, and ceases integration above that level of shaking.

Table 5-3. Scenario earthquakes from hazard disaggregation, shown modal magnitude and distance from PDX

| EQ | Mean recurrence interval (years) | *PGA* (g) | $M_w$ | $r_{Rup}$, (km) | $\varepsilon_0$ | Percentile | Source | Lon deg W | Lat deg N |
|---|---|---|---|---|---|---|---|---|---|
| 1 | 72 | 0.07 | 8.7 | 134 | -1.22 | 11% | Cascadia Megathrust – whole CSZ Characteristic | 124.330 | 45.489 |
| 2 | 225 | 0.16 | 9.12 | 134 | -0.28 | 39% | Ditto | 124.330 | 45.489 |
| 3 | 475 | 0.25 | 9.12 | 134 | +0.40 | 66% | Ditto | 124.330 | 45.489 |
| 4 | 975 | 0.35 | 9.34 | 84 | -0.27 | 39% | Ditto | 123.599 | 45.501 |
| 5 | 2,475 | 0.51 | 9.34 | 84 | +0.33 | 63% | Ditto | 123.599 | 45.501 |

Why do the same pairs of ($M_w$, $r_{Rup}$) cause both the 225-year and 475-year ground motion, even though the 475-year ground motion is 50% stronger? Ground motion is highly uncertain even given $M_w$ and $r_{Rup}$. Uncertainty is reflected by the columns labeled $\varepsilon_0$ and Prob, which refer to the number of standard deviations above or below the median (50$^{th}$ percentile) ground motion for the given ($M_w$, $r_{Rup}$) pair and the associated nonexceedance probability, respectively.

## 5.3.2 Ground Motion with HNTB Mean Recurrence Intervals

Figure 5-3 and Figure 5-4 shows the median ground motion in the five ruptures. The former shows peak ground acceleration; the latter, 5% damped spectral acceleration response at 1.0-second period, on the local soil conditions as estimated by OpenSHA. The maps reflect the effect of between-event uncertainty but not within-event variability. The project team later adjusted them uniformly by a calibration factor so that the OpenSHA estimate of ground motion matches that of GRI at PDX in the scenario that GRI considered for design. The project team also later added a spatially varying motion (the within-event term) to produce the blotchy simulations illustrated earlier in Figure 2-7. Twenty such simulations were produced for each of the maps shown in Figure 5-3 and Figure 5-4. Figure 5-3 shows median peak ground accelerations around PDX on the order of 0.16 to 0.37g.

The outlined boundary in Figure 5-3 and Figure 5-4 represents the portion of the Cascadia Subduction Zone modeled using OpenSHA to calculate shaking. As previously noted, the way the ground-motion prediction equation works, omitting the narrower portion of the Cascadia Subduction Zone south of about 43 degrees north latitude has no effect on estimated shaking in the Willamette

Valley, because shaking depends on the closest fault distance. The outlined portion is closer than the sections south of 43 degrees.

Omission of the southern segments might cause an underestimate in the number of earthquake-induced landslides on a portion of Interstate 5 south of 43 degrees north latitude. However, limitations in OpenSHA do not allow one to model a rupture area with a variable width. One can either model the southern sections as equally wide as the central sections, or omit them entirely. Including them would overestimate shaking and therefore landsliding along I-5. Omitting them would underestimate shaking and landslides along that portion.

Given the choice, the project team opted to omit them. Omitting them tends to produce less estimated landslide damage, a lower estimate of the time required to restore I-5, and a lower value of a resilient runway, if anything. As it turns out, the omission makes no difference, because I-5 is never the fastest route into the Willamette Valley under any of the simulations. More landslides along it would not change the benefit estimate.

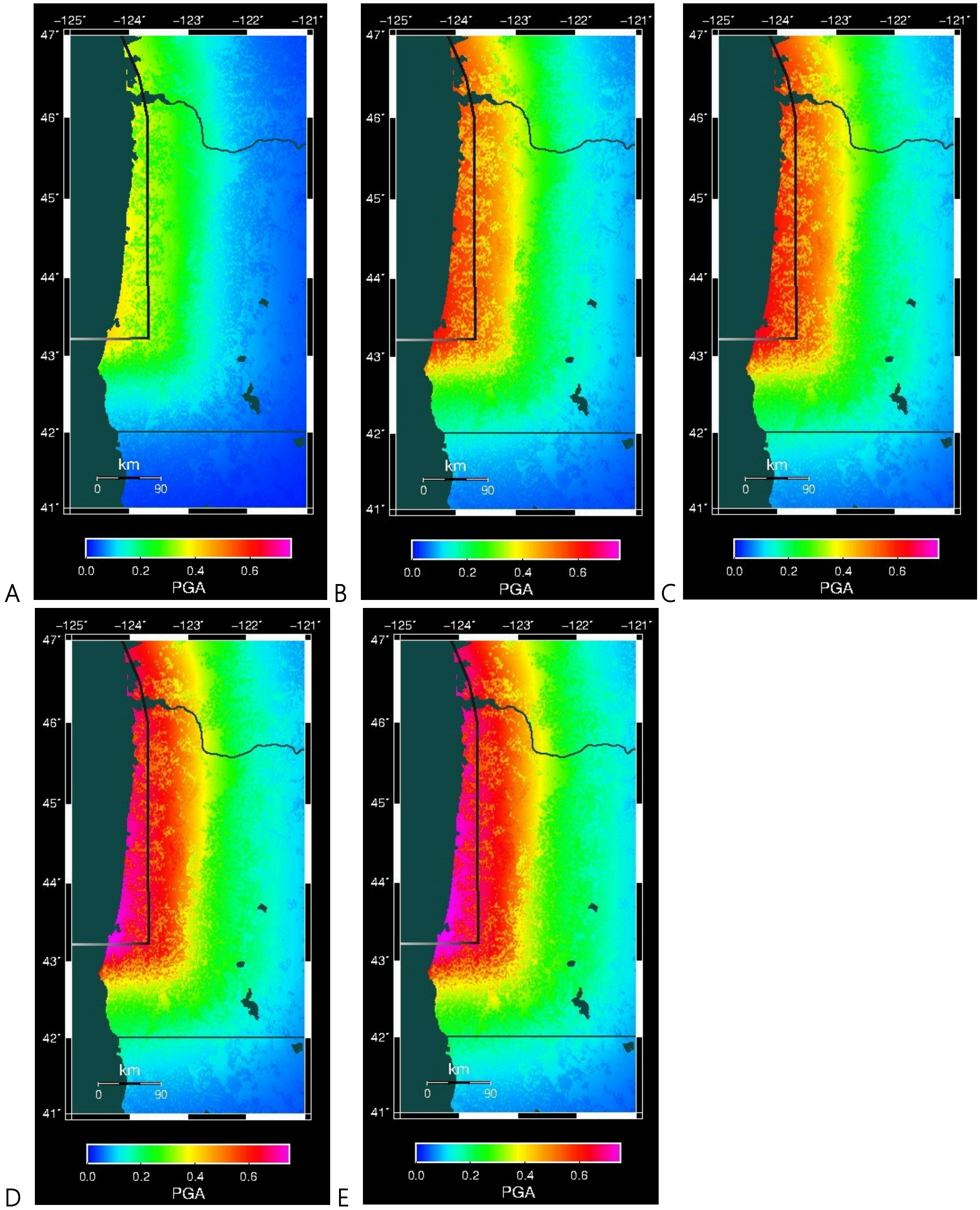


Figure 5-3. Peak ground acceleration (PGA) in Cascadia megathrust scenarios with 50-year exceedance probabilities of (A) 50%, (B) 20%, (C) 10%, (D) 5%, and (E) 2%

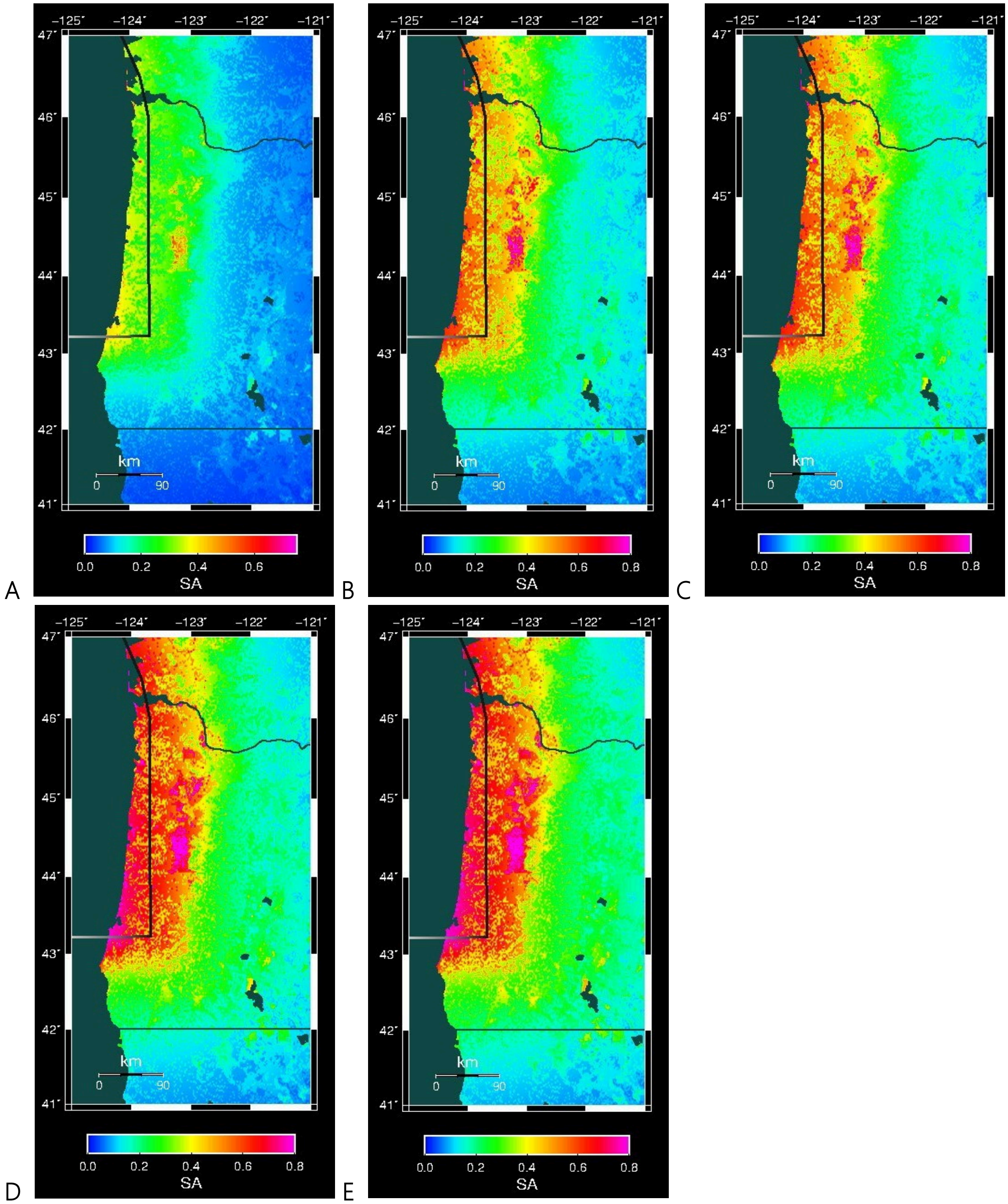


Figure 5-4. Damped elastic spectral acceleration response at 1.0-second period in Cascadia megathrust scenarios with 50-year exceedance probabilities of (A) 50%, (B) 20%, (C) 10%, (D) 5%, and (E) 2%

### 5.3.3 Calibrating OpenSHA Ground Motions to Match GRI (2020)

The PGA and SA10 maps are calibrated to match GRI's mean-plus-one-standard-deviation estimate of ground motion in the $M_W$ 9.0 CSZ event on a rock outcrop. The project team used OpenSHA to estimate motions at four nearby grid points labeled OpenSHA 00, 10, 01, and 11 in Figure 5-5. Table 5-4 presents values of PGA and SA10 at the four nearby gridpoints whose longitude and latitude values are shown. The table also shows the values spatially interpolated at the runway midpoint, plus GRI's values at that location and the ratio of the latter to the former. The table suggests that in this earthquake, location, soil condition, and nonexceedance probability, GRI's estimated ground motions are 92% of that of OpenSHA for peak ground acceleration and 81% for 1-second spectral acceleration response. The location denoted OpenSHA 00 is about 510 meters south and 430 meters west of the runway midpoint. The other gridpoints are approximately 1.55 km east, 2.22 km north, or both, from OpenSHA 00.


Figure 5-5. Calibrating OpenSHA ground-motion estimates to match GRI (2020)

Table 5-4. Calibration factor to adjust OpenSHA motions to match GRI's estimate

| Location ID | Longitude deg E | Latitude deg N | PGA, g | SA10, g |
|---|---|---|---|---|
| OpenSHA 00 | -122.6000 | 45.5800 | 0.435 | 0.408 |
| OpenSHA 10 | -122.5800 | 45.5800 | 0.428 | 0.403 |
| OpenSHA 01 | -122.6000 | 45.6000 | 0.435 | 0.408 |
| OpenSHA 11 | -122.5800 | 45.6000 | 0.428 | 0.403 |
| OpenSHA interpolated at calibration point | -122.5945 | 45.5846 | 0.433 | 0.407 |
| GRI estimated motion | Same | Same | 0.40 | 0.33 |
| **GRI ¸ OpenSHA** | | | **0.92** | **0.81** |

## 5.4 MEDICAL EVAUATION BENEFITS

Among the hospitals listed in Table 3-6 that are nearer PDX than HIO as shown in Figure 3-8 according to the list provided in chapter 4, PDX will provide transportation for medical resources to hospitals with 1,121 ICU or ED beds, of which 32%, or 360, are estimated to be unoccupied at the time of the earthquake. Thus, having a resilient runway at PDX would help to avoid up to $I_3$ – 360 fatalities, referred to here as avoided excess fatalities, where $I_3$ denotes the estimated number of severity-3 injuries, a number that varies by the earthquake size and time of day.

Table 5-5 presents severity-2 injuries in the PDX service area (the counties closer to PDX than to Hillsboro), severity-3 injuries, and the average number of avoided excess fatalities. Table 5-6 presents the acceptable costs to avoid the excess fatalities. Figures in the tables are rounded to two significant figures to reduce the appearance of excessive accuracy. Neither table accounts for delays transporting patients through PDX. A factor of $O$ = 0.67 seems reasonable, as it assumes that setting up emergency medical services or emergency medical transport to other hospitals might take 24 hours. Splitting benefits evenly between PDX and other resources further reduces the benefits, leaving about 1/3rd attributable to PDX.

Note that, although the average number of severity-3 injuries is less than 360 in some cases, in some of the 20 underlying simulations, the number exceeds 360. So, in some simulations, some severity-3 injuries lead to death. As a result, the average number of severity-3 injuries that lead to death can be greater than 0.

One can understand the apparent paradox through an analogy: a group of children attend a fair that has a ride requiring riders to be over 48 inches tall. Although the average height of the children may be 50 inches, some of them will be less than 48 inches tall, so some of the children will be unable to ride.

Table 5-5. Average numbers of severity-2 injuries, severity-3 injuries, and severity-3 injuries that lead to death because they exceed the available hospital resources

| Mean recur. int. (yr) | Severity-2 injuries | | | Severity-3 injuries | | | Avoided excess fatalities | | |
|---|---|---|---|---|---|---|---|---|---|
| | 2 PM | 2 AM | 5 PM | 2 PM | 2 AM | 5 PM | 2 PM | 2 AM | 5 PM |
| 72 | 1,000 | 250 | 720 | 160 | 32 | 110 | 63 | 0 | 28 |
| 225 | 3,000 | 990 | 2,200 | 490 | 110 | 360 | 270 | 14 | 160 |
| 475 | 3,600 | 1300 | 2,700 | 580 | 140 | 420 | 320 | 22 | 200 |
| 975 | 4,200 | 1,600 | 3,200 | 700 | 170 | 510 | 400 | 35 | 240 |
| 2,475 | 4,800 | 1,900 | 3,600 | 780 | 200 | 580 | 470 | 44 | 280 |

Table 5-6. Acceptable costs (in millions of 2020 USD) to avoid excess fatalities

| Mean recur. int. (years) | 2 PM | 2 AM | 5 PM | Average |
|---|---|---|---|---|
| 72 years | $390 | $0 | $170 | $110 |
| 225 | $1,800 | $85 | $1,000 | $560 |
| 475 | $2,000 | $140 | $1,200 | $690 |
| 975 | $2,500 | $210 | $1,500 | $880 |
| 2,475 | $2,900 | $270 | $1,700 | $1,000 |

Note that the results in Table 5-5 and Table 5-6 are strongly affected by within-event ground-motion variability. Ignoring within-event ground-motion variability, the expected number of excess severity-3 injuries leading to death was zero in all but one case: 32 deaths in a daytime, 2,475-year earthquake. Severity-2 casualties were generally less than half, and in the 72-year earthquake less than 1/10$^{th}$, those estimated with ground-motion uncertainty. Figure 5-6 shows the expected value of severity-2 and severity-3 injuries with and without ground-motion simulation in the counties whose emergency medical services would be transported through PDX.

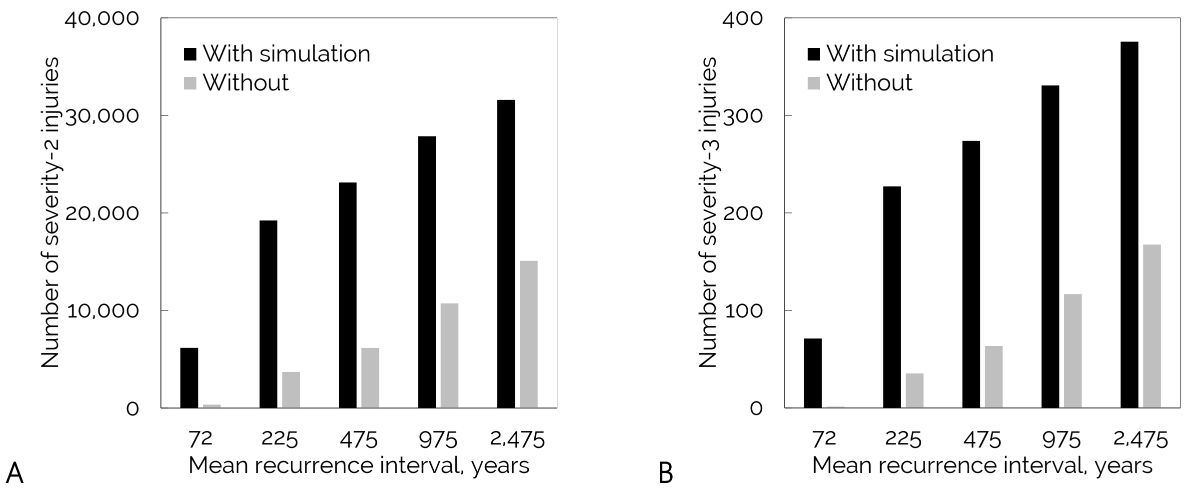


Figure 5-6. Effect of simulating within-event ground-motion variability for nonfatal injuries: (A) Hazus severity-2 injuries, and (B) Hazus severity-3 injuries

## 5.5 SAFETY-EVALUATION BENEFIT

### 5.5.1 Access Routes

The project team identified 10 freeway and U.S. and state highway routes from outside the Willamette Valley. Key north-south routes include I-5, OR-99E, OR- 99W, OR-214, OR-224, and OR-233. East-west routes include I-84, OR-22, US-20, US-26, and OR-58. Reasonable combinations include the following:

Table 5-7. Highway access routes

| Route ID | Mountain portion | Willamette Valley portion |
|---|---|---|
| 1. South from Seattle | I-5 | I-5 |
| 2. West from The Dalles | I-84 | I-84 |
| 3. West from Mt. Hood Village | US-26 | US-26 |
| 4. West from Mehama | OR-22 | OR-22 |
| 5. West from Sweet Home | US-20 | US-20 |
| 6. North from Redding A | I-5 | OR-99E |
| 7. North from Crescent Lake A | OR-58 | OR-99E |
| 8. North from Redding B | I-5 | OR-99W |
| 9. North from Crescent Lake B | OR-58 | OR-99W |
| 10. North from Redding C | I-5 | I-5 |

## 5.5.2 Access Delays from Landslides

### *5.5.2.1 Landslide Site Conditions*

One can drive into the Willamette Valley from the south, north, or east along seven mountainous routes: I-5 from Redding, I-5 from Olympia, I-84 from the Dalles, US26 from Warm Springs, US20 from the Sisters, OR20 from its intersection with US20, or OR58 from Crescent Lake. The project team estimated the distribution of slopes immediately adjacent to the paving along each of these routes, at 202 sample locations approximately equally spaced (6 km increments) along each route. Figure 5-7 shows the routes and the cumulative distribution function of the slope from the edge of the paving to a point 30 meters distant in plan. Positive slope refers to an uphill direction from the pavement; negative indicates downhill. The larger of the two slopes in absolute value is recorded for each sample location. The cumulative distribution function shows that approximately 25% of these samples have an uphill or downhill slope of at least 20 degrees, and 8% have a slope of at least 30 degrees.

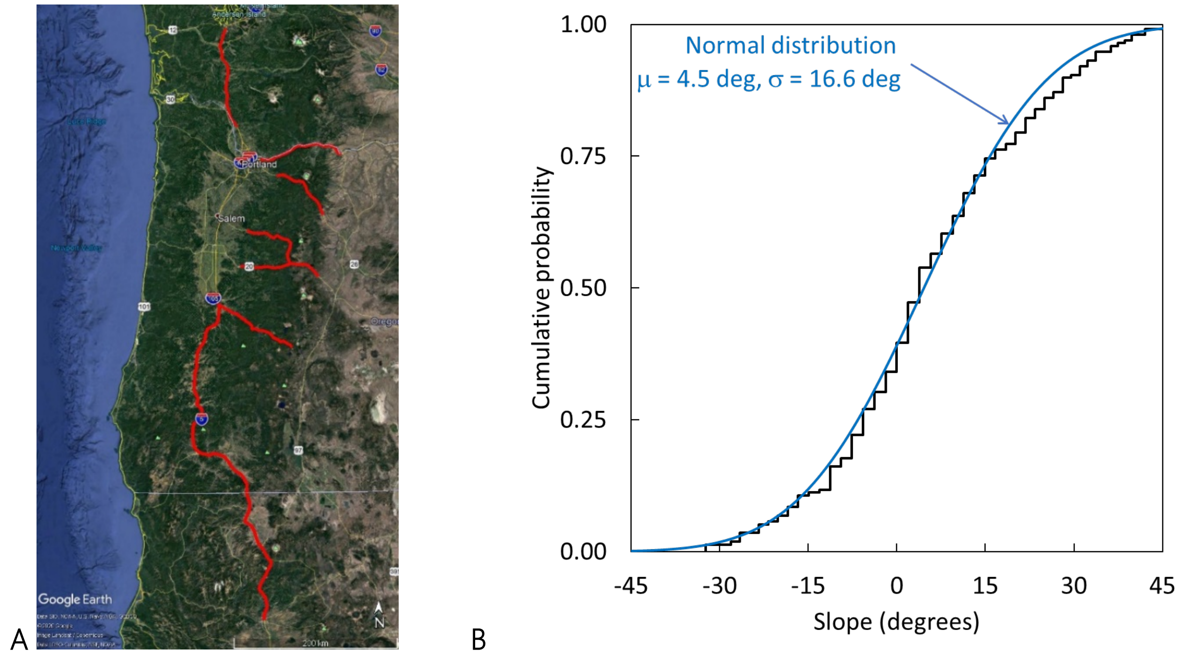


Figure 5-7. (A) Seven highway routes through the Cascades to the Willamette Valley; (B) Slope distribution along the route

Table 5-8 summarizes important attributes of the highway routes into the study area. $L$ denotes length, $J$ denotes the number of junctions with intersecting roads. $N$ is the number of sample points whose adjacent slopes were estimated. $\mu$ and $\sigma$ denote mean and standard deviation of slopes.

Table 5-8. Summary of highway hillside slope statistics for highway routes through the Cascades to the Willamette Valley

| Route | Stretch | $L$ (mi) | $J$ | $N$ | $\mu$ (deg) | $\sigma$ (deg) |
|---|---|---|---|---|---|---|
| I-5 | Redding-Eugene | 287 | 116 | 76 | 6.8 | 15.0 |
| I-5 | Woodland-Olympia | 81 | 31 | 23 | 4.0 | 8.6 |
| I-84 | Portland-The Dalles | 67 | 23 | 26 | 1.0 | 25.2 |
| OR-22 | Mehama-US-20 | 51 | 23 | 18 | 18.1 | 16.3 |
| OR-58 | Crescent Lake-Eugene | 68 | 54 | 19 | 16.5 | 14.7 |
| US-20 | Sweet Home-Sisters | 62 | 26 | 24 | 2.9 | 19.5 |
| US-26 | Mt Hood Village-Warm Springs | 59 | 35 | 16 | 0.8 | 12.1 |
| **All** | | **675** | **308** | **202** | **4.5** | **16.6** |

The table shows that the routes are unequal in terms of hilliness. The mean slope varies from 1 degree (US-26 and I-84) to 18 degrees (OR-22). The standard deviation varies from 9 degrees (I-5 from Woodland to Olympia) to 25 degrees (I-84). The table also shows that routes have junctions on average every 2.2 mi.

The project team extracted geologic units for the mountainous highway locations Figure 5-7(A) that lie within Oregon and therefore appear on the Walker and MacLeod (1991) Geologic Map of Oregon. The team interpreted each geologic unit as belonging to one of Wilson and Keefer's (1985) three geologic groups, A, B, or C. Results are shown in Table 5-8. The table groups samples by absolute value of slope, |α| in three ranges: 0 to 10 degrees, 10 to 20 degrees, more 20 degrees or greater.

Table 5-9 shows that about 30% of mountainous highway sample locations have geologic group A regardless of slope. For the remainder of mountainous highway locations, the chance that the geologic group is B increases with slope from about 40% on relatively low slopes (less than 10 degrees) to about 60% on relatively high slopes (20 degrees or greater), with a corresponding decrease in probability of geologic group C.

Table 5-9. Conditional probability of a site being in geologic group A, B, or C, conditioned on slope α

| \|α\|, degrees | A | | B | | C | | Total count |
|---|---|---|---|---|---|---|---|
| | Count | % | Count | % | Count | % | |
| 0 – 10 | 15 | 29% | 21 | 40% | 16 | 31% | 52 |
| 10 – 20 | 8 | 30% | 14 | 52% | 5 | 19% | 27 |
| 20+ | 11 | 30% | 23 | 62% | 3 | 8% | 37 |
| Total | 34 | 30% | 58 | 50% | 24 | 21% | 116 |

The project team used Bollman et al. (2013) to estimate the probability of saturated soil. It seems that coastal Oregon experiences saturated conditions about eight months out of the year (November through June), and dry conditions for the other four (July through October).

#### *5.5.2.2 PGA Along Mountainous Highways in Scenario Earthquakes*

Figure 5-8 shows peak ground acceleration in each of the five scenario earthquakes listed in Table 5-3. Red lines in the maps represent mountainous access routes into the Willamette Valley.

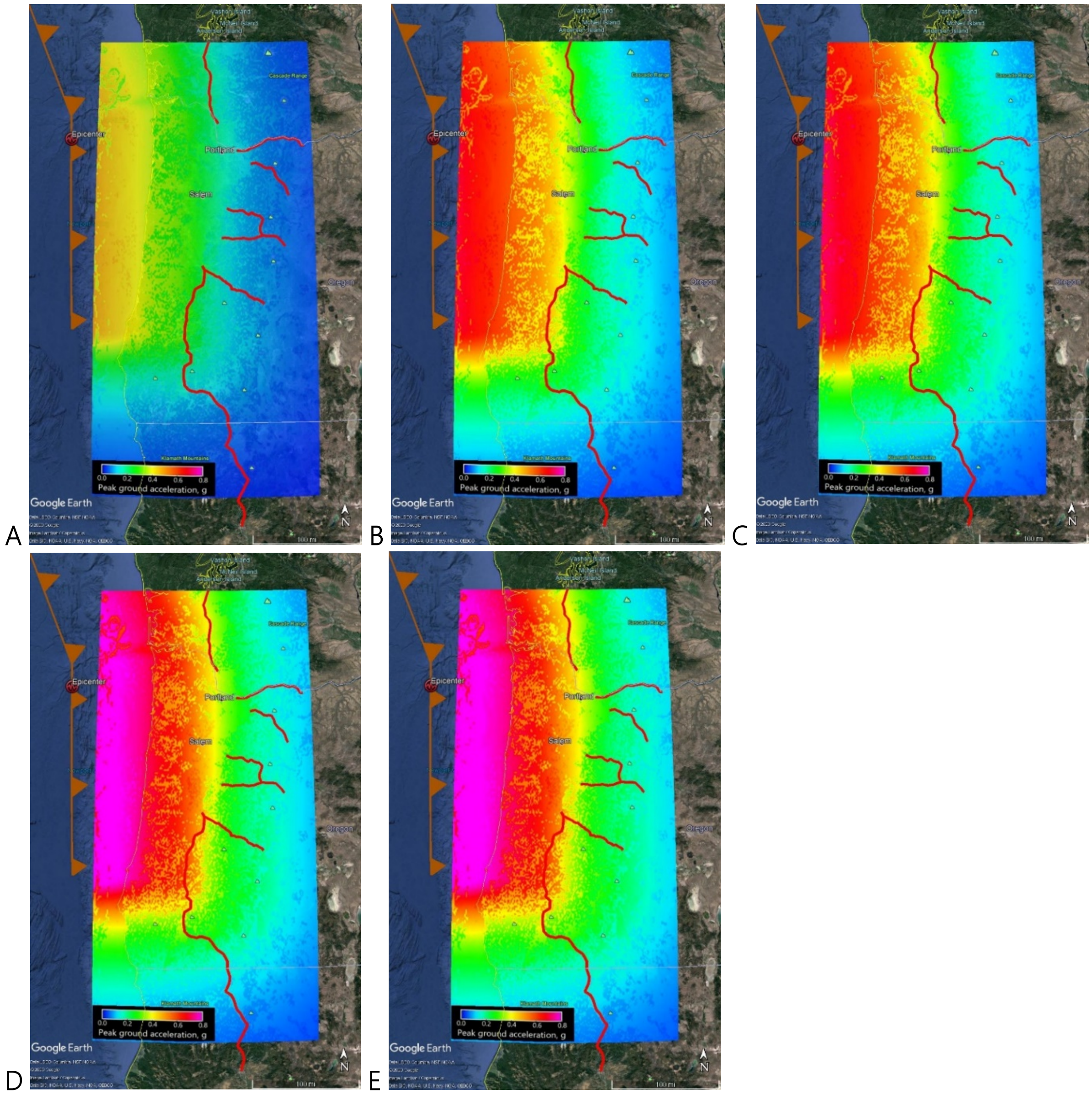


Figure 5-8. Estimated peak ground acceleration in each of 5 scenario earthquakes. Maps show between-event variability but not within-event variability.

#### *5.5.2.3 Number of Landslides and Duration of Repairs*

The landslide delay methodology detailed in chapter 4 produces the results shown in Table 5-10. In the table, the column labeled Earthquake denotes the same index to earthquakes as in Table 5-3. "Dry conditions" refers to the outcomes if the earthquake occurs during the four dry months; "saturated conditions," to the eight wet months. Columns labeled *L* denote the average number of landslides estimated along the subject routes, $\tau_L$ to the number of days required to fully restore highway landslides including 4 added days for reconnaissance, contracting, and for teams to arrive at landslides. Routes would have one lane open in about half the time shown.

Table 5-10. Estimated count and duration of landslide repairs, including 4 days for mobilization

| Mean recurrence interval, years | Dry conditions | | Saturated conditions | |
|---|---|---|---|---|
| | $L$, count | $\tau_L$, days | $L$, count | $\tau_L$, days |
| 72 | 120 | 31 | 900 | 190 |
| 225 | 270 | 61 | 1,300 | 280 |
| 475 | 340 | 75 | 1,370 | 290 |
| 975 | 340 | 74 | 1,400 | 300 |
| 2,475 | 380 | 84 | 1,400 | 310 |

Thus, the table shows that it will take about one to three months to restore full access if a large Cascadia Subduction Zone earthquake occurs in the summer months, and between six and 10 months for full access during the wet season, depending on earthquake magnitude and between-event variability.

The calculations assume 300 repair crews are available. The number is highly uncertain, but seemed reasonable to the Oregon Department of Transportation (D. Hamilton, Public Information Officer, Oregon Department of Transportation, verbal commun., July 27, 2020). Figures in the table are rounded to two significant figures and are probably accurate to no more than one significant figure.

Table 5-11 presents the estimated time to repair landslides along each mountainous route if the earthquake occurs during the four dry summer months. Columns refer to each route. Rows refer to the 5 scenario earthquakes. Values in the table represent the estimated restoration time in days, averaging over 20 realizations of ground motion. Table 5-12 presents similar information if the earthquake occurs during the eight wet months of fall, winter, and spring.

The tables include 4 days on average to account for reconnaissance, contracting, and for teams to arrive at landslides, collectively referred to here as mobilization time.

Table 5-11. Landslide repair duration $\tau_{L,r}$, dry conditions (days), plus 4 days mobilization time

| Mean recurrence interval, years | 1. I-5 from Seattle | 2. I-84 | 3. US-26 | 4. OR-22 | 5. US-20 | 6, 8, 10. I-5 from Redding | 7 and 9. OR-58 |
|---|---|---|---|---|---|---|---|
| 72 | 4 | 6 | 5 | 16 | 14 | 24 | 31 |
| 225 | 10 | 15 | 6 | 33 | 24 | 61 | 44 |
| 475 | 14 | 15 | 6 | 36 | 23 | 75 | 43 |
| 975 | 12 | 17 | 7 | 40 | 24 | 74 | 46 |
| 2,475 | 16 | 18 | 7 | 40 | 24 | 84 | 45 |

Table 5-12. Landslide repair duration $\tau_{L,r}$, saturated conditions (days), plus 4 days mobilization time

| Mean recurrence interval, years | 1. I-5 from Seattle | 2. I-84 | 3. US-26 | 4. OR-22 | 5. US-20 | 6, 8, 10. I-5 from Redding | 7 and 9. OR-58 |
|---|---|---|---|---|---|---|---|
| 72 | 92 | 31 | 21 | 58 | 38 | 190 | 58 |
| 225 | 110 | 80 | 66 | 93 | 77 | 280 | 87 |
| 475 | 110 | 80 | 70 | 96 | 78 | 290 | 87 |
| 975 | 120 | 87 | 78 | 100 | 81 | 300 | 91 |
| 2,475 | 120 | 91 | 81 | 100 | 83 | 310 | 91 |

The project team performed modest sensitivity studies on two of the more uncertain parameters. If it takes half as long to repair one slide—10 days rather than three weeks—then the durations scale accordingly: two to six weeks to full restoration during dry conditions, and three to five months in saturated conditions. If all cuts and fills are at least geologic group B (no C), landslide count and repair durations are only slight reduced—about 25% and 5%, respectively.

#### *5.5.2.4 Liquefaction-Induced Landslides are Overlooked*

The forgoing analysis omits liquefaction-induced landslides. How serious is the omission? The project team could find no statewide maps of liquefaction hazard along these routes, making it impractical to perform a liquefaction analysis. But "impractical" does not mean "unimportant." What are the possible implications of the omission?

First, the project team can at least note that omitting liquefaction from its analysis of earthquake-induced landslides would only underestimate access delays from landslides and thus underestimate the benefit of a resilient runway, adding conservativeness to the benefit-cost ratio calculated here.

But how significant might any underestimate be? Approximately 91 km out of 1,100 km (9%) of the length of mountainous highway routes in Figure 5-7 (the red lines) pass through Quaternary alluvium according to Walker and MacLeod's (1991) geologic map of Oregon, where one would expect any liquefaction to occur. Only some fraction of the Quaternary alluvium along mountainous routes is likely to be susceptible to liquefaction (typically saturated granular soils with low plasticity).

Do past earthquakes provide any sense of the scale of the underestimate? Important landslides have occurred because of soil liquefaction. In a notable lecture, Seed (1968, pg. 1116) provides a list of known earthquake-induced landslides in which liquefaction played a part: 56 to 73, dating between 373 BCE and 1966, most of them in the 150 years prior to his lecture. Seed does not seem to estimate the fraction of all earthquake-induced landslides that can be attributed to liquefaction. But out of thousands of earthquake-induced landslides, the fact that Seed found it practical to enumerate only several dozen that he could attribute to liquefaction, suggests that liquefaction-induced landslides are at most a second-order consideration in a regional risk analysis.

Jibson and Harp (1998) cataloged 11,000 individual landslides as small as one to two meters across that occurred in an area of about 10,000 $km^2$ of the Santa Susana Mountains after the January 17, 1994 Northridge earthquake. They report that "This area of greatest landslide concentration consists primarily of upper Miocene through Pleistocene clastic sediment having little or no cementation and that has been folded and uplifted owing to rapid tectonic deformation. This young, weak material lacks significant tensile strength and erodes readily to form steep-walled canyons that commonly head in nearly vertical slopes." These sedimentary rocks do not liquefy. Note however that December 1993 and January 1994 were dry; Los Angeles International Airport recorded no precipitation in the six weeks prior to the earthquake (www.wunderground.com, Los Angeles California weather history). The dry conditions would have inhibited the sort of liquefaction that concerns us.

Keefer et al. (1998) report investigations of 18 large landslides in the Summit Ridge area of the Santa Cruz Mountains after the $M_w$ 7.1 Loma Prieta earthquake of October 1989. They make no mention of liquefaction contributing to any of them, and report that where the failure plane could be inferred, it generally occurred within bedrock, suggesting that liquefaction played no significant role in landslides in the epicentral region. Again however, the earthquake occurred in a dry month with only about 30 mm of precipitation.

Tinsley and Dupre (1992) compare liquefaction hazard mapping and liquefaction outcomes around Watsonville in the $M_W$ 7.1 1989 Loma Prieta earthquake. Of all the Quaternary sediments they mapped near the Pajaro River and Corralitos Creek, about 15 km south of the epicenter, they identified about equal quantities of high, moderate, and low liquefaction susceptibility (Tinsley and Dupre 1992, p. 82). They observed liquefaction in perhaps 1 to 5% of the area of very-high susceptibility sediments, none in moderate and none in low.

While limited evidence offered here is far from exhaustive, it does hint that, while liquefaction-induced landslides may occur, omitting them likely underestimates the areal extent of landslides at the regional level by a relatively modest fraction. At this time, in the absence of detailed liquefaction hazard maps in this region, the project team judged that any error produced by omitting liquefaction-induced landslide is swamped by other variables explicitly considered here.

## 5.5.3 Access Delays from Highway Bridge Damage

Access to the study area requires many bridges to remain safe. The study area counties contain 2,309 bridges in the National Bridge Inventory. Of these, key routes in the study area with long detours have 61 bridges. They are shown as yellow circles in Figure 5-9. Table 5-13 presents estimated repair time by route: the longest average repair time to restore bridges. Columns in the table correspond to the routes shown in Table 5-7. Rows refer to earthquake scenarios listed in Table 5-3. Estimates have been rounded to two significant digits to reduce the appearance of excess accuracy.

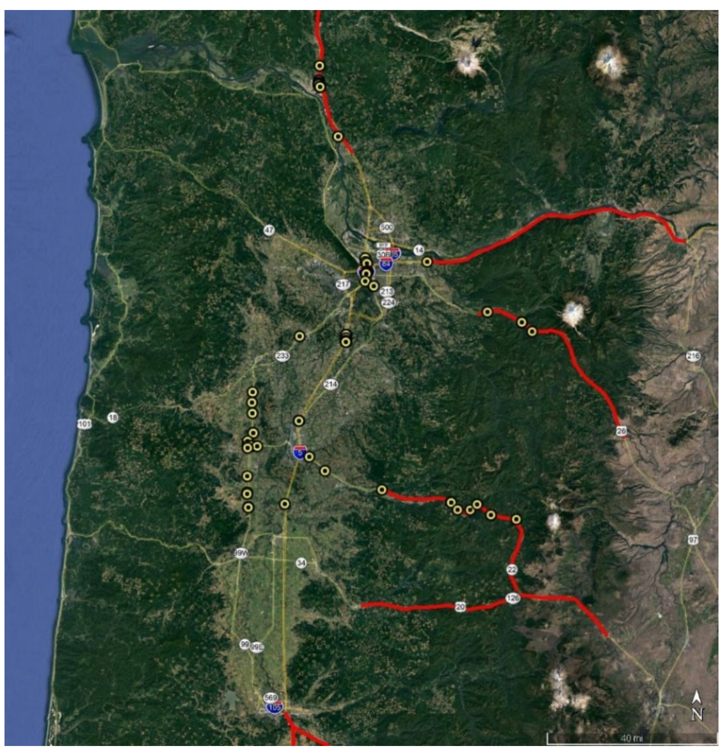

Figure 5-9. Freeway and highway bridges on access routes in the study area with long (>10 km) detours

Table 5-13. Expected value of bridge repair duration by route, including 4 days mobilization time

| Mean recurrence interval, years | 1. I-5 from Seattle | 2. I-84 from The Dalles | 3. US-26 | 4. OR-22 | 5. US-20 | 6. I-5 Redding to OR-99E | 7. OR-58 to OR-99E | 8. I-5 Redding to OR-99W | 9. OR-58 to OR-99W | 10. I-5 from Redding |
|---|---|---|---|---|---|---|---|---|---|---|
| 72 | 37 | 6 | 6 | 32 | 0 | 39 | 17 | 82 | 74 | 36 |
| 225 | 80 | 16 | 16 | 76 | 0 | 79 | 45 | 140 | 120 | 73 |
| 475 | 91 | 20 | 21 | 86 | 0 | 88 | 53 | 150 | 130 | 83 |
| 975 | 100 | 24 | 26 | 100 | 0 | 99 | 62 | 160 | 150 | 94 |
| 2,475 | 110 | 28 | 31 | 110 | 0 | 110 | 69 | 170 | 150 | 100 |

The project team also estimated the bridge repair durations, ignoring within-event ground-motion variability, to test the hypothesis that within-event variability matters. It does. Table 5-14 presents estimated bridge repair durations with median ground motions in each scenario earthquake. The figures that neglect within-event variability range between 25% and 80% of the figures that account for it, and they average about 56%. Ignoring within-event variability underestimates bridge repair time by half.

Table 5-14. Bridge repair duration by route, ignoring within-event ground-motion variability

| Mean recurrence interval, years | Earthquake | 1. I-5 from Seattle | 2. I-84 from The Dalles | 3. US-26 | 4. OR-22 | 5. US-20 | 6. I-5 Redding to OR-99E | 7. OR-58 to OR-99E | 8. I-5 Redding to OR-99W | 9. OR-58 to OR-99W | 10. I-5 from Redding |
|---|---|---|---|---|---|---|---|---|---|---|---|
| 72 | 1 | 12 | 4 | 4 | 13 | 0 | 10 | 8 | 28 | 28 | 10 |
| 225 | 2 | 42 | 6 | 10 | 45 | 0 | 33 | 28 | 75 | 75 | 33 |
| 475 | 3 | 51 | 7 | 13 | 54 | 0 | 45 | 36 | 84 | 84 | 45 |
| 975 | 4 | 63 | 8 | 17 | 69 | 0 | 54 | 45 | 100 | 100 | 54 |
| 2,475 | 5 | 72 | 11 | 21 | 78 | 0 | 63 | 54 | 110 | 110 | 63 |

## 5.5.4 Aggregate SAP Mobilization Time

Table 5-15 presents the time required to repair landslides and bridges roads along each of the 10 routes in each of the five scenario earthquakes considered here. The table reflects dry summer months from June to September when landslides are less likely. Table 5-16 presents analogous information for the wet fall, winter, and spring months from October through May when saturated hillsides are more likely to experience severe landslides in earthquakes.

Table 5-15. Aggregate road repair duration by route in dry months (June through September)

| Mean recurrence interval, years | Earthquake | 1. I-5 from Seattle | 2. I-84 from The Dalles | 3. US-26 | 4. OR-22 | 5. US-20 | 6. I-5 Redding to OR-99E | 7. OR-58 to OR-99E | 8. I-5 Redding to OR-99W | 9. OR-58 to OR-99W | 10. I-5 from Redding |
|---|---|---|---|---|---|---|---|---|---|---|---|
| 72 | 1 | 37 | 6 | 6 | 32 | 14 | 39 | 31 | 82 | 74 | 36 |
| 225 | 2 | 80 | 16 | 16 | 76 | 24 | 79 | 45 | 140 | 120 | 73 |
| 475 | 3 | 91 | 20 | 21 | 86 | 24 | 88 | 53 | 150 | 130 | 83 |
| 975 | 4 | 100 | 24 | 26 | 100 | 24 | 99 | 62 | 160 | 150 | 94 |
| 2,475 | 5 | 110 | 28 | 31 | 110 | 24 | 110 | 69 | 170 | 150 | 100 |

Table 5-16. Aggregate road repair duration by route in wet months (October to May)

| Mean recurrence interval, years | 1. I-5 from Seattle | 2. I-84 from The Dalles | 3. US-26 | 4. OR-22 | 5. US-20 | 6. I-5 Redding to OR-99E | 7. OR-58 to OR-99E | 8. I-5 Redding to OR-99W | 9. OR-58 to OR-99W | 10. I-5 from Redding |
|---|---|---|---|---|---|---|---|---|---|---|
| 72 | 92 | 31 | 21 | 58 | 38 | 190 | 58 | 190 | 74 | 190 |
| 225 | 110 | 80 | 66 | 93 | 77 | 280 | 87 | 280 | 125 | 280 |
| 475 | 110 | 80 | 70 | 100 | 78 | 290 | 87 | 290 | 150 | 290 |
| 975 | 120 | 87 | 78 | 100 | 81 | 300 | 91 | 300 | 130 | 300 |
| 2,475 | 120 | 91 | 81 | 100 | 83 | 310 | 91 | 310 | 150 | 310 |

Table 5-17 summarizes the time required to mobilize SAP evaluators either by road or through PDX, as a function of season, runway mitigation, and earthquake. The table contains five columns:

1. Earthquake mean recurrence interval in years, the same as in Table 5-3.
2. Time to mobilize SAP evaluators who must drive into the study area in dry months.
3. The same, but in wet fall, winter, and spring months.
4. Time to mobilize SAP evaluators through PDX, without a resilient runway. Season has no effect on this quantity.
5. The same, but with a resilient runway.

The table shows that, without a resilient runway, it is always faster to drive than to fly into the Willamette Valley, because landslides and bridges are repaired faster than the runway. With a resilient runway, it is always faster to fly than to drive.

Table 5-17. Time to mobilize SAP evaluators, in days, by road (depending on time of year) or PDX (depending on mitigation)

| Mean recurrence interval, years | $\tau_{Road}$, days, Jun-Sept | $\tau_{Road}$, days, Oct-May | $\tau_{Fly}$, days, without mitigation | $\tau_{Fly}$, days, with mitigation |
|---|---|---|---|---|
| 72 | 10 | 25 | 26 | 3 |
| 225 | 20 | 70 | 93 | 3 |
| 475 | 27 | 74 | 210 | 3 |
| 975 | 24 | 82 | 300 | 3 |
| 2,475 | 28 | 85 | 300 | 3 |

Table 5-18 presents the smaller of the two travel times—by road or air—as a function of season, mitigation to PDX's runway, and earthquake size. The table shows that a resilient runway at PDX reduces mobilization time in all five earthquakes by one to four weeks in dry months and three to 12 weeks in wet months. It shows that without a resilient runway, SAP evaluators would arrive faster by car than by air, even after waiting for landslide and bridge repairs, in all five scenario earthquakes.

One can now combine these results with estimates of the number of buildings that will have to be evaluated, to judge the benefit of a resilient runway for faster building safety inspection.

Table 5-18. Time required to mobilize remote SAP evaluators, depending on time of year and PDX runway mitigation

| Mean recurrence interval, years | $\tau$, remote SAP evaluator mobilization time, days | | | |
|---|---|---|---|---|
| | June-Sept | | Oct-May | |
| | without mitigation | with mitigation | without mitigation | with mitigation |
| 72 | 10 | 3 | 25 | 3 |
| 225 | 20 | 3 | 70 | 3 |
| 475 | 27 | 3 | 74 | 3 |
| 975 | 24 | 3 | 82 | 3 |
| 2,475 | 28 | 3 | 85 | 3 |

## 5.5.5 Estimated Building Inventory

Table 5-19 summarizes the estimated population in the study area, suggesting 20% population growth over the 17 years from 2002 to 2019 (the latest available as of this writing), equivalent to 1.08% annual growth and 24% growth over the 20 years from 2000 (probably the latest available census data underlying the 2002 inventory) to 2020 (the basis year for this study). The Hazus-MH building inventory estimates $N_{buildings}$ = 910,000 buildings in the study area (rounded to two significant figures to reduce the appearance of excessive accuracy), suggesting a current inventory of 1,100,000 building (again, rounded). Population has increased about 24% between 2000 and 2020 (extrapolated from the latest available census data as of this writing).

Table 5-19. Population of study-area counties

| FIPS | County | State | Population | |
|---|---|---|---|---|
| | | | 2002 | 2019 |
| 41005 | Clackamas | OR | 352,075 | 404,980 |
| 41047 | Marion | OR | 293,853 | 333,950 |
| 41051 | Multnomah | OR | 677,951 | 790,670 |
| 41053 | Polk | OR | 64,900 | 79,730 |
| 41067 | Washington | OR | 472,063 | 583,595 |
| 41071 | Yamhill | OR | 87,636 | 104,990 |
| 53011 | Clark | WA | 369,140 | 488,241 |
| 53015 | Cowlitz | WA | 94,467 | 110,593 |
| 53059 | Skamania | WA | 9,864 | 12,083 |
| Total | | | 2,423,951 | 2,908,832 |

## 5.5.6 Estimated Number of Safety Evaluations

Table 5-20 presents the estimated number of buildings that will require post-earthquake safety evaluation, (denoted $N = N_{green} + N_{yellow} + N_{red}$), the number that can be immediately re-occupied once they are evaluated (denoted by $N_{green} + 0.75 \times N_{yellow}$), and this latter number as a fraction of all 2.9 million buildings in the study area (denoted by $Q$). The rows refer to the scenario earthquakes of Table 5-3. Quantities in the table are rounded to two significant figures to reduce the appearance of excessive accuracy. They may only be accurate to 1 significant figure.

Table 5-20. Estimated demand for post-earthquake building safety evaluation

| Mean recurrence interval, years | Evaluations, $N = N_{green} + N_{yellow} + N_{red}$ | Re-occupiable, $N_{green} + 0.75 \times N_{yellow}$ | $Q$ |
|---|---|---|---|
| 72 | 410,000 | 340,000 | 31% |
| 225 | 700,000 | 550,000 | 49% |
| 475 | 750,000 | 580,000 | 52% |
| 975 | 810,000 | 600,000 | 54% |
| 2,475 | 850,000 | 610,000 | 55% |

## 5.5.7 Improved Safety-Evaluation Resilience Associated with Resilient Runway

As of August 2020, there were $L$ = 180 local certified SAP evaluators (people whose addresses appear to be within the study area; J. Barnes, California Governor's Office of Emergency Services, written commun., August 24, 2020). Judging by relative population, 300 certified SAP evaluators live in the Seattle-Tacoma metropolitan area. As of August 2020, there were a total of 10,693 certified SAP evaluators nationwide (same source). Removing those living in the Portland and Seattle-Tacoma areas, that leaves 10,213 SAP evaluators who could be mobilized to the Pacific Northwest. Assuming they were allocated by relative population, approximately 3,880 of the 10,213 remote SAP evaluators might be asked to go to the Portland area, the remainder to the Seattle-Tacoma area. Cal OES estimates that approximately one in three certified SAP evaluators can be mobilized at any one time (that is, $F$ = 0.33). Each team of SAP evaluators is estimated to complete $R$ = 13 evaluations per day.

Following the procedures presented in chapter 4, the project team found the following safety-evaluation resilience benefits from a resilient runway at PDX. Table 5-21 presents the time required to complete evaluation T, by season and depending on whether liquefaction at PDX's runway has been mitigated. The table also repeats information about placards from Table 5-20 for ease of reference.

The table shows that without a resilient runway, safety evaluation takes one to four months, depending on earthquake size and season. A resilient runway reduces that time by one to 11 weeks, meaning that a resilient runway will allow up to 610,000 buildings to be re-occupiable almost three months sooner.

Table 5-21. Time to complete building safety evaluation, T, days

| Mean recurrence interval, years | Evaluated buildings, $N$ | Reoccupiable buildings, $N_{green}$ + 0.75 × $N_{yellow}$ | Time to complete evaluation, $T$, days | | | |
|---|---|---|---|---|---|---|
| | | | June-Sept | | Oct-May | |
| | | | no mitigation | with mitigation | no mitigation | with mitigation |
| **72** | 410,000 | 340,000 | 33 | 27 | 48 | 27 |
| **225** | 700,000 | 550,000 | 60 | 44 | 110 | 44 |
| **475** | 750,000 | 580,000 | 67 | 47 | 120 | 47 |
| **975** | 810,000 | 600,000 | 73 | 50 | 120 | 50 |
| **2,475** | 850,000 | 610,000 | 76 | 52 | 130 | 52 |

Table 5-22 presents the estimated delay for the average evaluated building, in days. The table shows that the average building that must be evaluated waits between 21 and 103 days for SAP evaluators to evaluate the building, depending on season and earthquake size. Having a resilient runway allows SAP evaluators to reduce the loss of resilience by up to three months, because they can arrive in the Portland area via PDX.

Table 5-22. Average time a building awaits safety evaluation, days

| Mean recurrence interval, years | Reoccupiable buildings, $N_{green}$ + 0.75 × $N_{yellow}$ | Fraction of all buildings, $Q$ | Evaluation delay for average building, days | | | |
|---|---|---|---|---|---|---|
| | | | June-Sept | | Oct-May | |
| | | | no mitigation | with mitigation | no mitigation | with mitigation |
| **72** | 340,000 | 31% | 21 | 15 | 35 | 15 |
| **225** | 550,000 | 49% | 39 | 23 | 85 | 23 |
| **475** | 580,000 | 52% | 45 | 25 | 92 | 25 |
| **975** | 600,000 | 54% | 49 | 27 | 97 | 27 |
| **2,475** | 610,000 | 55% | 52 | 28 | 103 | 28 |

Table 5-23 presents the reduced delay between the mainshock and when the average damaged building gets evaluated. It shows that in earthquake 1, the average building can be evaluated six days sooner in summer, three weeks sooner in fall through spring. The weighted average of the two figures (the weight being the fraction of the year that the soil is dry or wet) is 16 days. In larger earthquakes, the average improvement in the largest earthquake—affecting over 600,000 buildings—is 75 days in fall through spring, with a weighted average of 58 days, that is, two months.

Table 5-23. Improved average safety-evaluation time, days

| Mean recurrence interval, years | Average reduction in safety-evaluation delay, days | | |
|---|---|---|---|
| | June-Sept | Oct-May | Weighted average |
| 72 | 6 | 20 | 16 |
| 225 | 16 | 62 | 46 |
| 475 | 20 | 67 | 51 |
| 975 | 22 | 70 | 55 |
| 2,475 | 24 | 75 | 58 |

Table 5-24 recaps the improvement in safety-evaluation resilience provided by having a resilient runway. The first four columns recap attributes of the five earthquakes considered here. The last three columns (columns 4 through 7) recap the benefit of a resilient runway in how it allows building safety inspectors to evaluate buildings faster and allow faster re-occupancy of safe ones.

1. EQ denotes an identifier (1 through 5).
2. Mean recurrence interval measures the relative likelihood of the earthquake, with longer mean recurrence intervals being less likely in one year.
3. CSZ earthquake magnitude denotes the moment magnitude of the earthquake; all five most likely earthquakes occurring on the Cascadia Subduction Zone, abbreviated CSZ.
4. Percentile refers to the non-exceedance probability of shaking at PDX, which reflects that shaking is uncertain and can be higher or lower than average for a given earthquake magnitude and location.
5. Re-occupiable buildings denotes the number of buildings that suffer frightening looking damage but that would ultimately be assigned a green placard, plus a fraction of those that would be assigned a yellow placard but only to modestly restrict use of the building.
6. Q denotes the fraction of all buildings in the study area that must be evaluated, but can be re-occupied once they are evaluated.
7. Average reduction in safety-evaluation delay measures how much sooner the average building is examined by a safety assessment program (SAP) evaluator. The reduction applies to buildings that

can be re-occupied because building safety evaluators can arrive faster from outside the study area by flying into PDX, thanks to its resilient runway.

Table 5-24. Recap of improved safety-evaluation resilience, days

| EQ | Mean recurrence interval, years | CSZ earthquake magnitude | Per-centile | Re-occupiable buildings | Fraction of all buildings, *Q* | Average reduction in evaluation delay, days |
|---|---|---|---|---|---|---|
| 1 | 72 | 8.7 | 11% | 340,000 | 31% | 16 |
| 2 | 225 | 9.12 | 39% | 550,000 | 49% | 46 |
| 3 | 475 | 9.12 | 66% | 580,000 | 52% | 51 |
| 4 | 975 | 9.34 | 39% | 600,000 | 54% | 55 |
| 5 | 2475 | 9.34 | 63% | 610,000 | 55% | 58 |

## 5.6 ESTIMATED NATIONAL DEFENSE BENEFIT

As noted in section 3, the Portland Air National Guard Base Finance Office (2019) estimates the economic impact of the 142nd Wing to be $130 million per year, or $356,000 per day. Table 5-25 presents a weighted average benefit-cost ratio to estimate the daily value of this expenditure: 4.35 times the expense.

Table 5-25. Weighted average benefit-cost ratio for use in benefit transfer assessment of the defense benefit of a resilient runway

| Source | Expenditure | Expenditure 2020 USD | *BCR* |
|---|---|---|---|
| U.S Air Force 2017 p. 99 | $239 million (2012 USD) | $268 million | 3.5 |
| U.S. Air Force 2017 p. 103 | $562 million (2017 USD) | $591 million | 5.22 |
| U.S. Air Force 2019 p. 110 | $33.6 million (2019 USD) | $33.8 million | 2.97 |
| Hill et al. 2009 p. 22 | $104 million (2006 USD) | $132 million | 2.59 |
| Weighted average | | | 4.35 |

Thus, the U.S. government derives an estimated 4.35 times $356,000 per day of defense value from the operation of the U.S. Air Force 142nd Wing Oregon Air National Guard, or $1.55 million per day. This value is not realized if the 142nd Air Wing cannot service its mission. The aircraft cannot be transferred to another location without a working runway, and national defense cannot be deferred to a later date. Thus, each day sooner the runway is restored, the nation saves $1.55 million.

It seems reasonable therefore to assign a $130 million annual benefit, or $356,000 per day, to the functionality of PDX's runways.

Using $1.55 million loss of defense value per day of runway downtime, the downtimes depicted in Table 3-2, a 0.06-g threshold level of shaking required to initiate downtime, and a 49-year mean recurrence interval for that level of shaking, the project team estimated the following values of average loss per year and present value of future loss under as-is and mitigated (retrofitted) conditions. The difference between the two is the defense benefit. Present value calculations use a real discount rate that seems appropriate to discounting military benefit: 30-year U.S. treasury rate minus current inflation, which produces a real discount rate of 0.85%. Applying a 100-year useful project life produces a defense benefit of $28 million, as shown in Table 5-26. Dollar amounts are rounded to two significant figures to reduce the appearance of excess accuracy.

Table 5-26. Defense benefit of a resilient runway

| Condition | Per year | Present value |
|---|---|---|
| As-is | $480,000 | $32,000,000 |
| Mitigated | $60,000 | $4,000,000 |
| Benefit | $420,000 | $28,000,000 |

# 6. References Cited

Abrahamson, N. A., Kuehn, N., Gulerce, Z., Gregor, N., Bozognia, Y., Parker, G., Stewart, J., Chiou, B., Idriss, I. M., Campbell, K., and Youngs., R. (2018). *Update of the BC Hydro Subduction Ground-Motion Model using the NGA-Subduction Dataset*. Pacific Earthquake Engineering Research Center, University of California, Berkeley, PEER Report No. 2018/02.

Allianz Global Corporate & Specialty (2020). *Allianz Risk Barometer 2020 - Business Interruption*. https://www.agcs.allianz.com/news-and-insights/expert-risk-articles/allianz-risk-barometer-2020-business-interruption.html

Appleby, C.A., Burn, W.J., Hairston-Porter, R.W., and Bauer, J.M. (2019). *Coseismic Landslide Susceptibility, Liquefaction Susceptibility, and Soil Amplification Class Maps, Clackamas, Columbia, Multnomah, And Washington Counties, Oregon*. Open-File Report O-19-09, Oregon Department of Geology and Mineral Industries, Portland, 55 p.

Applied Technology Council (1985). *ATC-13 Earthquake Damage Evaluation Data for California*. Redwood City, CA, 492 pp.

Applied Technology Council (2005). *ATC-20-1: Field Manual: Postearthquake Safety Evaluation of Buildings*, 2nd Edition, Redwood City, CA, 144 pp.

Basoz, N. and Mander, J.B. (1999). *Enhancement of the Highway Transportation Lifeline Module in HAZUS, Final Pre-Publication Draft (#7)*. National Institute of Building Sciences, Washington DC

Bollman, M.A., King, G.A., Watrud, L.S., and Johnson, M.G. (2013). Seasonal soil moisture patterns in contrasting habitats in the Willamette Valley, Oregon. Northwest Science, 87(2): 161-177

Bruneau, M., Chang, S.E., Eguchi, R.T., Lee, G.C., O'Rourke, T.D., Reinhorn, A,M., Shinozuka, M., Tierney, K., Wallace, W.A., and. von Winterfeldt, D. (2003). A Framework to quantitatively assess and enhance the seismic resilience of communities, *Earthquake Spectra*, 19 (4): 733–752

Burns, W.J., Mickelson, K.A., and Madin, I.P. (2016). *Landslide Susceptibility Overview Map of Oregon*. Open-File Report O-16-02, Oregon Department of Geology and Mineral Industries, Portland, 52 p.

California Department of Transportation and California Geological Survey (2012). *63rd Annual Highway Geology Symposium Proceedings, May 7-10, 2012, Redding, CA*, 511 p.

Cimellaro, G.P., Reinhorn, A.M., and Bruneau, M. (2010). Seismic resilience of a hospital system. *Structure and Infrastructure Engineering*, 6 (1-2): 127-144, DOI:10.1080/15732470802663847

Data.gov (2013). *Geologic Map of Oregon*, https://catalog.data.gov/dataset/geologic-map-of-oregon-ngmdb [accessed 21 Jun 2020]

Detweiler, S.T., and Wein, A.M., eds. (2018). *The HayWired Earthquake Scenario—Engineering Implications*. U.S. Geological Survey Scientific Investigations Report 2017–5013–I–Q, 429 p., https://doi.org/10.3133/sir20175013v2 [accessed April 22, 2020]

Earthquake Engineering Research Institute (2010). *EERI Special Earthquake Report — June 2010. Learning from Earthquakes. The Mw 8.8 Chile Earthquake of February 27, 2010.* Oakland, California, 20 p. https://www.eeri.org/site/images/eeri_newsletter/2010_pdf/Chile10_insert.pdf [accessed May 15, 2020]

EQE International (1994). *The January 17, 1994 Northridge, CA Earthquake An EQE Summary Report, March 1994.* Transportation. https://www.lafire.com/famous_fires/1994-0117_NorthridgeEarthquake/quake/06_EQE_transportation.htm [accessed May 15, 2020].

EQE International and the Governor's Office of Emergency Services (1995). The Northridge Earthquake of January 17, 1994: Report of Data Collection and Analysis, Part A: Damage and Inventory Data, EQE International, Irvine, CA, 322 p.

Federal Highway Administration (2013). *Federal Highway Administration Design Manual: Deep Mixing for Embankment and Foundation Support*. Federal Highway Administration (2020). *National Bridge Inventory (NBI)*. Washington, DC, https://www.fhwa.dot.gov/bridge/nbi.cfm [accessed Apr 20, 2020]

Felzer, K.R. and Brodsky, E.E. (2006) Decay of aftershock density with distance indicates triggering by dynamic stress. Nature, 441(8): 735-738

Ferreira, M.A., Oliviera, C.S., and Mota de Sa, F. (2011). Estimating human losses in earthquake models: a discussion. Spence, R., So. E., and Scawthorn, C., eds. Human Casualties in Earthquakes. Progress in Modeling and Mitigation. Springer, 255-266.

Field, E.H., T.H. Jordan, and C.A. Cornell (2003). OpenSHA: A Developing Community-Modeling Environment for Seismic Hazard Analysis, Seismological Research Letters, 74, no. 4, p. 406-419.

Forgione, M. (2019). New Zealand earthquake: Christchurch airport plans to reopen Wednesday; extra flights added. Los Angeles Times. Retrieved from https://www.latimes.com/archives/la-xpm-2011-feb-22-la-trb-new-zealand-quake-20110222-story.html

Franklin, J. and Gabbatt, A., (2010). Chilean military takes control of quake-hit cities. *The Guardian*, March 1, 2010, https://www.theguardian.com/world/2010/mar/01/chile-military-earthquake-cities-looting [accessed May 15, 2020]

Golshani, F., and Kashani, H. (2018). A probabilistic model for evaluating the impact of prepositioning of rescue centers of earthquake consequence management. *Proc. Creative Construction Conference 2018, CCC 2018, 30 June - 3 July 2018, Ljubljana, Slovenia*

GRI (2020). *Geotechnical Services South Runway Seismic Mitigation Design Portland International Airport (PDX) Portland, Oregon*. Beaverton OR, 198 p

Halpern N.A., Goldman D.A., Tan K.S., and Pastores, S.M. (2016). Trends in critical care beds and use among population groups and Medicare and Medicaid beneficiaries in the United States: 2000-2010. *Critical Care Medicine* 44(8):1490-1499.

Hill, J, Franklin, D, Jolly, K, and Townsend, MJ (2009). *Kansas Military Analysis Fiscal and Economic Impact of Military Activity in Kansas*. Wichita: Center for Economic Development and Business Research, W. Frank Barton School of Business, 82 p.

HNTB Corporation (2015). *Port of Portland Corporate Seismic Risk Assessment Study*. Belleview, WA, 337 p.

Hopkins, T.C., Beckham, T.L., Sun, C., and Pfalzer, B. (2005) *Kentucky Geotechnical Database*. Report KTC-05-03/SPR227-01-1F, Kentucky Transportation Center, Lexington KY.

IMPLAN (2020). *IMPLAN Sectoring & NAICS Correspondences*. https://implanhelp.zendesk.com/hc/en-us/articles/115009674428-IMPLAN-Sectoring-NAICS-Correspondences [accessed April 22, 2020].

Jena, A.B., Mann, N.C., Wedlund, L.N., & Olenski, A. (2017). Delays in emergency care and mortality during major U.S. marathons. *The New England Journal of Medicine*, 376 (15): 1441–1450. https://doi.org/10.1056/NEJMsa1614073

Jibson, R.W. (2007). Regression models for estimating coseismic landslide displacement. *Engineering Geology* 91(2-4):209–218.

Jibson, R.W. and Harp, E.L. (1998). Research on landslides triggered by the Northridge earthquake: documentation of effects and analytical modeling to create seismic landslide hazard maps. *Proceedings of the NEHRP Conference and Workshop on Research on the Northridge, California Earthquake of January 17, 1994*, II:142-149

Jibson, R.W., Harp, E.L., Michael, J.M. (2000). A method for producing digital probabilistic seismic landslide hazard maps. *Engineering Geology* 58(3-4):271–289.

Kaptan, K. (2014). An organizational metamodel for hospital emergency departments. *Disaster Medicine and Public Health Preparedness*, 8 (5): 436-444

Keefer, D.K., Griggs, G.B., and Harp, E.L. (1998). Large landslides near the San Andreas Fault in the Summit Ridge area, Santa Cruz Mountains, California. The Loma Prieta, California, Earthquake of October 17,1989—Landslides. U.S. Geological Survey Professional Paper 1551-C. C71:C128

Kuehn, N., Bozorgnia, Y., Campbell, K.W., and Gregor, N. (2020). *Partially Nonergodic Ground-Motion Model for Subduction Regions using NGA-Subduction Database*. PEER Report 2020/04, Pacific Earthquake Engineering Research Center, UC Berkeley.

Leontief, W. (1936). Quantitative input and output relations in the economic system of the United States. *Review of Economics and Statistics*, 18, 105-125.

Li, P., Rose, A., and Eduardo, B. (1999). Construction of an Input-Output income distribution matrix for the U.S. In Hewings, G., Sonis, M., Madden, M., and Kimura, Y. (eds) *Understanding and Interpreting Economic Structure*. Springer, Heidelberg.

McCrink, T.P. and F.G. Perez (2017). HayWired scenario mainshock—earthquake-induced landslide hazards. Chapter F in S.T. Detweiler and A.M. Wein, eds. The HayWired Earthquake Scenario—Earthquake Hazards. Scientific Investigations Report 2017–5013–A–H. US Geological Survey, Reston VA, p. 69-90

MercoPress (2010). Santiago airport reopens domestic terminal and activity should reach 50%. March 4, 2010. https://en.mercopress.com/2010/03/04/santiago-airport-reopens-domestic-terminal-and-activity-should-reach-50 [accessed May 15, 2020]

Metro Research Center (2016). *Population Forecast to 2060 Portland-Vancouver-Hillsboro, OR-WA, Metropolitan Statistical Area*. Portland, OR, 8 p.

Miller, R.E., and Blair, P.D. (2009). *Input-output Analysis: Foundations and Extensions, 2nd ed*. Cambridge University Press, New Jersey

Multi-Hazard Mitigation Council (2005). *Natural Hazard Mitigation Saves: An Independent Study to Assess the Future Savings from Mitigation Activities*. National Institute of Building Sciences, Washington, DC.

Multi-Hazard Mitigation Council (2019). *Natural Hazard Mitigation Saves: 2019 Report*. Principal Investigator Porter, K.; Co-Principal Investigators Dash, N., Huyck, C., Santos, J., Scawthorn, C.; Investigators: Eguchi, M., Eguchi, R., Ghosh., S., Isteita, M., Mickey, K., Rashed, T., Reeder, A.; Schneider, P.; and Yuan, J., Directors, MMC. Investigator Intern: Cohen-Porter, A. National Institute of Building Sciences. Washington, DC. www.nibs.org

Nako, A., Shike, C., Six, J., Johnson, B.m and Dusicka, P. (2009). *Seismic Vulnerability of Oregon State Highway Bridges: Mitigation Strategies to Reduce Major Mobility Risks*. No. OR-RD-10-08, Oregon Dept. of Transportation, 64 p.

(NIBS and FEMA) National Institute of Building Sciences and Federal Emergency Management Agency (2012). *Multi-hazard Loss Estimation Methodology Earthquake Model Hazus®-MH 2.1 Technical Manual.* Federal Emergency Management Agency, Washington, DC, 718 pp.

Oregon Department of Transportation (2019) Maintenance District Map. Salem, OR, 1 p. https://www.oregon.gov/odot/Data/Documents/DistrictMaintMap.pdf [accessed July 222, 2020]

Park, H.S., Cox, D.T., Alam, M.S., and Barbosa, A.R. (2017). Probabilistic seismic and tsunami hazard analysis conditioned on a megathrust rupture of the Cascadia Subduction Zone. *Frontiers in Built Environment*, https://doi.org/10.3389/fbuil.2017.00032 [accessed July 22, 2020]

Parker, G.A., Stewart, J.P., Boore, D.M., Atkinson, G.M., and Hassani, B. (2020). *NGASubduction Global Ground Motion Models with Regional Adjustment Factors*. PEER Report 2020/03, Pacific Earthquake Engineering Research Center, UC Berkeley.

Parker, R., Bruce, J., Bump, T., Craigie, M., Tapogna, J., Clark, B., and Duy, T. (2020). *Responding to the Economic Impacts of Coronavirus: A Proposed Oregon Economic Recovery and Resilience Framework*. University of Oregon Institute for Policy Research and Engagement. 12 p. https://oeda.biz/wp-content/uploads/2020/04/Oregon-Recovery-and-Resilience-Organizational-Framework-Pandemic-2020.pdf [accessed May 14, 2020]

Paul, J.A., George, S.K., Yi, P.F., and Lin, L. (2006). Transient modeling in simulation of hospital operations for emergency response. *Prehospital and Disaster Medicine* 21 (4): 223-236

Paul, J.A., and Hariharan, G. (2012). Location-allocation planning of stockpiles for effective disaster mitigation. *Annals of Operations Research* 196:469-490

Paul, J.A., and MacDonald, L. (2016). Location and capacity allocations decisions to mitigate the impacts of unexpected disasters. *European Journal of Operational Research* 251 (1): 252-263

Port of Portland (2019). Portland International Airport (PDX) Monthly Traffic Report December, 2018: Calendar Year Report. 5 p. https://popcdn.azureedge.net/pdfs/Dec2018webstats.pdf [accessed Sept. 7, 2020]

Portland International Airport (2019). *Airport Emergency Plan*. Portland, 133 p.

Porter, K.A. (2009a). Cracking an open safe: more HAZUS vulnerability functions in terms of structure-independent spectral acceleration. *Earthquake Spectra* 25 (3), 607-618, https://www.sparisk.com/pubs/Porter-2009-Safecrack-MDF.pdf

Porter, K.A. (2009b). Cracking an open safe: HAZUS vulnerability functions in terms of structure-independent spectral acceleration. *Earthquake Spectra* 25 (2), 361-378, https://www.sparisk.com/pubs/Porter-2009-Safecrack-Casualty.pdf

Porter, K.A. (2010). Cracking an open safe: uncertainty in HAZUS-based seismic vulnerability functions. *Earthquake Spectra*, 26 (3), 893-900 https://www.sparisk.com/pubs/Porter-2010-Safecrack-COV.pdf

Porter, K.A. (2018). An earthquake urban search and rescue model for earthquake response and its application to the HayWired scenario. Detweiler, S.T. and Wein, A.M. eds., *The HayWired Earthquake Scenario—Engineering Implications*. Scientific Investigations Report 2017–5013–I–Q, Reston, VA: United States Geological Survey, ch. M, p. 99-192, https://doi.org/10.3133/sir20175013 and www.sparisk.com/pubs/HayWired-2018-vol2.pdf

Porter, K. (2020). *A Beginner's Guide to Fragility, Vulnerability, and Risk*. University of Colorado Boulder, 128 pp., https://www.sparisk.com/pubs/Porter-beginners-guide.pdf

Portland Air National Guard Base Finance Office (2019). Oregon Air National Guard Financial Impact Summary Portland Air National Guard Base 2018. Portland, OR, 2 p. https://www.142fw.ang.af.mil/Portals/38/documents/FY18%20142%20FW%20Financial%20Summary.pdf?ver=2019-05-01-122934-517 [accessed Sept. 7, 2020]

Reasenberg, P.A., and L.M. Jones (1989). Earthquake hazard after a mainshock in California. Science, 243: 1173–1176.

Reasenberg, P.A., and L.M. Jones (1994). Earthquake aftershocks: update. Science. 265: 1251-1253.

RNZ News (2011). Christchurch airport open to emergency flights only. https://www.rnz.co.nz/news/canterbury-earthquake/69181/christchurch-airport-open-to-emergency-flights-only [accessed May 15, 2020]

Rose, A. (2009). *Economic Resilience to Disasters: Community and Regional Resilience Institute (CARRI) Research Report 8*. CARRI Institute, Oakridge, TN

Rose, A., Stevens, B., and Davis, G. (1988). *Natural Resource Policy and Income Distribution*. John Hopkins University Press, Baltimore MD

Rose, A., Wei, D., and Prager, F. (2012). Distributional impacts of greenhouse gas emissions trading: alternative allocation and recycling strategies in California. *Contemporary Economic Policy* 30(4): 603-617.

Saavedra, J.L. (2010). Massive earthquake hits Chile, 214 dead. Reuters February 26, 2010. https://www.reuters.com/article/us-quake-chile/massive-earthquake-hits-chile-214-dead-idUSTRE61Q0S920100227 [accessed May 15, 2020]

Seed, H.B. (1968). Landslides during earthquakes due to liquefaction. *Journal of the Soil Mechanics and Foundations Division*, ASCE, 94 (SM5), pp. 1053-1122

Skybrary (2014). *Boeing F-15 Strike Eagle*. https://www.skybrary.aero/index.php/F15 [accessed Sept. 7, 2020]

Snyder, D.T. (2008). Estimated Depth to Ground Water and Configuration of the Water Table in the Portland, Oregon Area. Scientific Investigations Report 2008-5059, U.S. Geological Survey, 52 p.

Spence, R., So. E., and Scawthorn, C., eds. (2011). *Human Casualties in Earthquakes: Progress in Modeling and Mitigation*. Springer, 322 p.

Sun, L., Hopkins, T.C., Beckham, T.L., and Ni, B. (2005) *Examination of Economical Methods for Repairing Highway Landslides*. Research Report KTC-05-04/SPR-180-98-1F, Kentucky Transportation Center, Lexington, KY, 37 p.

Taylor, L., Schneider, K., and Midena, K. (2011). 'Terminals rocking' as quake hits airport. Courier Mail, February 22, 2011 https://www.couriermail.com.au/travel/travel-news/terminals-rocking-as-earthquake-hits-christchurch-airport/news-story/23f746d74956fccd6463c569827c80fc?sv=b90a80ddaa3ed0a7569be4db67830429 [accessed May 15, 2020]

Tinsley, J.C. and Dupre, W.R. (1992) Liquefaction hazard mapping, depositional faces, and lateral spreading ground failure in the Monterey Bay area, Central California, during the 10/17/89 Loma Prieta earthquake. *Proceedings from the 4th Japan-U.S. Workshop on Earthquake Resistant Design of Lifeline Facilities and Countermeasures for Soil Liquefaction: Tokai University Pacific Center, Honolulu, Hawaii, May 27-29, 1992*. 1:71-85.

U.S. Air Force (2017). *United States Air Force Working Capital Fund Appropriate 4930 Fiscal Year (F.Y.) 2018 Budget Estimates*. Washington, DC. 127 p.

U.S. Air Force (2019). *United States Air Force Working Capital Fund Appropriate 4930 Fiscal Year (F.Y.) 2020 Budget Estimates*. Washington, DC. 127 p.

U.S. Air Force (ND). History. *142nd Wing*. https://www.142fw.ang.af.mil/Resources/History/ [accessed Sept 7, 2020]

U.S. Bureau of Economic Analysis (2020). *Personal Income and Employment by County and Metropolitan Area: Personal Income and Employment by Major Component (CAINC4)*. https://apps.bea.gov/iTable/iTable.cfm?reqid=70&step=1#reqid=70&step=1

U.S. Bureau of Labor Statistics (ND). *CPI Inflation Calculator*. https://www.bls.gov/data/inflation_calculator.htm [accessed September 24, 2020]

U.S. Department of Defense (2020). *Military Compensation: Annual Pay Adjustment*. https://militarypay.defense.gov/Pay/Basic-Pay/AnnualPayRaise/ [accessed November 4, 2020]

U.S. Department of Transportation (2015). *Guidance on Treatment of the Economic Value of a Statistical Life (VSL) in U.S. Department of Transportation Analyses-2015 Adjustment*. Washington, DC, 13 p., https://www.transportation.gov/sites/dot.gov/files/docs/VSL2015_0.pdf [accessed 13 Oct 2020]

United States Geological Survey (ND). Unified Hazard Tool. https://earthquake.usgs.gov/hazards/interactive/

United States Geological Survey National Earthquake Information Center (NDa). M 8.8 - offshore Bio-Bio, Chile. https://earthquake.usgs.gov/earthquakes/eventpage/official20100227063411530_30/executive [accessed May 15, 2020]

United States Geological Survey National Earthquake Information Center (NDb). M 6.1 - South Island of New Zealand. https://earthquake.usgs.gov/earthquakes/eventpage/usp000huvq/executive [accessed May 15, 2020]

United States Geological Survey National Earthquake Information Center (NDc). M 6.7 - 1km NNW of Reseda, CA. https://earthquake.usgs.gov/earthquakes/eventpage/ci3144585/executive [accessed May 15, 2020]

Vanmarcke, E. H., & Fenton, G. A. (1991). Conditioned simulation of local fields of earthquake ground motion. Structural Safety, 10(1-3), 247-264.

Verdin, K.L., Godt, J.W., Funk, C., Pedreros, D., Worstell, B., Verdin, J., (2007). *Development of a Global Slope Dataset for Estimation of Landslide Occurrence Resulting from Earthquakes.* Colorado: U.S. Geological Survey, Open-File Report 2007-1188, 25 p.

Wald, D.J. and Allen, T.I. (2007). Topographic slope as a proxy for seismic site conditions and amplification. *Bulletin of the Seismological Society of America*, 97, 1379-1395.

Walker, G.W., and MacLeod, N.S. (1991). Geologic Map of Oregon. U.S. Geologic Survey, 3 sheets.

Wang, Y., Summers, R.D., and Hoffmeister, R.J. (2002). *Landslide Loss Estimation Pilot Project in Oregon*. Open-File Report O-02-05, State of Oregon Department of Geology and Mineral Industries, Portland OR, 47 p.

Washington State Department of Natural Resources (2013). *Modeling a Magnitude 9.0Earthquake on the Cascadia Subduction Zone off the Pacific Coast*. 4 p. https://www.dnr.wa.gov/Publications/ger_seismic_scenario_cascadia.pdf [accessed April 22, 2020]

Webb, G., Tierney, K., and Dahlhamer, J. (2000). Business and disasters: empirical patterns and unanswered questions. *Natural Hazards Review*, 1, 83-90.

Wei, D., Koc, E., Rose, A., Chen, Z., and Soibelman, L. (2020). *Socioeconomic Dimensions of Resilience to Seaport and Highway Transportation Network Disruptions*. Final Report to Caltrans, METRANS Center, University of Southern California, Los Angeles, CA

Wein, A.M., Felzer, K.R., Jones, J.L., and Porter, K.A. (2017). HayWired scenario aftershock sequence. Chapter G in Detweiler, S.T. and Wein, A.M., eds., The HayWired Earthquake Scenario—Earthquake Hazards. Scientific Investigations Report 2017–5013–A–H. US Geological Survey, Reston VA: 91-112, https://doi.org/10.3133/sir20175013

Werner, S.D., Cho, S., Taylor, C.E., Lavoie, J.P., Huyck, C.K., Chung, H., and Eguchi, R.T. (2006). *Technical Manual: REDARS™ 2 Methodology and Software for Seismic Risk Analysis of Highway Systems*. Report MCEER-06-SP08, Buffalo NY: Multidisciplinary Center for Earthquake Engineering Research.

Wilson, R. C., and Keefer D. K. (1985). Predicting areal limits of earthquake induced landsliding, evaluating earthquake hazards in the Los Angeles region. Joyner, W.B., Fumal, T.E., and Ziony, J.I., eds. *Future Directions in Evaluating Earthquake Hazards of Southern California*. U.S. Geological Survey Professional Paper 1360, 317-493.

Zhao, J.X., Zhang, J., Asano, A., Ohno, Y., Oouchi, T., Takahashi, T., Ogawa, H., Irikura, K., Thio, H.K., and Somerville, P.G. (2006). Attenuation relations of strong ground motion in Japan using site classification based on predominant period. Bulletin of the Seismological Society of America 96 (3): 898–913

Zhao, J. X., Liang, X., Jiang, F., Xing, H., Zhu, M., Hou, R., Zhang, Y., Lan, X., Rhoades, D. A., Irikura, K., Fukushima, Y., and Somerville, P. G. (2016). Ground-motion prediction equations for subduction interface earthquakes in Japan using site class and simple geometric attenuation functions. *Bulletin of the Seismological Society of America* 106 (4): 1,518-1,534.